Winter 12-15-2021

Human PLCG2 Haploinsufficiency Results in a Novel Immunodeficiency

Joshua Brandon Alinger
Washington University in St. Louis

WASHINGTON UNIVERSITY IN ST. LOUIS

Division of Biology and Biomedical Sciences
Molecular Microbiology and Microbial Pathogenesis

Dissertation Examination Committee:
Anthony French, Chair
Marco Colonna
Brian Edelson
Todd Fehniger
Deborah Lenschow

Human *PLCG2* Haploinsufficiency Results in a Novel Immunodeficiency

by
Joshua Brandon Alinger

A dissertation presented to
the Graduate School
of Washington University in
partial fulfillment of the
requirements for the degree
of Doctor of Philosophy

May 2022
St. Louis, Missouri

Table of Contents

List of Figures

List of Tables

Acknowledgments

I would like to first and foremost thank my patients for their participation, without which this work would not be possible.

To my mentor, Tony French, for his day-to-day enthusiasm and support which gave me new inspiration and hope for a career in science.

To my thesis committee members, Todd, Marco, Debbie, and Brian, whose insight and suggestions paved the way for this work.

To my best friend and co-worker, Allyssa Daugherty, who spent countless hours in lab and outside of lab keeping me (relatively) sane.

To my fellow Pediatrics graduate students, Annelise Mah, Emma Walker, and Ying Lim, who continue to provide me with scientific inspiration, friendship, and moral support.

To Marshall Bloom, Tim Bauler and my former NIH colleagues and mentors, who convinced me that I was good enough to embark on this journey.

And last but not least, to the WUSTL Medical Scientist Training Program and our funding sources, for providing me with the means and opportunity to complete this work.

Thank you all,

Joshua B. Alinger

Washington University in St. Louis
May 2022

Dedicated to my late mother and grandmother.

ABSTRACT OF THE DISSERTATION

Human *PLCG2* Haploinsufficiency Results in a Novel Immunodeficiency

by

Joshua B. Alinger

Doctor of Philosophy in Biology and Biomedical Sciences

Molecular Microbiology and Microbial Pathogenesis

Washington University in St. Louis, 2022

Anthony R. French MD PhD, Chair

NK cells are critical for the recognition and lysis of herpesvirus-infected cells. Patients with NK cell immunodeficiency may suffer from unusually severe and/or recurrent herpesvirus infections; however, the genetic cause is frequently unknown. *PLCG2* encodes a signaling protein in NK cell and B cell receptor signaling, in which dominant-negative or gain-of-function mutations may cause cold urticaria, antibody deficiency, or autoinflammation. However, loss-of-function mutations and *PLCG2* haploinsufficiency have never been reported in human disease. We examined 2 families with autosomal dominant NK cell immunodeficiency with dual high-dimensional techniques, mass cytometry and whole-exome sequencing, to identify the cause of disease. We identified two novel heterozygous loss-of-function mutations in *PLCG2* that impaired NK cell function, including calcium flux, granule movement, and target killing. Although expression of mutant *PLCG2* protein in vitro was normal, phosphorylation of both mutants was diminished. In contrast to PLAID and APLAID, B cell function remained intact. *Plcg2*+/- mice, as well as targeted CRISPR knock-in mice, also displayed impaired NK cell function with preserved B cell function, phenocopying human *PLCG2* haploinsufficiency. We report the first known cases of *PLCG2* haploinsufficiency, a clinically and mechanistically distinct syndrome from previously

reported mutations. Therefore, these families represent a novel disease, highlighting a role for *PLCG2* haploinsufficiency in herpesvirus-susceptible patients and expanding the spectrum of *PLCG2*-related disease.

Chapter 1: Natural Killer Cells

Section 1.1 Natural Killer Cells and the Immune Response to Herpesviruses

Herpesviridae is a ubiquitous family of large DNA viruses, eight of which are capable of infecting humans. The seroprevalence of these viruses in adults exceeds 80-90% and nearly all humans are infected by one or more members of the family[1]. Herpesviruses predate both the arrival of adaptive immunity in jawed vertebrates and the speciation of mammals. Thus, nearly all mammals, as well as many other organisms, have cospeciated with one or more herpesviruses in the presence of an adaptive immune system. During this protracted period of coevolution, herpesviruses have evolved to evade the immune system and latently infect the mammalian host[1]. Many of these viruses have evolved specific mechanisms to evade adaptive immunity in particular, such as the active suppression of endogenous major histocompatibility complex (MHC) expression and the expression of virally derived MHC-like immunoevasins. Despite this, most immunocompetent individuals are capable of controlling herpesviruses and rarely develop severe disease.

While adaptive immunity is capable of limiting herpesvirus infections, the active evasion of antigen presentation suggests the need for other cell types to recognize and suppress viral infection. This assistance comes in the form of the Natural Killer (NK) cell, designed to detect the downregulation of class I MHC (MHC-I) and other signs of viral infection (as well as other pathological conditions such as cellular transformation). Mammals infected with herpesviruses are capable of recognizing infection via what has been coined the “missing self” hypothesis[2]. Upon infection with many types of DNA viruses, MHC-I expression may be reduced, and this reduction

is recognized by a reduction in NK cell inhibitory receptor signaling. At baseline, the presence of MHC-I on the surface of nearly all nucleated cells maintains NK cells in an inhibited state to prevent autoreactivity. This threshold of activation may be adjusted by activating receptors, recognizing stress signals or viral proteins, and cytokines secreted by other cell types during infection. The subsequent activation of NK cells results in several effector functions, including NK cell proliferation, the degranulation of cytolytic granules to lyse infected target cells, and the secretion of inflammatory cytokines such as TNFα and IFNγ (figure 1.1).

The study of murine cytomegalovirus (MCMV) in mice that express the Ly49H receptor, an activating receptor specific for MCMV-encoded m157, has provided an invaluable model for the study of NK cell activation[3,4]. The host tropism of MCMV is restricted to mice, however the pathology and response to MCMV resembles human infection with human cytomegalovirus (HHV-5). While mice are naturally infected with MCMV via the oral-fecal route, the virus is introduced either intravenously or intraperitoneally in the laboratory setting and extensive work has been done to study the immune response to MCMV during infection via these routes. Given the close relationship and interactions of natural killer cells with other cell types during infection, it is worth noting the (particularly innate) immunological events occurring during MCMV infection.

After intraperitoneal injection, MCMV may be detected within the spleen as early as 6 hours after infection, predominantly within the endothelial or fibroblastic stromal cells of the marginal zone[5]. The spleen appears to be the first target of infection and is required for further dissemination, as splenectomized mice display decreased viral replication within the liver and other sites[6]. As such,

the spleen is commonly examined during MCMV, particularly during the early phases before dissemination to the liver. By two days post-infection, MCMV may be detected within a variety of splenocytes including neutrophils, dendritic cells (classical CD8+ XCR1+ dendritic cells), NK cells and to a minor extent, B and T lymphocytes[5]. As the first cellular target, stromal cells have the potential to sense viral infection and replication via Toll-like receptor 3 (TLR3) or cytosolic sensors which cause subsequent expression of type I interferon (IFN). MCMV encodes at least one gene capable of inhibiting TLR3 signaling in infected cells, m45, which may limit the importance of stromal derived type I interferon (IFN-I)[7]. Nonetheless, IFN-I is detected early in infection, peaking around 36 hours and remains at this level until 48 hours post-infection, decreasing to baseline thereafter. The main producers of IFN-I during MCMV are plasmacytoid dendritic cells (pDC), detecting MCMV infection in a TLR9 dependent manner[8]. TLR9 recognizes unmethylated CpG DNA which uncommon in the mammalian genome, likely derived from apoptotic bodies/exosomes of virally infected cells and/or direct recognition of viral particles themselves[8]. Since pDC are rarely directly infected during MCMV infection, they remain shielded from MCMV-encoded immunoevasins which are expressed within infected cells[9]. The production of IFN-I induces the expression of interferon stimulated genes (ISGs) typically via the IFNAR receptor complex, leading to phosphorylation of the transcription factors STAT1 and STAT2 (as well as IRF9) with subsequent translocation to the nucleus[10]. MCMV encodes at least one protein capable of inhibiting STAT2 signaling, m27, to prevent the induction of ISGs[9]. Nonetheless, this pathway appears to be intact during MCMV infection as IFNAR deficient mice remain more susceptible to MCMV infection than wild-type mice suggesting that IFN-I is still protective during infection[11]. In addition to stimulation of virally infected cells, IFN-I also interacts with several immune cell types, including dendritic cells (inducing maturation and cytokine production) as well

as NK cells both indirectly and directly. Indirectly, IFN-I stimulates the expression of IL-15 and the high affinity IL-15Ra receptor on classical dendritic cells (cDC) which are critical for the trans-presentation of IL-15 to NK cells[12-14]. IL-15 is a critical cytokine for both NK cell survival/homeostasis as well as proliferation[15-17]. IL-15 may also synergize with IL-18 to induce NK proliferation, though IL-18 alone is unable to induce NK proliferation[18]. Subsequently, IL-15 creates a positive feedback loop within cDC whereby autocrine IL-15 signaling induces CD40 and allows for CD40-CD40L interactions between cDC and pDC[19]. This interaction licenses an increase in the cDC secretion of IL-12, required for NK cell IFNγ expression[20]. Directly, IFN-I signaling is also required for NK cell proliferation and maintenance, inhibiting the expression of the NKG2D ligand and stress signal Rae-1 on NK cells, thus preventing NK cell fratricide during infection[21]. IFN-I is also capable of inducing IFNγ expression in NK cells during LCMV infection in a STAT4 dependent manner[22]. However, IFN-I may also have negative regulatory effects in this scheme, as IFN-I is capable of inhibiting IL-12 expression in dendritic cells[23]. In addition to IL-12, IL-18 is also required for optimal NK cell IFNγ secretion[24]. Both IL-12 and IL-18 are expressed highly during early infection, peaking at 36 hours and then decreasing thereafter despite increasing levels of viral titers[5]. The reason for this decrease in IL-12 and IL-18 is not entirely clear, but likely stems from a negative regulatory program induced within pDC and CDC, and possibly involves IFN-I signaling.

As discussed previously, herpesviruses possess several mechanisms to evade T cell immunity by the active inhibition of antigen presentation. MCMV is no exception to this rule and encodes at least three proteins that inhibit MHC-I expression at various stages: m04, m06 and m152[5]. However, deletion of these genes in MCMV does not alter the kinetics of the T cell response to

MCMV. T cell immunity to MCMV involves gamma-delta and natural killer T cells as well as conventional CD4 and CD8 T cells, though the primary proliferating effector cells are CD8 T cells[5]. The uptake of viral antigen in cDC via cross-presentation thus appears sufficient to induce protective CD8 responses in spite of active downregulation of MHC-I on infected cells. This downregulation of MHC-I instead allows for NK cell activation, assisted by the activating receptor Ly49H which recognizes the viral protein m157 in select inbred mouse strains (C57BL/6 but not BALB/c for example)[3,25].

Ly49H plays an important role in the NK cell recognition of MCMV infected cells and is stochastically expressed on approximately 50% of splenic NK cells[26]. A paper on the role of Ly49H and NK cell activation during MCMV, Dokun et al (Nat Immunol 2001), describes a biphasic process of NK cell activation[26]. Early in infection, NK cells are stimulated to produce IFNγ and this process is unbiased in regard to Ly49H- or Ly49H+ NK cells. This likely reflects the large increase in IL-12 and IL-18 (both required for IFNγ production) that has been described by numerous groups.

Despite the fact that NK cell-derived IFNγ early in infection is independent of Ly49H, infection with MCMV lacking the Ly49H ligand m157 (Δm157 MCMV) causes an increase in numerous cytokines including IFNγ. This is likely a reflection of increased viral titers in the Δm157 MCMV infection stemming from lack of early control of viral replication. The production of IFNγ peaks at 36 hours post-infection and returns to baseline by 48 hours. NK cell counts in the spleen decrease by more than 75% after expression of IFNγ reaching a nadir at 2 days post-infection and then rapidly expanding thereafter[27]. This decrease could be attributed to NK migration out of the spleen;

however, there is no concurrent increase in NK cell numbers in other tissues, suggesting that NK cell death may be responsible for this decrease[27]. Expansion of NK cells from two days post-infection onward results in a Ly49H+ biasing of the NK cell pool, increasing from 50% to 90% Ly49H+ by 4 days post-infection. Ly49H- cells proliferate little if at all during this phase and neutralization of Ly49H (either genetically using BxD8 mice or via antibody neutralization) abrogates this activation[26,28]. These data imply that Ly49H signaling is sufficient and necessary to cause NK cell proliferation during MCMV infection. Interestingly, receptor stimulation (including through Ly49H) is capable of inducing IFNγ in vitro even in the absence of IL-12 and IL-18, however IFNγ is not secreted during this phase indicating that IFNγ secretion is possibly actively inhibited during this phase[29,30].

A later paper supports the importance of Ly49H mediated cytotoxicity but not IFNγ in the spleen during this specific proliferation phase of infection[31]. In contrast to *Ifng* -/- mice, mice deficient in perforin (required for NK cell and CD8 cytotoxicity) have remarkably increased titers in comparison to wild-type controls at 5 days post-infection. Interestingly, single deficiencies in IL-12, IL-18, IFN-I or Batf3 (resulting in the elimination of IL-15 presenting cDCs) result in viral control comparable to wild-type mice. However, simultaneous deletion of IL-12 and IFN-I results in a substantial reduction in granzyme B and perforin levels as well as an increase in viral titers in the spleen. In this particular study, IFNγ was not required for efficient viral control at this time point in the spleen, though it was partially required for efficient viral control in the liver suggesting that there may be organ specific or kinetic differences in the NK response to MCMV. However, a previous study found that while IFNγ was not required for viral control in the spleen at late time points (5-6 days), there was an increase in viral titers in the *Ifng* -/- mice at earlier time points (3 days)[32]. Overall, these studies suggest that IFNγ is capable of restraining viral growth but given

the short kinetics of its secretion and the large increase in Ly49H mediated cytotoxicity later in infection, it may be partially redundant with Ly49H induced cytotoxicity.

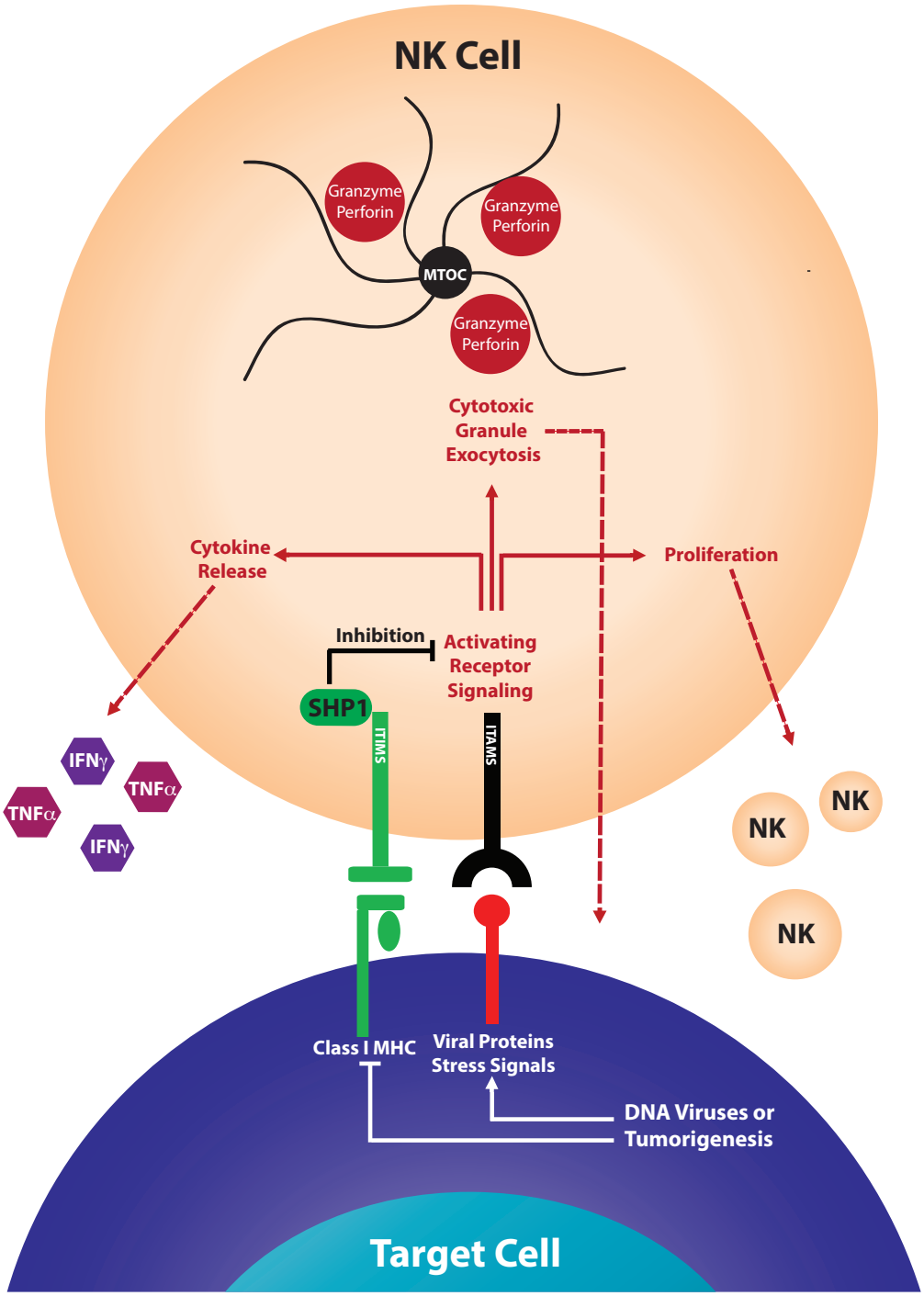

Figure 1.1 Model of NK Cell Activation

The activation of NK cells results in several effector functions, including NK cell proliferation, the exocytosis of cytolytic granules to lyse infected target cells, and the secretion of inflammatory cytokines such as TNFα and IFNγ.

Section 1.2 NK Cells in Human Disease

Many genetic conditions (reviewed in figure 1.2) affecting granule movement such as Chediak-Higashi syndrome (*LYST)*, Griscelli Syndrome (*RAB27A)*, and familial hemophagocytic lymphohistiocytosis (*PRF1, STX11, STXBP2, UNC13D,* among others), may affect NK cell degranulation and function. Forms of Severe Combined Immunodeficiency (SCID) such as JAK3 deficient SCID can also present with both low T and NK cells. However, all of these patients may also present with T cell deficiency which often underlies the more severe clinical presentation in these patients. Thus, a variety of immunologic disorders may impact NK cell function; however, the broader immunodeficiencies in these patients often present a more pressing clinical concern. Thus, NK cell disorders are defined as immunodeficiencies in which the NK cell deficiency is the primary immunologic phenotype [33].

To date, only a handful of monogenic NK cell disorders have been described. These examples may be grouped into two classifications: classical and functional NK cell deficiencies [33]. Classical NK cell deficiencies are defined as genetic disorders in which all or a major subset of NK cells fail to develop properly, resulting in NK cell cytopenias. This group includes the first published case of a NK cell deficiency in which the patient presented with overwhelming cytomegalovirus (CMV) infection due to what was eventually ascribed to GATA2 deficiency, a transcription factor involved in the maturation of NK cells in the $CD56^{dim}$ NK cell subset[34,35]. Indeed, this presentation of herpesvirus susceptibility is common to NK cell disorders as expected by their role in antiviral defense. The remaining described classical NK cell disorders include mutations in other transcription factors (IRF8) or DNA repair molecules (MCM4) and may similarly present with recurrent viral infections. [36,37].

By contrast, functional NK cell disorders present with normal circulating levels of NK cells with diminished function. Clinical NK cell function testing is typically performed using a chromium based K562 killing assay or a CD107 degranulation assay, both involving the incubation of primary patient peripheral blood mononuclear cells with a target tumor line, K562, to measure either target killing or the induction of patient NK cell degranulation[38]. Examples of functional NK cell disorders are even more rare, with only one genetic cause (mutations in *FCG3A*/CD16, impairing antibody-dependent cellular cytotoxicity) previously described[39,40]. However, a number of patients present with herpesvirus susceptibility in the form of either severe or recurrent infections with reduced clinical NK cell function who do not receive genetic diagnoses.

NK cells have also been implicated in the development or progression of a number of autoimmune or autoinflammatory syndromes including multiple sclerosis, rheumatoid arthritis, systemic lupus erythematosus (SLE), autoimmune thyroid disease, psoriasis, systemic juvenile idiopathic arthritis (sJIA), and juvenile dermatomyositis (JDM)[41-52]. Many of these studies offer only correlative evidence in the form of decreased NK cell numbers or function in the context of active disease; however, NK cells are known to play an important role in immunoregulation either by the secretion of immunomodulatory cytokines or by the direct targeting of activated T cells [53-55]. NK cells also regulate humoral immunity through the negative regulation of T follicular helper cells, an overabundance of which has been implicated in the development of autoantibodies and autoimmune disease [56,57]. Thus, in addition to the expected viral immunodeficiency in patients with NK cell disorders, a variety of other phenotypes, including but not limited to autoimmunity and immunodysregulation, may be present in these patients. Nonetheless, a more thorough investigation of the role of NK cells in autoimmunity is needed to understand the mechanism and/or role of NK cell dysfunction in these diseases.

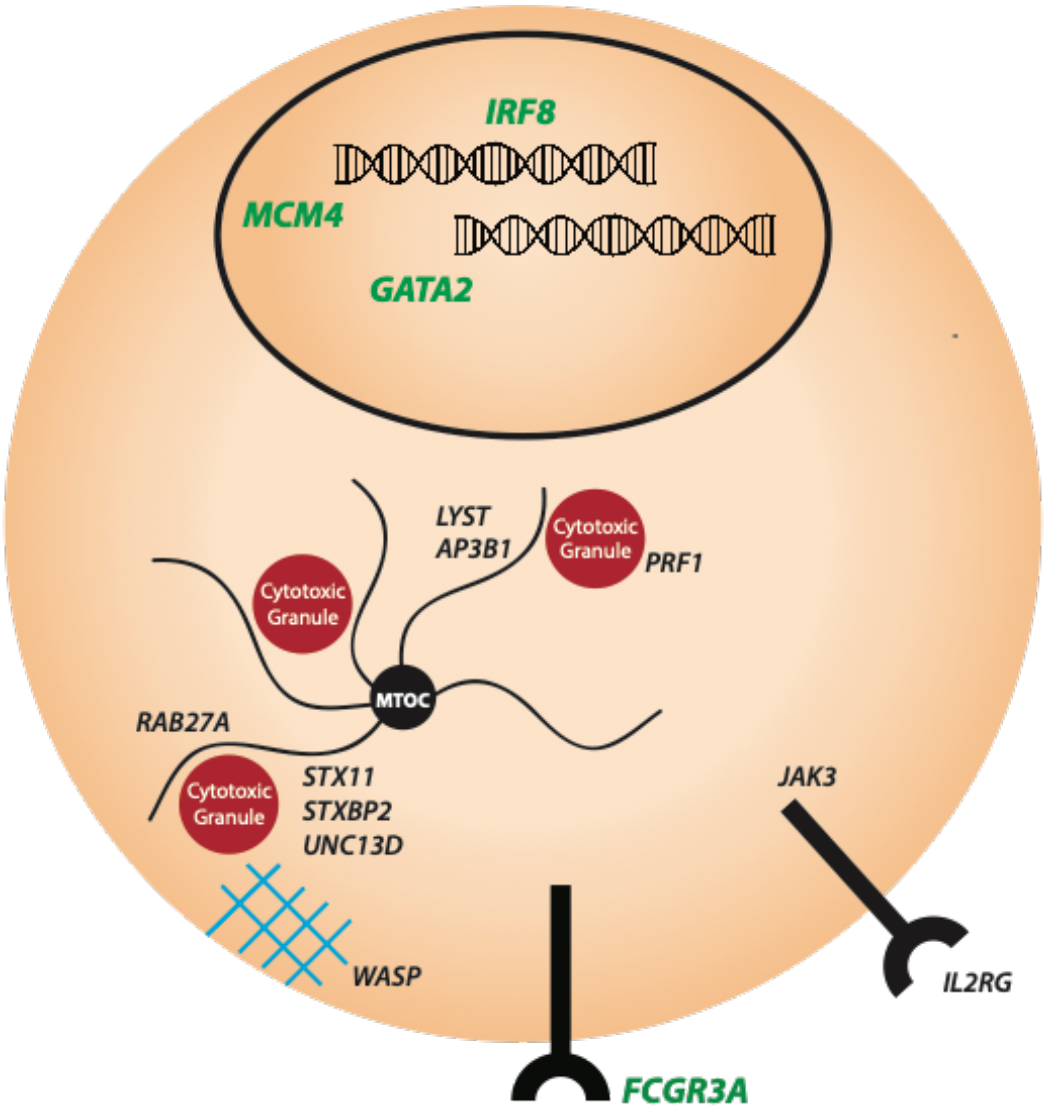

Figure 1.2 Human Disorders Impacting NK Cell Function

NK cell function and development can be impacted by a number of genetic conditions, however many conditions (shown in bold black) affect other cell types such as CD8 T cells. Only four genetic causes of specific NK cell deficiency (shown in green bold) have been previously described.

Section 1.3 Human NK Cell Receptors and Signaling

Human NK cells can be differentiated into two main circulating classes, the $CD56^{Bright}$ and $CD56^{Dim}$ NK cell subsets[58-60]. $CD56^{Bright}$ NK cells are generally thought to be cytokine-producing and immunomodulatory; however, with proper cytokine stimulation can be cytolytic[61]. Nonetheless, $CD56^{Dim}$ NK cells are considered the major cytotoxic NK cell subset in human blood and are the only subset capable of CD16-mediated antibody-dependent cellular cytotoxicity (ADCC).

Human NK cells use a variety of germline-encoded receptors to recognize viral and/or stress ligands present on the surface of cells. including the Natural Cytotoxicity Receptors (NCR) NKp30, NKp44, and NKp46, as well as NKG2C, NKG2D, the ADCC receptor CD16 and certain ITIM-deficient KIR receptors which are capable of triggering cytotoxicity[62]. NK cells also express costimulatory receptors that may also be found on T cells including NKp80, DNAM-1, 2B4, and NTA-B. The vast majority of NK cell receptors signal through either CD3ζ or DAP12; however, exceptions to this exist that signal through DAP10 or FcεRIγ (NKG2D and KIR2DL4, respectively). While certain details about costimulatory receptor signaling in NK cells remain to be solved, their signaling through SAP, hemITAM, or ITT domains remains largely conserved as it functions in T cells. NK cell receptor expression, ligands, and signaling mechanisms are reviewed with references in table 1.1.

NK cell receptor signaling through DAP12, FcεRIγ, and CD3ζ (representing the majority of NK cell receptors) proceeds in an analogous fashion to T cell receptor signaling[63]. The recruitment of these ITAM-bearing adaptor molecules and an aspartic acid residue in their hydrophobic tail to NK receptors is facilitated by a charged, basic residue within the cytoplasmic domain of each NK receptor[64,65]. The strength of the interaction between these residues dictates receptor:adaptor

specificity, though few examples are absolute. Upon engagement between these residues, Src family members such as Lck lead to the tyrosine phosphorylation of several substrates including Grb2, PI3K and Syk family members such as ZAP-70. The activation of Syk family members through tyrosine phosphorylation in turn leads to another round of substrate phosphorylation, including poly-phosphorylation of LAT. LAT is a scaffold protein through which many members of this signaling cascade may dock to phosphotyrosine residues with SH2 domains, including the Grb2-SLP76 complex, Vav, and Phospholipase-Cγ (PLCγ)[66]. The Vav-Rac pathway is subsequently able to activate the MAP Kinase pathway via MEK and ERK to support cytotoxicity and cytokine secretion[67]. Meanwhile, the recruitment of PLCγ to LAT enables recruitment of its respective kinase, Itk (a member of the Tec family of kinases) to allow for phosphorylation and catalytic activation of PLCγ[68,69]. The catalysis of PIP_2 into IP_3 and DAG via PLCγ is a key triggering event in NK receptor activation as IP_3-induced calcium flux is critical for the mobilization of cytolytic granules, while localized DAG formation serves as a homing target for granule movement[70-72]. The regulation and activation of PLCγ is reviewed in Chapter 2. At many steps of this process, the counter-regulation of this cascade through inhibitory receptors is achieved through KIR activated SHIP, SHP-1, and SHP-2 phosphatases that may dephosphorylate a number of substrates, disabling the formation of the signalosome[73]. Figure 1.3 summarizes this signaling cascade.

NKG2D is also a major NK cell receptor expressed on human NK cells that differs significantly in its activation from the pathway described above. In using DAP10 in lieu of other adaptor molecules, DAP10 activation occurs independent of Syk kinases and relies specifically on *PLCG2*, contrasting the promiscuity that DAP12, FcεRIγ, and CD3ζ share in their use of either *PLCG1* or

PLCG2[74]. While DAP10 also requires SLP-76 and Grb2, Vav1 instead of Vav2/3 is preferentially used in NKG2D/DAP10 signaling[67]. Intriguingly, while most NK receptors are capable of activating calcium flux alone, NKG2D requires either costimulation or crosslinking with another NK cell receptor for productive activation, a process that depends in part on the synergistic activation of *PLCG2*[75,76]. NKG2D crosslinking alone is also insufficient to trigger cytokine secretion in contrast to certain other NK cell receptors such as CD16[76]. Thus, NKG2D/DAP10 signaling represents a unique departure from the NK signaling paradigm presented above. Nonetheless, the importance of NKG2D is underscored by its critical role in various models of malignancy investigated using NKG2D knockout mice[77].

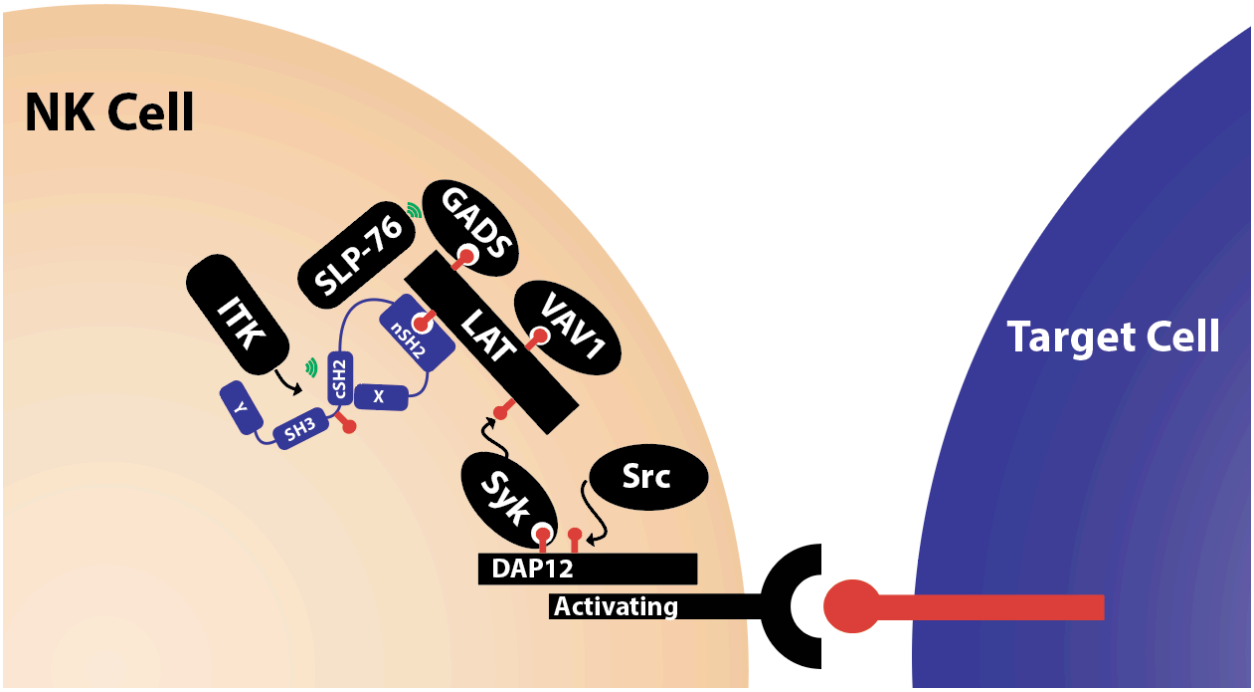

Figure 1.3 NK Cell Signaling through DAP12

Briefly, the association of activating receptors and DAP12 lead to the recruitment of Src, Syk, and the poly-phosphorylation of LAT. Phosphotyrosine residues on LAT serve to scaffold a number of downstream signaling molecules including VAV, SLP-76 and PLCG-2 (shown in simplified domain structure in blue).

Table 1.1: Human NK Cell Receptors, Ligands, and Signaling

Receptor	Type	Ligand	Adaptor	Expression
NKp80	Coreceptor[78]	AICL[79]	hemITAM[80]	Most circulating[78]
DNAM-1	Coreceptor[81]	Nectin-2, PVR[82]	ITT-1 Motif[83]	Most circulating[83]
2B4	Coreceptor[84]	CD48[85,86] Viral HA[87]	SAP[88,89]	Most circulating[90]
NTB-A	Coreceptor[91]	NTB-A[92] Viral HA[87]	SAP[93] EAT-2[94]	Most circulating[92]
NKp30	Natural Cytotoxicity Receptor[95,96]	B7-H6[97], BAG6, BAT3[98] pfEMP1[99]	CD3ζ[98]	Most circulating[96]
NKp44	Natural Cytotoxicity Receptor [100]	PCNA[101] 21spe-MLL5, HSPG, NID1, PDGF-DD [102]	DAP12[103]	Activated NK Cells[104]
NKp46	Natural Cytotoxicity Receptor [105,106]	Properdin[107] Viral HA[108] PfEMP1[99]	DAP12[103]	Most circulating[105,106]
NKG2D	Activating Receptor	MIC-A[109], MIC-B[110], ULPB[111]	DAP10[112]	Most circulating[112]
NKG2C	Activating Receptor (complex with CD94)	HLA-E[113,114]	DAP12[115]	Small populations, CMV seropositive+ [116]
CD16	ADCC Receptor[117-119]	IgG[118]	CD3ζ[120]	$CD56^{Dim}$>$CD56^{Bright}$[58]
KIR2DS1 KIR2DS4 KIR3DS1	HLA-specific NK Receptors	HLA-C2[121] HLA-Cw4[122] HLA-A*11[123] Bacterial RecA[124] HIV[125], HLA-Bw4[126] HCV, HLA-F[125]	DAP12[115]	Stochastic[127]
KIR2DL4	HLA-specific NK Receptor	HLA-G[128]	FcεRIγ[129]	Most circulating [128]

Chapter 2 Phospholipase-Cγ

Section 2.1 Phospholipase-C Signaling

Humans express thirteen isozymes of phospholipase-C enzymes grouped into β, -γ, -δ, -ε, -η, and -ζ families depending on sequence, domain structure, and regulation[130-139]. This diverse family of enzymes links a variety of cell surface receptors to downstream cellular functions, united by their common catalytic function of converting phosphatidylinositol 4,5-bisphosphate (PIP_2) at the cell membrane into 1,4,5-trisphosphate (IP_3) and diacylglycerol (DAG)[130,140]. The canonical cascade of phospholipase-C activation results in the release of endoplasmic reticulum stored calcium as well as the influx of extracellular calcium through calcium release activated channels (CRAC) such as ORA1 and ORA2[141]. The cell type and signaling context determines the consequence of this activation; however, the role of calcium as a second messenger is well established in a wide number of processes ranging from the stimulation of cell growth and proliferation to cellular motility to lymphocyte activation[142].

Nearly all isozymes in the phospholipase-C family contain a common set of domains including a 1) N-terminal Plecktstrin homology (PH) domain functioning to bind PIP_2, PIP_3 or Rac GTPases[143-147], 2) EF-hand domains enabling catalysis[148], membrane targeting[149] or G-protein dependent signaling[150], and 3) a calcium-binding C2 domain critical for the structural stabilization of the X/Y boxes of the catalytic triose phosphate isomerase (TIM) domain[144,151,152]. Beyond this common core of catalytically critical domains, each isozyme within the phospholipase-C family contains a unique set of regulatory domains that enables their specific activities.

Phospholipase-C-gamma (PLCγ) isozymes are unique within the family for their additional split PH domain, tandem Src homology 2 (SH2) domains and a Src homology 3 (SH3) domain that allows for interaction with specific receptor tyrosine kinases and scaffolding molecules. The split PH domain enables phosphorylation-independent Rac GTPase activation of PLCγ (specifically *PLCG2* more so than *PLCG1*)[153–155]. The two SH2 domains of PLCγ consist of a N-terminal SH2 (nSH2), enabling binding to the lymphocyte scaffold protein LAT[69,156,157] and an autoinhibitory C-terminal SH2 (cSH2)[158] which may also enable protein-protein contacts critical for signalosome assembly[159]. Meanwhile, the SH3 domain allows for interaction of PLCγ with SLP-76, completing the T and NK cell receptor signalosome composed of PLCγ, LAT, SLP-76 and the SLP-76 adaptor Gads[160].

The association of PLCγ with either receptor tyrosine kinases or with signalosome-recruited Tec kinases (such as Itk or Btk) results in the tyrosine phosphorylation of PLCγ kinases at multiple sites[161,162]. These sites in *PLCG1* include Tyr771, Tyr775, Tyr783, and Tyr1254. The interaction of Tyr783 is critical for rearrangement of the autoinhibitory cSH2 domain and subsequent association of the X and Y catalytic domains[161,163,164]. The analogous site in *PLCG2*, Tyr759, is likely similarly regulated, although phosphorylation of both Tyr753 and Tyr759 are required for optimal *PLCG2* signaling in B cells[165].

While *PLCG1* is ubiquitously expressed, *PLCG2* is restricted to the hematopoietic lineage[166]. T cell receptor (TCR) signaling appears largely unrestricted in its use of either *PLCG1* or *PLCG2* for signal transduction, although *PLCG1* is traditionally thought of as the key molecule in TCR activation. Contrastingly, B cell receptor signaling has long been known to be specifically

dependent upon *PLCG2* signaling[167,168]. In contrast to the nSH2 and SH3 domains binding to LAT and SLP-76, respectively, in TCR signaling, B cell receptor (BCR) signaling requires the cSH2 and C2 domain interfaces of *PLCG2* to associate with BLNK and the B cell signalosome[168]. Thus, unique features of these domains in *PLCG2* versus *PLCG1* may engender this process to the former isozyme. Moreover, unlike *PLCG1*, *PLCG2* is uniquely able to engage Rac through the split PH domain and this interaction is required for optimal BCR signal transduction[168,169].

As described in chapter 1, *PLCG2* is also critical to NK cell function; however, the use of *PLCG1* or *PLCG2* in NK cells is most likely NK cell receptor dependent. Canonical NK receptors such as NKp46 use a signaling cascade closely related to TCR signaling and likely are unrestricted in their use of either isozyme. Certain receptors such as NKG2D use a Vav2/3-Rac-mediated signal transduction that, similar to BCR signaling, may require the split PH domains of *PLCG2* to associate and optimally activate catalytic function[67]. However, a clear mechanism for why NK cell function is more dependent upon *PLCG2* than *PLCG1* is not clear.

PLCG2 expression is not solely restricted to B, T, or NK cells. A number of other cell types use and require *PLCG2* for function. Macrophages require *PLCG2* for trafficking of Toll-like receptor 4 (TLR4) to the endosomes and optimal interferon regulatory factor 3 (IRF3) activation to sense virally derived nucleic acids[170]. *PLCG2* is also required downstream of M-CSF receptor signaling for optimal monocyte differentiation, as well as downstream of IL-3 and GM-CSF signaling in hematopoietic development[171,172]. Platelet adhesion downstream of glycoprotein Ib (GPIb)-von Willebrand factor complex signaling is also dependent upon *PLCG2*[173]. RANKL-induced activation of osteoclasts is also specifically dependent on *PLCG2*, and this restriction of RANKL

signaling to *PLCG2* also applies to RANKL regulation of lymphatic architecture[174], demonstrating a wide range of functions uniquely dependent on this gene.

A schematic representation and a summary of the known domain structures and functions of *PLCG2* are included in figure 2.1 and table 2.1, respectively.

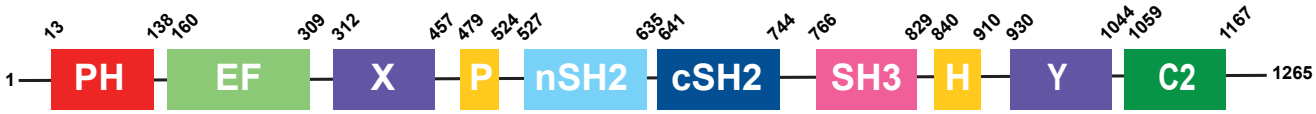

Figure 2.1 Phospholipase-C-γ2 Domain Structure

The human *PLCG2* sequence was analyzed using IntroPro protein sequence analysis and classification software[160]. Abbreviations: PH, Plecktstrin homology. SpPH, split Plecktstrin homology. SH2, Src homology.

Table 2.1 Phospholipase-Cγ2 Interpro-Predicted Domain Structure

***PLCG2* Domain**	**Amino Acid Residues**	**Function**
PH Domain	13-138	PIP_2, PIP_3 or Rac GTPase binding[143-147]
EF Hand	160-309	Supports catalytic domain structure[148], membrane targeting[149] and G-protein dependent signaling[150]
TIM, X-Box	312-457	PIP_2 Catalysis
N-terminal SpPH	479-524	Phosphorylation-independent Rac GTPase activation of PLCγ
N-terminal SH2	527 - 635	Binding to lymphocyte LAT[69,156,157]
C-terminal cSH2	641 - 744	Autoinhibitory[158] B cell signalosome assembly[159].
SH3	766 - 829	SLP-76 binding[175]
C-terminal SpPH	840-910	Same as N-terminal SpPH
TIM, Y-Box	930 - 1,044	PIP_2 Catalysis
C2 Domain	1,059 - 1,167	Structural stabilization of the X/Y boxes of the catalytic domain[144,151,152]

Table 2.1 Legend

The human *PLCG2* sequence was analyzed using IntroPro protein sequence analysis and classification software[160]. Abbreviations: PH, Plecktstrin homology. TIM, triose phosphate isomerase. SpPH, split Plecktstrin homology. SH2, Src homology.

Section 2.2 Mouse Models of Phospholipase-C

Although mice homozygous for *Plcg1* are embryonically lethal, dying at embryonic day 9[176], *Plcg2* knockout mice develop normally and serve as an important tool for the study of *Plcg2* in immune function. These mice were first reported to have defects in B cell development and function[177]; however, subsequent studies also described defects in NK cell cytotoxicity[178,179], lymphatic development[174], male fertility[180], and osteoclastogenesis[174]. Consistent with the role of *Plcg2* in signaling, mice deficient in *Plcg2* have decreased calcium flux after BCR stimulation leading to a reduction in B cell development and function, impairing the humoral response. Two groups subsequently described the role of *Plcg2* in NK cells, demonstrating the absolute requirement for *Plcg2* in murine NK cells. Colonna et al. described that murine NK cells express trivial amounts of *Plcg1*[178], and NK cells deficient for *Plcg2* thus have reductions in cytotoxicity, activating receptor induced cytokine secretion, and susceptibility to MCMV in vivo. Colucci et al. later mechanistically attributed this to a defect in NK cell activating receptor calcium flux which led to decreased malignant and virally infected cell clearance, but did not affect either NK cell development or NK cell-target conjugate formation[179].

Several N-ethyl-N-nitrosourea (ENU) mutagenesis studies have produced mice with spontaneous mutations in *Plcg2* that serve as an interesting study in the role of this enzyme in immune function. The first described model was the *Ali5* mouse, a mouse heterozygous[142] for a gain-of-function mutation in *Plcg2* at D993G[181]. This gain-of-function mutation led to severe spontaneous inflammation and autoimmunity in this model. Somewhat paradoxically, these mice were later found to be resistant to an experimental model of *Helicobacter*-induced mucosa-associated lymphoid tissue (MALT) lymphoma, possibly as a result of increased regulatory T cell (Treg)

numbers and a decrease in proinflammatory cytokine after infection, compared to wild-type controls[182]. A related phenotype is seen in the *Ali14* mouse model, which are heterozygous for a distinct gain-of-function mutation at Y495C of the split PH domain of *Plcg2*, and exhibit a wide range of phenotypes from hypergammaglobulinemia to infertility[142]. Contrastingly, *Queen* mice possess a heterozygous mutation at I346R of the X-box catalytic domain and have been described as having defects in B cells function, presumably as a result of a loss-of-function mutation at that position[183].

Section 2.3 *PLCG2* in Human Disease

Mutations of *PLCG2* in humans have been previously reported as well and are summarized in table 2.2. Somatic mutations of *PLCG2* have been reported in chronic lymphocytic leukemia treated with the Btk kinase inhibitor Ibrutinib[184]. The canonical Ibrutinib *PLCG2* escape mutant, R665W, confers a Btk-independent gain-of-function mutation; however, other mutations have been reported at P664, P665, S707, L845, D993, D140 and M1141[185-187]. Indeed, nearly 80% of patients with progressive CLL have mutations in *PLCG2*, demonstrating the importance of *PLCG2* in Btk signaling and B cell development[185,187].

The first germline mutations of *PLCG2* was reported in 2012 by Milner et al. in a cohort of 27 patients with fully penetrant cold urticaria, as well as varying degrees of recurrent sinopulmonary infections, antibody deficiency, autoimmune disease, and allergic disease[188-190]. In these patients with PLAID (*PLCG2*-associated antibody deficiency and immune dysregulation), deletions of either exon 19 or exons 20-22 result in the deletion of portions of the autoinhibitory C-terminal SH2 (cSH2) domain and SH3 domain. Intriguingly, while these mutations resulted in reduced calcium flux at physiological temperatures, cold temperatures result in increased mast cell

degranulation due to a temperature sensitive gain-of-function mechanism with these deletions. Though this gain-of-function is likely due to the loss or dysfunction of the autoinhibitory cSH2 domain, the loss-of-function phenotype was described in a later study to be the result of a deletion of an interaction surface on the cSH2 domain critical for B cell signalosome assembly, resulting in dominant-negative inhibition of B cell signaling[159].

The second inherited syndrome involving *PLCG2* was reported later the same year, this time involving a dominantly inherited autoinflammatory disease involving blistering skin lesions, granulomatous inflammation, lung disease, ocular inflammation, arthralgias, enterocolitis, and mild antibody deficiency[191]. Whole exome sequencing identified a heterozygous point mutation at a highly conserved site, S707Y in the cSH2 domain that, unlike PLAID, conferred gain-of-function activity even at physiologic temperatures. This gain-of-function activity was hypothesized then to lead to increased lymphocyte and neutrophil activation resulting in non-specific autoinflammation and the syndrome was coined APLAID (autoinflammation and *PLCG2*-associated antibody deficiency and immune dysregulation). The mild immunodeficiency, which presented in the form of decreased circulating memory B cells and immunoglobulins, is hypothesized to be the result of substrate-depletion and tachyphylaxis, though this mechanism has not been experimentally tested. An additional patient with inflammatory lesions, uveitis, interstitial lung disease and IBD was also later described with a novel mutation in *PLCG2* at L848P[192]. Recently, other mutations in patients with APLAID-like disease have been reported at R730K, N798S, and M1141L, demonstrating that mutations in other domains may also result in APLAID (personal communication with Ivona Aksentijevich).

Rare variants in *PLCG2* have also been implicated as a protective variant in Alzheimer's disease. Along with the microglial receptor *TREM2*, patients with a mutation at P522R in *PLCG2* are protected from Alzheimer's with an odds-ratio of 0.68[193]. Although this mutation lies within an interdomain region between the split-PH and nSH2 domain, functional characterization of this mutant show a weak hypermorphic phenotype, possibly leading to increased microglial activation and thus potential clearance of amyloid plaques[194]. However, the exact mechanism of this protection has not been thoroughly explored and thus remains to be seen. Known mutations in both mouse and human *PLCG2* are summarized in table 2.2.

Table 2.2 Reported Mutations in PLCγ2

Species	Mutation	Name	Type	Domain	Mechanism	Phenotype
Mouse	D993G[181]	*Ali5*	Germline	X-box	GOF	Autoinflammation and autoimmunity, MALT lymphoma resistance[182]
	Y495C[142]	*Ali14*	Germline	spPH	GOF	Inflammatory arthritis and infertility[142]
	I346R[183]	*Queen*	Germline	TIM-Barrel	Unknown	Reduced T-independent IgM response[195]
Human	P664S[186] P665W[186] S707Y[186] ΔS707-A708[186] L845F[186,187] D993Y[185]		Somatic	cSH2 cSH2 cSH2 cSH2 spPH Y-Box	Unknown	Ibrutinib resistance in Chronic Lymphocytic Leukemia
	ΔW646-R685[188] ΔY686-W806[188]	PLAID	Germline	cSH2	LOF & GOF	Cold urticaria, antibody deficiency, allergic disease, autoimmunity
	S707Y[191] L848P[192]	APLAID	Germline	cSH2 spPH	GOF	Granulomatous inflammation, inflammatory bowel disease, uveitis, arthralgias, antibody deficiency
	P522R		Germline	nSH2	GOF	Protective variant in Alzheimer's disease[194]

Table 2.2 Legend
Previously reported mutations in mouse and human PLCγ2 are summarized. Abbreviations: GOF, Gain-of-function. LOF, Loss-of-function. PLAID, PLCγ2-associated antibody deficiency and immune dysregulation. APLAID, autoinflammation and PLCγ2-associated antibody deficiency and immune dysregulation. spPH, split Pleckstrin homology domain. cSH2, C-terminal Src homology domain. nSH2, N-terminal Src homology domain.

Chapter 3: Human *PLCG2* Haploinsufficiency is a Novel NK Cell Immunodeficiency

Joshua B. Alinger[1], Emily M. Mace[3,7], Justin. R. Porter[2], Annelise Y. Mah[1], Allyssa L. Daugherty[1] , Li Stephanie[1], Allison A. Throm[1], Jeanette T. Pingel[1], Nermina Saucier[1], Albert Yao[1], Ivan K. Chinn[3], James R. Lupski[4], Mohammad Ehlayel[5], Michael Keller[6], Greg R. Bowman[2], Megan A. Cooper[1], Jordan S. Orange[3,7], Anthony R. French[1*]

[1]Division of Rheumatology, Department of Pediatrics, St. Louis Children's Hospital, Washington University School of Medicine. St. Louis, MO, USA.

[2]Department of Biochemistry and Molecular Biophysics, Washington University School of Medicine. St. Louis, MO, USA.

[3]Department of Pediatrics, Baylor College of Medicine; Center for Human Immunobiology, Texas Children's Hospital. Houston, TX, USA.

[4]Department of Molecular and Human Genetics, Baylor College of Medicine, Texas Children's Hospital. Houston, TX, USA.

[5]Hamad Medical Center. Doha, Qatar.

[6]Children's National Medical Center, Washington DC, USA.

[7]Department of Pediatrics, Vagelos College of Physicians and Surgeons, Columbia University, New York, NY, USA.

Abstract

Although most individuals effectively control herpesvirus infections, some suffer from unusually severe and/or recurrent infections requiring anti-viral prophylaxis. A subset of these patients possess defects in NK cells, innate lymphocytes which recognize and lyse herpesvirus-infected cells; however, the genetic etiology is rarely diagnosed. *PLCG2* encodes a signaling protein in NK cell and B cell receptor-mediated signaling, among other cell types. Dominant-negative or gain-of-function mutations in *PLCG2* cause cold urticaria, antibody deficiency, or autoinflammation. However, loss-of-function mutations and *PLCG2* haploinsufficiency have never been reported in human disease. Using mass cytometry and whole-exome sequencing, we identified novel heterozygous mutations in *PLCG2* in two families with severe and/or recurrent herpesvirus infections. In vitro studies demonstrated that these mutations were loss-of-function and resulted in impaired NK calcium flux, granule movement, and cytotoxicity. In contrast to dominant-negative or gain-of-function *PLCG2* mutations, B cell function remained intact. *Plcg2*+/- mice, as well as targeted CRISPR knock-in mice, also displayed impaired NK cell function with preserved B cell function, phenocopying human *PLCG2* haploinsufficiency. We report the first known cases of *PLCG2* haploinsufficiency, a clinically and mechanistically distinct syndrome from previously reported mutations. Therefore, these families represent a novel disease, highlighting a role for *PLCG2* haploinsufficiency in herpesvirus-susceptible patients and expanding the spectrum of *PLCG2*-related disease.

Section 3.1 Introduction

Nearly all individuals will encounter herpesviruses such as herpes simplex virus 1 (HSV1) or cytomegalovirus (CMV) in their lifetime[196]. Although most will present with only limited recurrences, some patients will continue to have unusually severe and/or recurrent herpesvirus infections[197]. A subset of these patients possess defects in natural killer (NK) cells, innate lymphocytes which recognize and lyse herpesvirus-infected cells[2,34,198]. NK cell deficiency (NKD) can result from either aberrant NK cell development (classical NKD) or reduced NK cell function (functional NKD), typically evaluated by measuring NK cell killing and CD107 degranulation after incubation with K562 target cells[198]. Despite these diagnostic tools, there is minimal understanding of the genetics underlying functional NKD, and most patients do not receive a definitive diagnosis. Herein, we present a novel syndrome of functional NK cell immunodeficiency caused by heterozygous loss-of-function mutations in *PLCG2*.

NK cells recognize herpesvirus-infected cells using an array of germline-encoded activating receptors, such as CD16, NKG2D and 2B4[199]. Many activating receptors signal via a pathway involving Src and Syk kinases, LAT, and *PLCG2*-induced secondary messengers[199]. *PLCG2* (encoding phospholipase-C-γ2) is recruited to LAT, phosphorylated, and subsequently cleaves PIP_2 into IP_3 and DAG. This critical process initiates an increase in cytosolic calcium via both extracellular influx as well the release of intracellular calcium stores, leading to the polarized mobilization of cytotoxic granules towards the target cell[72]. *PLCG2* is expressed in hematopoietic cells and is related to the ubiquitously-expressed *PLCG1*. While *PLCG1* is sufficient for many signaling pathways including mitogen and TCR signaling, *PLCG2* is uniquely necessary for NK cell and B cell signaling, as demonstrated by their profound disruption in *Plcg2*-/- mice[178,179,200].

Although *PLCG2* is traditionally thought of as a NK- and B- cell signaling molecule, it also plays a role in several other cell types including platelets[173], neutrophils[201], monocytes, and macrophages[171].

Mutations in *PLCG2* have been previously reported in a separate domain (the C-terminal SH2 domain, cSH2), causing the syndromes PLAID and APLAID. PLAID is caused by exonic deletions compromising the cSH2 domain and results in gain-of-function at sub-physiologic temperatures[159,188,189]. At normal temperatures, PLAID acts in a dominant-negative manner to dysregulate immune signaling. While NK cell degranulation is reduced in PLAID, B cell and mast cell dysregulation underlie the predominant clinical phenotypes in these patients, including antibody deficiency and cold urticaria[159,188,189]. APLAID is caused by a constitutive gain-of-function mutation (S707Y) and results in autoinflammation and B cell immunodeficiency (perhaps as a result of substrate depletion)[191]. Herein, we demonstrate that heterozygous loss-of-function mutations in *PLCG2* result in a clinical phenotype distinct from PLAID and APLAID, extending the spectrum of disease seen with human mutations in *PLCG2*.

Section 3.2 Materials, Methods and Statistics

Data Availability Statement

With the exception of whole-exome sequencing data, the distribution of which may compromise research participant privacy and/or consent, the data that support the findings of this study are available from the corresponding author upon reasonable request.

Patients and Sample Collection

All human samples were obtained using written informed donor consent and were used with the approval of either the Washington University School of Medicine Institutional Review Board or the Baylor College of Medicine Institutional Review Board for the Protection of Human Subjects. All samples were obtained in compliance with the Declaration of Helsinki. Peripheral blood mononuclear cells (PBMC) were isolated by density centrifugation over Ficoll-Paque according to manufacturer's instructions prior to liquid nitrogen cryopreservation in fetal bovine serum and DMSO.

Animal Studies

Plcg2 mice were generated by Jim Ihle (St. Jude Children's Research Hospital)[200] and backcrossed onto a B/6 background for 10 generations by Marco Colonna (Washington University)[178]. Mice were maintained under specific pathogen–free conditions and used between 8 and 14 weeks of age. Mouse experiments were performed in both male and female mice with equivalent results. All experiments were approved and conducted in accordance with Washington University Animal Care and Use Committee guidelines for animal care and use.

Exome Sequencing

For kindred A, exome sequencing was performed as previously described[202]. Briefly, genomic DNA was extracted from whole blood or saliva and coding regions enriched using SureSelect All Exon (Agilent Technologies) followed by next-generation sequencing (Illumina) at St. Louis Children's Hospital through the Genome Technology Access Center at Washington University. For kindred B, whole exome sequencing was performed on genomic DNA by Baylor Genetics as

previously described[203,204]. After quality control, alignment and variant calling, exome data was analyzed using institution-specific pipelines to identify potential variants. Medium or high impact variants (i.e. non-synonymous changes, early stops, frameshifts and splice site mutations) with minor allele frequencies less than 0.01 in ExAC[205] were prioritized and potential variants were cross-referenced between kindreds. Both kindreds were negative for variants in known genes associated with immunodeficiency and immunodysregulation[206], including HLH mutations[207] and NK cell associated mutations in MCM4, GATA2, IRF8, FCGR3A (CD16) and KLRC2 (NKG2C)[35-37,198,208].

Transfection Experiments

293T cells (ATCC CRL-3216) were cultured in Dulbecco's modified eagle media supplemented with 10% fetal bovine serum. Cells were transfected with a mammalian expression vector driven under MND promoter containing N-terminal FLAG tagged PLCG2 (WT or relevant mutation) using Lipofectamine LTX (Invitrogen) and incubated for 24 hours. Cells were then stimulated with 100□M pervanadate and either lysed with RIPA buffer or fixed using 1.6% formaldehyde 15 minutes post-stimulation. Western blot analysis of protein expression was performed using anti-FLAG (Sigma, clone M2) or Actin (Santa Cruz Biotechnology, clone C-11). PLCG2 phosphorylation was analyzed by flow cytometry as described below using PE anti-PLCG2 Y759 (clone K86-689.37, BD).

NK Cell Cytotoxicity Assays

PBMCs isolated as described above were thawed and allowed to rest for 1 hour in Roswell Park Memorial Institute (RPMI) media supplemented with 20% FBS, pyruvate, non-essential amino

acids, glutamine and HEPES. Cells were then seeded into 96 well U-bottom plates along with CellTrace Violet (Invitrogen) labeled K562 (ATCC, CCL-243) tumor target cells at a PBMC:K562 ratio of 50:1. After incubation for 4 hours, 7-AAD (BD) was added and target cell death was quantified using flow cytometry. Mouse NK cell assays were performed similarly except that NK cells were isolated from spleen using EasySep Mouse NK Cell Enrichment (Stem Cell Technologies) and then mixed with CellTrace Violet labeled YAC-1 (ATCC, TIB-160) or RMA-S cells (kind gift from Wayne Yokoyama).

Microscopy

For analysis of NK-target cell conjugates, fixed cell confocal microscopy was performed using patient NK cells and K562 erythroblast target cells. $3x10^6$ PBMC from patient or heathy donor were incubated with K562 target cells for 45 minutes then fixed, permeabilized and stained with anti-perforin Alexa Fluor 488 (clone dg9), anti-tubulin biotin followed by Pacific Blue conjugated streptavidin, and phalloidin Alexa Fluor 568. Images were acquired on a Zeiss AxioPlanII with a Yokogawa CSU-10spinning disk and Hamamatsu ORCA-ER camera. Excitation lasers (405 nm, 488 nm, 561 nm, 647 nm) were merged through a Spectral Applied Research laser merge. Images were taken throughout the volume of cell conjugates using 0.5μm steps. Acquisition and analysis were performed using Velocity software (PerkinElmer). For measurement of actin accumulation, analysis was performed as described previously[209]. Briefly, area and intensity of F-actin at the immunological synapse were measured for a defined area. Cortical F-actin intensity from both NK and target cells was subtracted from this measurement to generate a quantitative measure of specifically accumulated actin at the synapse. For MTOC polarization, MTOC were defined as the highest intensity staining of α-tubulin and the distance between this and the center of the

immunological synapse was measured for 30 conjugates each from patient and healthy donor. Granule convergence was analyzed as previously described[210]. Distance between individual lytic granules and the MTOC were measured and the mean of these was calculated for each cell.

Mass Cytometry

Mass cytometry is a high-dimensional single cell analysis technique based on flow cytometry but differs in its use of metal tagged antibodies in lieu of fluorophores. Procedure performed as described previously[211,212] and acquisition was performed using a CyTOF instrument (Fluidigm). Data was analyzed and viSNE was performed using Cytobank[213,214]. Briefly, for the panel in table 3.2, PBMCs were isolated, thawed and rested as detailed above. Cells were stained with cisplatin to track cell viability. Between $1x10^6$ and $3x10^6$ PBMCs per time point were stained with metal conjugated extracellular antibodies (Fluidigm), seeded in 96-well U bottom plates and stimulated with either a cocktail of A) 500U/mL IFNα (Peprotech), 500ng/mL LPS (Invivogen), 50ng/mL IL-12 (Peprotech), and 500U/mL IL-2 (Proleukin), and CD16/CD3/IgM crosslinking (using surface staining antibodies followed by anti-mouse IgG, Biolegend) for 0, 3 and 15 minutes. Cells were then fixed in 1.6% formaldehyde and permeabilized in 100% methanol. After washes, intracellular staining was performed before DNA staining using Cell-ID Intercalator-Ir (Fluidigm). For the panel in table 3.3, cells were stained with cisplatin to track cell viability. Between $1x10^6$ and $3x10^6$ PBMCs were unstimulated or mixed with 1:1 K562 cells and 500U/mL IL-2 (Proleukin) in the presence of GolgiStop (BD), GolgiPlug (BD) and metal-conjugated CD107 antibody (Fluidigm). Cells were then stained with conjugated extracellular antibodies (Fluidigm) or antibodies conjugated to the desired metal using Maxpar Antibody Labeling Kit (Fluidigm). Cells

were fixed in CytoFix/CytoPerm (BD), washed in Perm Buffer (eBioscience) and stained with intracellular antibodies before DNA staining using Cell-ID Intercalator-Ir (Fluidigm).

Flow Cytometry

Where indicated, flow cytometry was performed using either surface staining alone at room temperature for 15 minutes or surface staining in combination with methanol permeabilized intracellular staining at room temperature for 60 minutes before acquisition using a Fortessa X-20 (BD). Data analysis performed using Cytobank[214] or FlowJo. Human antibodies used in this study: APC CD56 (clone 5.1H11, Biolegend), Pacific Blue CD3 (clone OKT3, Biolegend), APC Cy7 CD14 (Clone HCD14, Biolegend), FITC NKG2D (clone 1D11, Biolegend), FITC CD16 (clone 3G8, BD), PE NKp44 (clone P-44-8, Biolegend), PE 2B4 (clone C1.7, Biolegend), PE-Cy7 CD19 (clone HIB19, Biolegend), APC IgM (clone MHM-88, Biolegend), APC-Cy7 HLA-DR (clone L243, Biolegend), and Alexa Fluor 488 total PLCG2 (clone K86-1161, BD). Mouse antibodies used in this study: BV786 CD45 (clone 30-F11, BD), BV421 NK1.1 (clone PK136, BD), BV510 IgM (clone R6-60.2, BD), FITC CD11b (clone M1/70, Biolegend), PE-Cy7 CD27 (clone LG3A10, Biolegend), PE CD4 (clone GK1.5, Biolegend), PerCP IgD (clone 11-26c.2a, Biolegend), APC B220 (clone RA3-6B2, BD), APC-Cy7 CD3 (clone 17A2, Biolegend), APC-R700 CD8 (clone RPA-T8, BD), FITC CD43 (clone S11, Biolegend), PE CD24 (clone 30-F1, Biolegend), PE-Cy7 CD11b (clone M1/70, BD), PE Ly49H (clone 3D10, BD), and APC-Cy7 CD19 (clone 1D3, BD).

ELISA

Human serum IgG and IgM levels were analyzed using commercially available ELISA kits (Invitrogen) according to manufacturer instructions. Briefly, ELISA plates were coated with capture antibody overnight before washing, blocking and incubation with diluted patient sera or standard. Plates were then washed again, incubated with HRP-conjugated detection antibody, washed again and incubated with TMB substrate solution. Solution was then stopped with 1M phosphoric acid and absorbance was measured at 450nm.

Calcium Flux Analysis

For human samples, NK cells were enriched using RosetteSep Human NK Cell Enrichment (Stem Cell Technologies). 1-2x10^6 enriched NK cells were then loaded with Indo-1 dye (Invitrogen) and labelled with PE or FITC conjugated mouse IgG antibodies against the NK cell receptors 2B4 and NKG2D. Kinetic measurements of calcium flux were obtained using a BD Fortessa X-20 at baseline and then upon antibody crosslinking using anti-mouse IgG. Mouse calcium flux analysis was similarly performed: NK cells were isolated from spleen using EasySep Mouse NK Cell Enrichment (Stem Cell Technologies), loaded with Indo-1, labelled with APC NK1.1 followed by crosslinking and acquisition as above. Patient B.II.4 was performed similarly except that expansion beforehand was required due to limited patient sample and anti-NKp44 and anti-NKG2D were used for crosslinking. NK cells were expanded as previously described[215]. Briefly, 10^6 PBMCs from patient B.II.4 or healthy control were co-incubated with 10^6 irradiated (100Gy) K562-mbIL15-41bbl (Kind gift from Dario Campana, National University of Singapore) for 7 days. After 7 days, cells were removed and assessed for purity. T cells ($CD3^+$) were present at less than <1%. 100U/mL of recombinant IL-2 (Proleukin) was added to the culture and incubated for 7 more days

with partial media exchange every 2 days. After 14 days total, NK cells expanded 10 to 15-fold with >95% purity ($CD56^+CD3^-$) and were then used for cytotoxicity and calcium flux assays. For murine B cell calcium flux analysis, naive B cells were gated on whole splenocytes ($B220^+CD27^-$) and treated as above, with the exception of using anti-mouse IgM as the crosslinking antibody. Human B cell calcium flux analysis was performed from PBMCs (gated as CD19+) with the exception of using anti-human IgM as the crosslinking antibody.

Statistics

Normal internal reference ranges for human NK cell cytotoxicity and mass cytometry were determined using 25 healthy controls; outliers were removed using ROUT (Robust regression and Outlier removal) and the central 95th percentile was determined. Upper and lower bounds are visualized by dashed lines. Unless normality was established after D'Agostino & Pearson omnibus test for normality, pairwise comparisons are made using Mann-Whitney U test with Bonferroni correction for multiple comparisons Where noted, comparisons between healthy controls and patients are performed using age and gender matched healthy control donors. All statistics performed using Graphpad Prism.

Molecular Dynamics, Structural Analysis, and Conservation Analysis

Structural diagrams were generated using PyMOL v2.0 (PyMOL Molecular Graphics System). Conservation analysis of the G595 and L183 residues were generated using M-Coffee with ESPript secondary structure analysis[216-218]. For molecular dynamics, 134.9μs of aggregate simulation time of the SH2 domain (107 aa) with wild-type (69.4μs) and G595R mutant (65.5μs) sequences was ran with GROMACS 2016.1 at 300K using the AMBER03 force field with explicit TIP3P

solvent[219-221]. Salt was added to neutralize the system and create a solution concentration of 100mM (13 Na^+/14 Cl^- for wild-type, 16 Na^+/18 Cl^- for G595R). Simulations were prepared by placing the starting structure for each sequence in a dodecahedron box that extended 1.0Å beyond the protein in any dimension. Each system was then energy minimized with the steepest descent algorithm until the maximum force fell below 100 kJ/mol/nm using a step size of 0.01 nm and a cutoff distance of 1.2 nm for the neighbor list, Coulomb interactions, and van der Waals interactions. For production runs, all bonds were constrained with the LINCS algorithm and virtual sites were used to allow a 4fs time step[222]. Cutoffs of 1.0 nm were used for the neighbor list, Coulomb interactions, and van der Waals interactions. Before being run in production, systems were equilibrated with position restraints for all heavy atoms for 1ns. The Verlet cutoff scheme was used for the neighbor list. The stochastic velocity rescaling (v-rescale) thermostat was used to hold the temperature at 300 K. Conformations were stored every 10ps[223]. The initial structure for both simulations was a homology model of Swiss Model threading the human PLCG2 sequence onto 4EY0, a crystal structure of the close human paralog, *PLCG1*[224]. The human paralog was used (rather than the murine homolog) because the crystal structure contains both nSH2 and cSH2 domains and so provided more information about the course of the C-terminal amino acids of the nSH2 domain than the murine homolog structure 2DX0[225]. A microstate decomposition was built using khybrid clustering with a radius of 1.5Å and 5 rounds of kmedoids updates on the entire 135μs dataset using backbone atoms (C, $C\alpha$, N, O) and $C\beta$ (except residue 595) to produce 2314 states[226]. Using the cluster centers derived in this way, the data for the wild-type and the mutant was reassigned separately and generated separate Markov state models on this shared state space. Transition probabilities were fit with the transpose method[227]. The state space had near complete coverage for

both sequences with the wild-type sampling 2204/2315 states and the mutant sampling 2150/2315 states. The lagtime was 1.5 ns and was determined using the implied timescales test.

Section 3.3 Heterozygous *PLCG2* Mutations in Functional NK Cell Disorder Patients

We identified patients from two unrelated nonconsanguineous families with autosomal dominant immunodeficiency, characterized by recurrent infections and reduced NK cell killing. In family A (Figure 3.1A), patient A.I.2 is a CMV/HSV1-seronegative 52-year-old Caucasian female with a history of arthralgias, antiphospholipid syndrome, and late-onset recurrent *Staphylococcal* septicemia. Her daughter, A.II.3, is a 19-year-old female with a history of arthralgias and autoimmunity (positive antinuclear antibody and type 1 diabetes), as well as recurrent HSV1 gingivostomatitis requiring prophylactic valacyclovir. Family B (Figure 3.1B) consists of patient B.II.4, a 9-year-old Qatari male with a history of CMV myocarditis, as well as adenoviral hepatitis. There was no history of immunodeficiency or autoimmunity in any other family members. Clinical NK cell testing in both families revealed reduced NK cell K562 killing, despite intact CD107 degranulation against K562 cells and normal cytotoxic granule contents (Figure 3.1C, Table 3.1). Flow cytometry of peripheral blood demonstrated normal NK cell percentages and absolute counts inconsistent with classical NKD (Figure 3.1D, Table 3.1). Further clinical immunology evaluation of immunoglobulin levels (IgM, IgG, IgA, and IgE), protective antibody titers, T cell mitogen stimulation, and immune subpopulation analysis was also unremarkable (Table 3.1)

Patients and unaffected relatives underwent whole-exome sequencing which revealed novel heterozygous *PLCG2* missense variants. Patients A.I.2 and A.II.3 possessed heterozygous mutations (c.1783G>A, p.G595R) in *PLCG2*, located in the N-terminal SH2 domain (nSH2). An

additional healthy HSV1-seropositive 17-year-old sibling (A.II.2) with the mutation was identified; however, her borderline-normal NK cell killing suggests incomplete penetrance, a common feature of autosomal dominant immune syndromes[228]. Patient B.II.4 possessed a different heterozygous mutation in *PLCG2* (c.547C>T, p.L183F), located in the N terminus of *PLCG2,* within EF-hand domains, which, along with the nearby PH domain, is responsible for membrane localization in the phospholipase-C family[149,229]. Patient B.I.1 also possessed this mutation but was not available for evaluation. The locations of these mutations and other reported *PLCG2* mutations are diagrammed in Figure 3.1E.

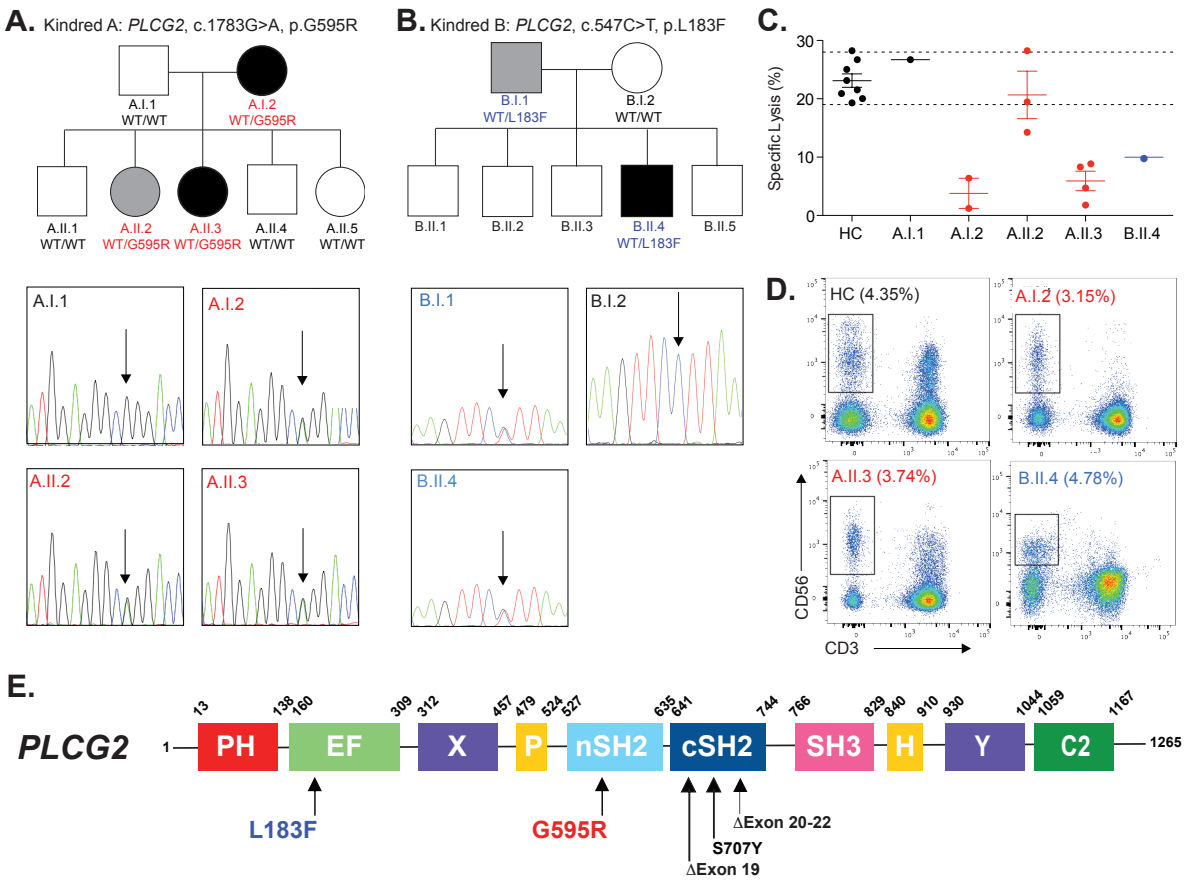

Figure 3.1: Familial NK Cell Deficiency Associated with Novel Heterozygous *PLCG2* Mutations

(A) Pedigree of family A; affected heterozygotes are shown in black symbols while unaffected or unevaluated heterozygotes are shown in gray or white, respectively. WT, wild-type allele. Sanger-sequencing chromatograms are shown for patients and unaffected relatives. Arrow denotes site of heterozygosity. (B) Pedigree and sanger sequencing of family B is displayed as in subfigure A. (C) NK cell killing against K562 cells is quantified after incubation for four hours at a peripheral blood mononuclear cell (PBMC) to K562 ratio of 50:1. Upper and lower internal reference ranges are displayed with dashed lines. See supplementary appendix for generation of reference ranges. Each point represents a unique biologic replicate, either a separate blood draw (patients) or a separate individual (controls). (D) Flow cytometry evaluation of NK cells ($CD3^-$ $CD56^+$) in healthy control (HC) versus patients A.I.2, A.II.3 and B.II.4. Percentage of NK cells in the lymphocyte gate is displayed. Internal normal NK cell reference range, 2.8% to 15.5%. (E) The location of variants, including previously reported PLAID (Exon 19 or 20-22 deletions) and APLAID (S707Y) variants are displayed with the domain structure of *PLCG2*. PH, Pleckstrin homology; nSH2, N-terminal Src Homology 2; cSH2, C-terminal SH2; SH3, Src Homology 3. Except where limited by patient sample availability (B.II.4 in subfigures C and D), all data is representative of two or more independent experiments. All error bars represent standard deviation from the mean.

Table 3.1: Clinical Characteristics and Phenotypes of *PLCG2* Haploinsufficiency Patients

	Patient A.I.2	**Patient A.II.3**	**Patient B.II.4**
Mutation	G595R	G595R	L183F
Absolute Lymphocyte Count*	Normal	Normal	Normal
Absolute Neutrophil Count*	Normal	Normal	Normal
Herpesvirus Infections	None	HSV1 Gingivostomatitis	CMV Myocarditis
Bacterial Infections	Recurrent Sepsis	None	None
Hepatitis, Unknown Origin	Negative	Negative	Positive
HSV1 Serology*	Negative	Positive	Negative
CMV Serology*	Negative	Positive	Positive
Antinuclear Antibody*	Positive	Positive	Negative
Other Autoimmunity	Antiphospholipid Syn.	Type I Diabetes	None
Absolute NK Cell Count*	Normal	Normal	Normal
NK Cell Cytotoxicity*	Reduced	Reduced	Reduced
NK Cell Perforin/Granzyme*	Normal	Normal	Normal
NK Cell CD107 Degranulation*	Normal	Normal	Normal
NK Cell Maturity ($CD57^+$)	Increased	Increased	Increased
$NKG2C^+$ NK Cells	(CMV Seronegative)	Negative	Negative
Monocytes/DCs	Reduced	Reduced	Reduced
T_{FH} Phenotype	$T_{FH2}>T_{FH1}$	$T_{FH2}>T_{FH1}$	$T_{FH2}>T_{FH1}$
B Cell Count*	Reduced	Reduced	Normal
Class Switched Memory B Cells	Normal	Normal	Normal
IgA/IgG/IgM*	Normal	Normal	Normal
IgE*	Not Evaluated	Normal	Normal
Pneumococcal Antibody Titers*	Normal	Not Evaluated	Normal
T Cell Mitogen Stimulation*	Not Evaluated	Not Evaluated	Normal

*Measured in clinical laboratory

Section 3.4 Mass Cytometry Reveals Monocytopenia with Normal B and NK Cell Development

As immunodeficiencies commonly arise from aberrant immune cell development or signaling, mass cytometry (CyTOF, Table 3.2) was employed to analyze these processes in the peripheral blood. Consistent with clinical studies, NK cell abundance, as well as the distributions of immunomodulatory $CD56^{Bright}$ and cytotoxic $CD56^{Dim}$ NK cells, were intact (Figure 3.2A). Family A demonstrated reduced B cells with preserved naïve to class-switched memory B cell percentages, suggesting a defect in B cell output but not activation (Figure 3.2B). In support of this, serum immunoglobulins, seroconversion, and IgM-induced calcium flux were normal (Figure 3.2C-D, Table 3.1). Although T cell development and calcium flux were unperturbed (data not shown), the distribution of T follicular-helper cells (T_{FH}) was altered with increased T_{FH2} cells and decreased T_{FH1} cells in both families (Figure 3.3A), a pattern seen previously in human autoimmunity[230]. The abundance of monocytes and dendritic cells, but not other myeloid cells (i.e., granulocytes), was reduced in both families as well (Figure 3.3B, Table 3.1). Human monocyte activation with macrophage colony stimulating factor (MCSF) is dependent on *PLCG2* induced calcium flux, possibly contributing to the observed monocytopenia and bacterial susceptibility in patient A.1.2[171].

Table 3.2: CyTOF Panel for PBMC Subpopulation and Signaling Analysis

Antigen	Clone	Tag
CD45	HI30	089Y
CCR6	G034E3	141Pr
CD19	HIB19	142Nd
CD45RA	HI100	143Nd
pPLCG2	K86-689.37	144Nd
CD4	RPA-T4	145Nd
IgD	IA6-2	146Nd
CD11c	Bu15	147Sm
CD16	3G8	148Nd
CD127	A019D5	149Sm
pSTAT5	47	150Nd
CD123	6H6	151Eu
pAKT	D9E	152Sm
pSTAT1	58D6	153Eu
pBtk/Itk	24a/BTK	154Sm
CD27	L128	155Gd
CXCR3	G025H7	156Gd
pSTAT3	4/P-Stat3	158Gd
pMAPKAPK2	27B7	159Tb
CD14	M5E2	160Gd
CD80	2D10.4	161Dy
pLCK	4/LCK-Y505	162Dy
pJAK2	D4A8	163Dy
IkBa	L35A5	164Dy
CD45RO	UCHL1	165Ho
pNFKB	K10-895.12.50	166Er
pERK	D13.14.4E	167Er
CD8	SK1	168Er
CD25	2A3	169Tm
CD3	UCHT1	170Er
pZAP70	17a	171Yb
IgM	MHM-88	172Yb
HLA-DR	L243	173Yb
pSTAT4	38/p-Stat4	174Yb
PD-1	EH12.2H7	175Lu
CD56	NCAM16.2	176Yb
CD11b	ICRF44	209Bi

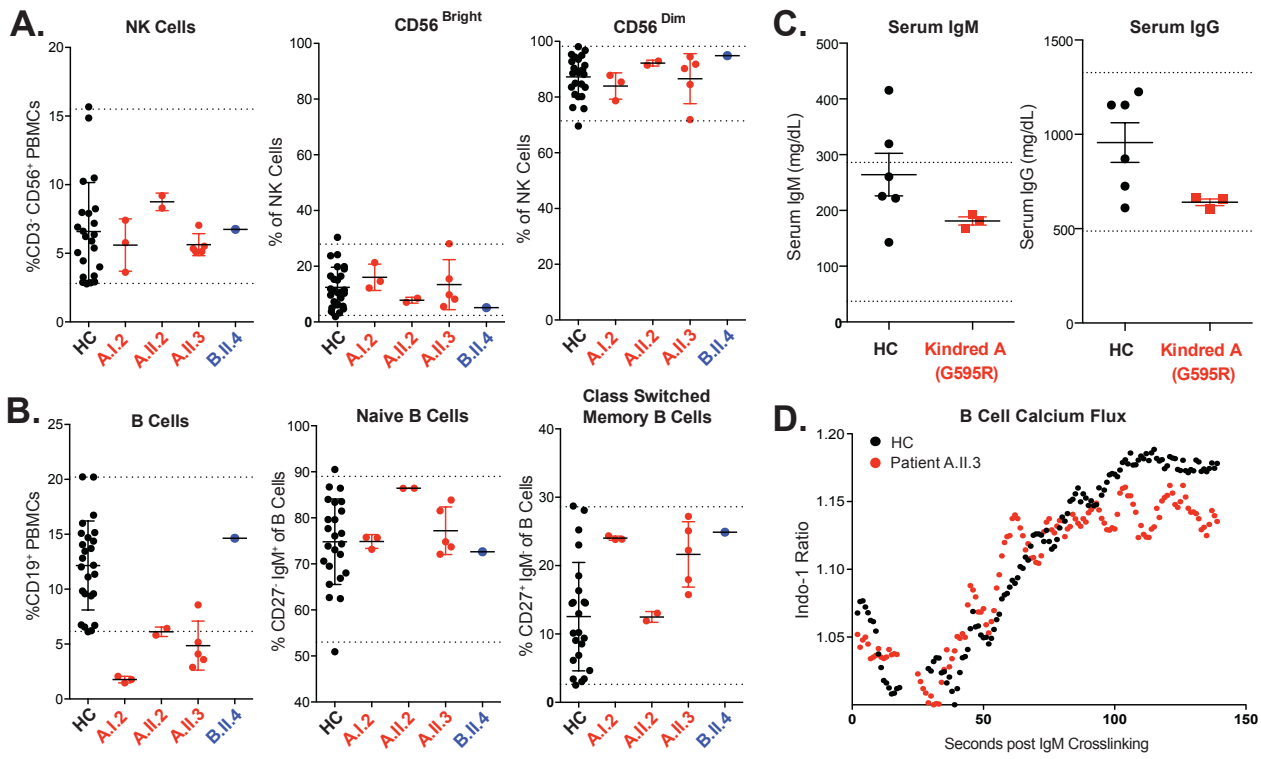

Figure 3.2: Analysis of NK Cells and B Cells in *PLCG2* Haploinsufficiency
(A) Mass cytometry was performed to quantify total ($CD3^{-}CD56^{+}$), $CD56^{Bright}$ and $CD56^{Dim}$ NK cells in the peripheral blood of HC (healthy controls), G595R patients A.I.2, A.II.2, A.II.3 and L183F patient B.II.4. Internal reference ranges are shown as visualized by dashed lines (see Methods). NK cell reference range, 2.8% to 15.5%. Each patient data point represents a unique biological replicate from a different blood draw. (B) B cells ($HLADR^{+}CD19^{+}$) are quantified and displayed as a percentage of PBMCs. Memory formation and class-switching is assessed by quantification of $CD27^{+}$ IgM^{-} cells within the B cell compartment. Normal B cell reference range, 6.2% to 20.2%. Each patient data point represents a unique biological replicate from a different blood draw. (C) ELISA quantification of serum IgG and IgM obtained from HC versus patients A.I.2, A.II.2 and A.II.3 (pooled above). Reference ranges courtesy of Mayo Clinic; IgG 487-1,327 mg/dL and IgM 37-286 mg/dL. Error bars represent standard deviation from the mean. (D) Indo-1 analysis of calcium flux in primary B cells (gated $CD19^{+}$ from peripheral blood mononuclear cells) after crosslinking with anti-IgM.

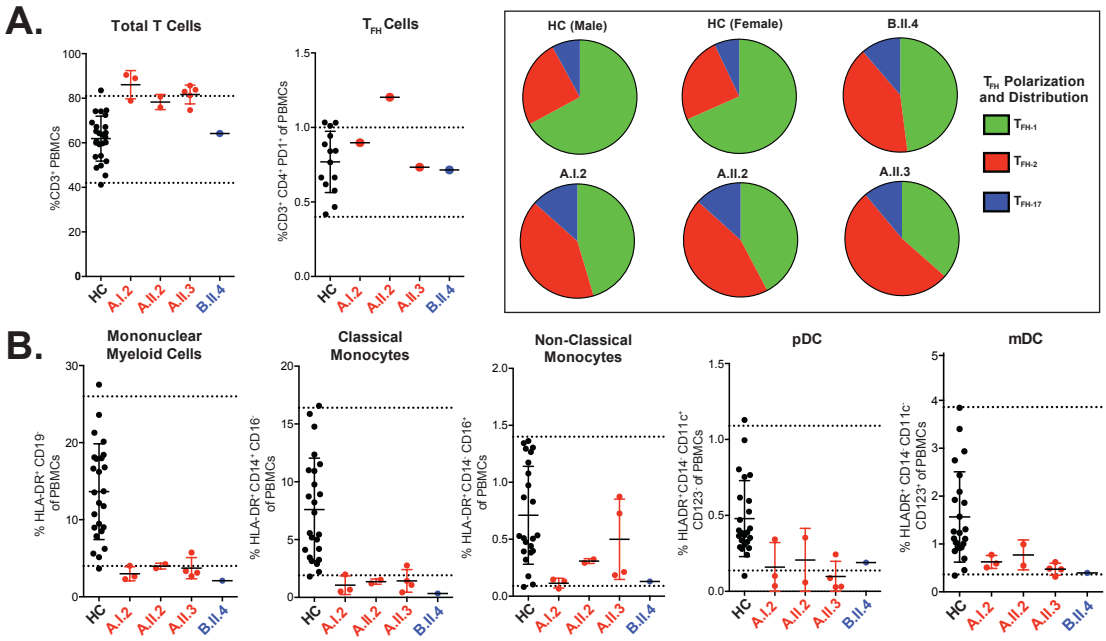

Figure 3.3: Analysis of T Cells and Myeloid Cells in *PLCG2* Haploinsufficiency

(A) Mass cytometry was performed to quantify total T cells ($CD3^+$) and T-follicular helper cells (T_{FH}, $CD3^+$ $CD4^+$ $PD\text{-}1^+$ $CCR6^-$) in the peripheral blood of HC (healthy controls), G595R patients A.I.2, A.II.2, A.II.3 and L183F patient B.II.4. Internal reference ranges are shown as visualized by dashed lines (see Methods). Each patient data point represents a unique biological replicate from a different blood draw. Error bars represent standard deviation. Distribution of polarized T_{FH} cells is graphically displayed from each patient and two HC. $T_{FH\text{-}1}$ gated from $CXCR3^+$ $CCR6^-$ T_{FH} cells, $T_{FH\text{-}2}$ gated from $CXCR3^-$ $CCR6^-$ T_{FH} cells, $T_{FH\text{-}17}$ gated from $CXCR3^-$ $CCR6^+$ T_{FH} cells. (B) Myeloid lineage cells are quantified and displayed as a percentage of PBMCs. Normal reference ranges for all myeloid cells, 4.1% to 26.3%; classical monocytes, 1.91% to 16.4%; non-classical monocytes, 0.1% to 1.4%; pDC, 0.1% to 1.1%; mDC, 0.4% to 3.8%. Each patient data point represents a unique biological replicate from a different blood draw. Error bars represent standard deviation from the mean.

Section 3.5 Hypophosphorylation of *PLCG2*

CyTOF analysis of NK cell signaling revealed hypophosphorylation of *PLCG2* in both families (Figure 3.4A). Family A demonstrated a reduction in the magnitude of *PLCG2* phosphorylation while family B displayed a slower accumulation of phospho-*PLCG2*. *PLCG2* hypophosphorylation was also confirmed by flow cytometry in patients A.I.2 and A.II.3; however, patient A.II.2 had normal *PLCG2* phosphorylation (Figure 3.5A/B) consistent with her borderline-normal NK cell killing (Figure 3.1C). Upstream Btk/Itk, ZAP70/Syk, and Lck phosphorylation was intact, suggesting an intrinsic defect in *PLCG2* (Figures 3.4B, 3.6). MAPKAPK2, activated by PKC downstream of *PLCG2*-induced DAG, was similarly hypophosphorylated (Figure 3.6)[231]. Total *PLCG2* protein levels in family A were analyzed to establish whether hypophosphorylation was the result of functional inhibition or reduced protein expression. Total *PLCG2* protein levels were normal in NK cells (Figure 3.4C), as well as in all other cell types examined (Figure 3.7), suggesting that the G595R mutation compromises function and not protein expression. Analysis of *PLCG2* protein levels in patient B.II.4 was not feasible due to limited samples. Notably, this analysis also revealed differential *PLCG2* expression between immune cell subsets, including physiologically lower *PLCG2* expression in monocytes and $CD56^{Dim}$ NK cells than in T cells, B cells, and $CD56^{Bright}$ NK cells (Figure 3.7).

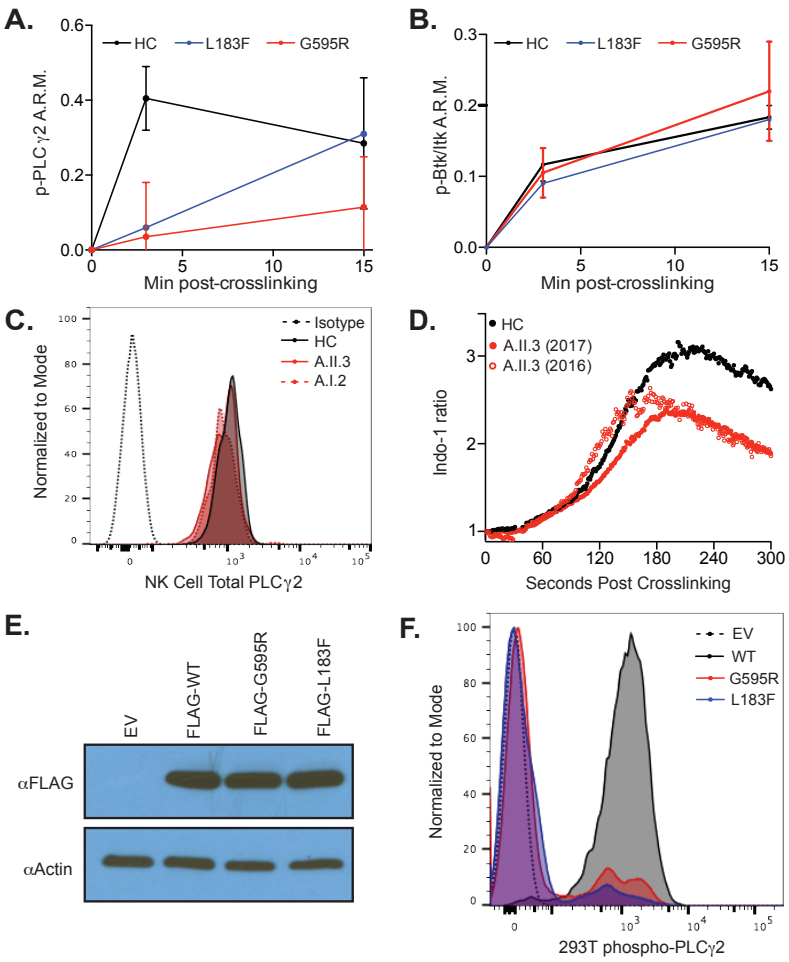

Figure 3.4: Loss-of-Function Mutations in *PLCG2* and Haploinsufficiency Cause NK Cell Dysregulation

(A) *PLCG2* phosphorylation in CD56^{Dim} NK cells after CD16 crosslinking is quantified by CyTOF, normalized to time 0 using an arcsinh transformation in three healthy controls (HC; two females, one male), two G595R patients (A.II.3 and A.I.2) and one L183F patient (B.II.4). A.R.M., Arcsinh ratio of mean. Error bars represents standard deviation from the mean. (B) Btk/Itk phosphorylation is shown as in subfigure A. (C) Total *PLCG2* levels in CD56^{Dim} NK cells is quantified by flow cytometry in a healthy control versus G595R patients. Isotype, Isotype control (dotted black line). HC, healthy control (solid black line). A.II.3, G595R patient (solid red line). Patient A.I.2, G595R patient, (dotted red line). (D) Indo-1 calcium flux analysis in G595R patient A.II.3 was assessed in naïve enriched human CD56^{Dim} NK cells after crosslinking with NKG2D and 2B4. Open and closed red circles represent two unique blood samples acquired one year apart (E) Western blot analysis for *PLCG2* protein expression in HEK293T cells transfected with wild-type or mutant FLAG-tagged *PLCG2*. EV, empty vector. (F) Phosphorylation of FLAG-tagged wild-type or mutant *PLCG2* after 15 minutes of pervanadate stimulation in 293T cells is quantified using phospho-flow cytometry. EV, empty vector. Except where limited by patient sample availability (B.II.4 in subfigures A and B), all data is representative of two or more independent experiments.

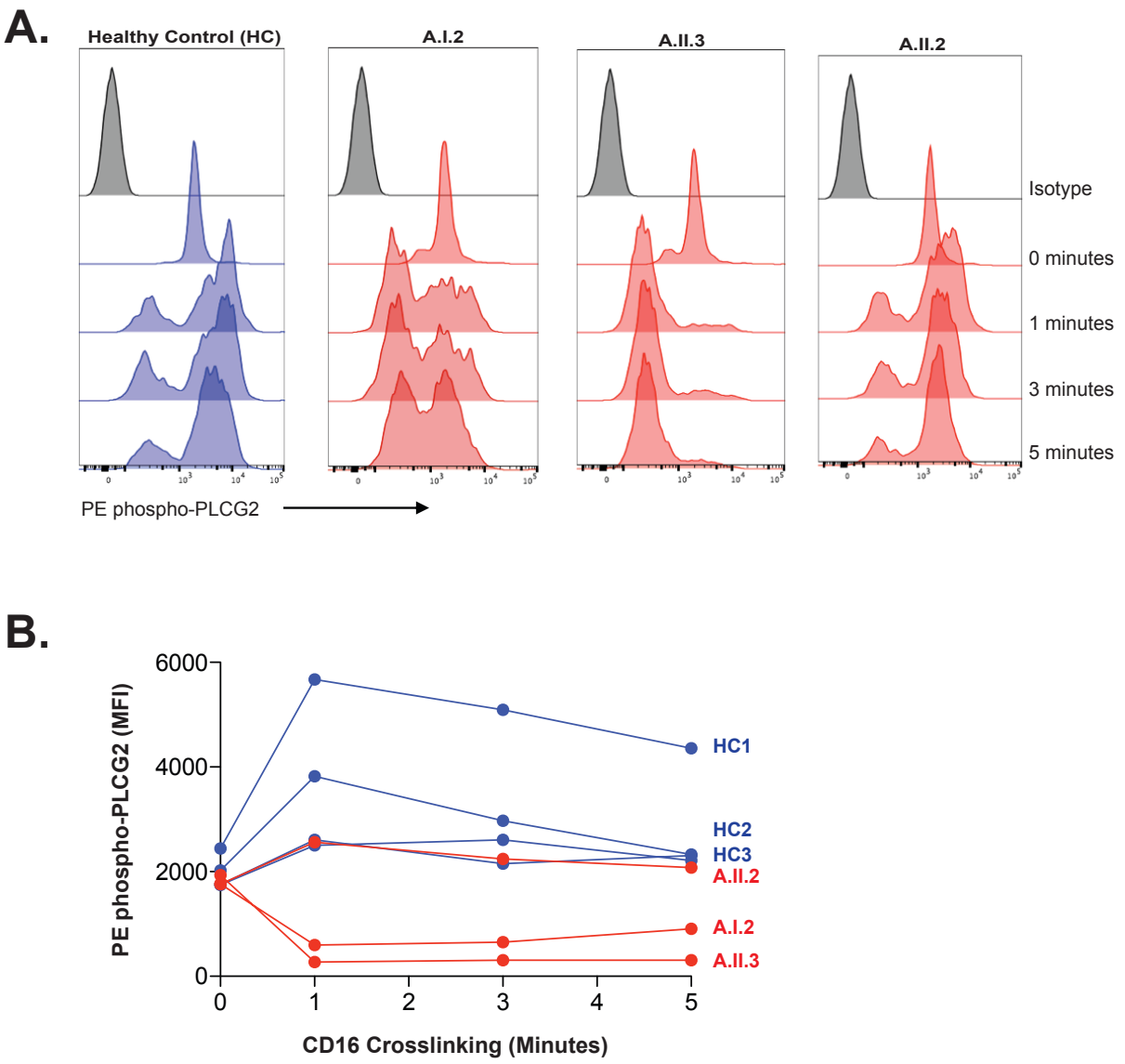

Figure 3.5: Family A phospho-*PLCG2* Flow Cytometry
(A) Briefly, patient PBMCs were labeled with APC-CD56, BV421-CD3 and unconjugated mouse anti-CD16 monoclonal antibody and washed. Cells were rested, warmed to 37C, and goat-anti mouse antibody was added to crosslink CD16 and stimulate *PLCG2* phosphorylation. At indicated time points, cells with fixed in formaldehyde, methanol permeabilized and stained with PE-phospho*PLCG2* before flow cytometry. Representative histograms are shown in (A). Median fluorescent intensity (MFI) of PE-phospho*PLCG2* is graphed by time in (B).

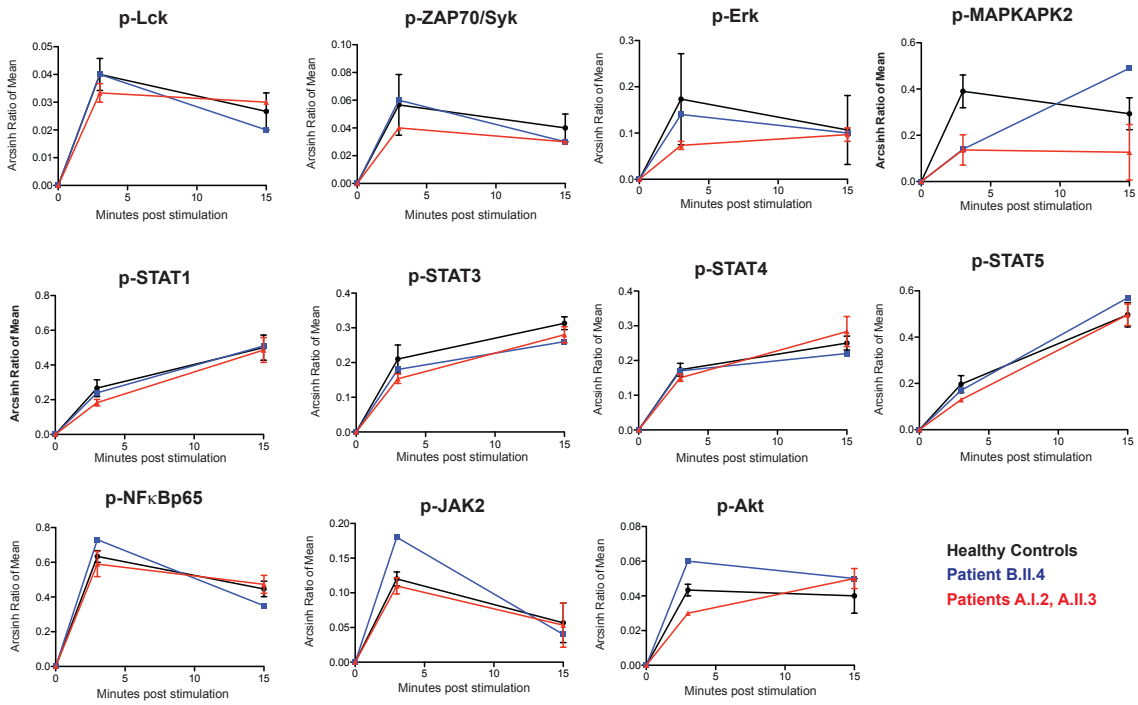

Figure 3.6: CyTOF Analysis of CD56^{Dim} NK Cell Signaling

PBMCs were stimulated with 50ng/mL IL-12, 500U/mL IL-2, 500U/mL IFNα, 500ng/mL LPS and 1ug anti-mouse crosslinking antibody for CD16/CD3/IgM per 10^6 cells for 0, 3 or 15 minutes before fixation. Analysis of signaling pathways was performed using mass cytometry to measure phosphoprotein levels after stimulation in CD56^{Dim} NK cells (gated as CD3$^-$ CD56$^+$ CD16$^+$). Values normalized to time 0 using an arcsinh transformation of the mean in three healthy controls (HC, black), two G595R patients (A.II.3 and A.I.2, red) and one L183F patient (B.II.4, blue). HC, healthy control. A.R.M., Arcsinh ratio of mean. Error bars represents standard deviation from the mean.

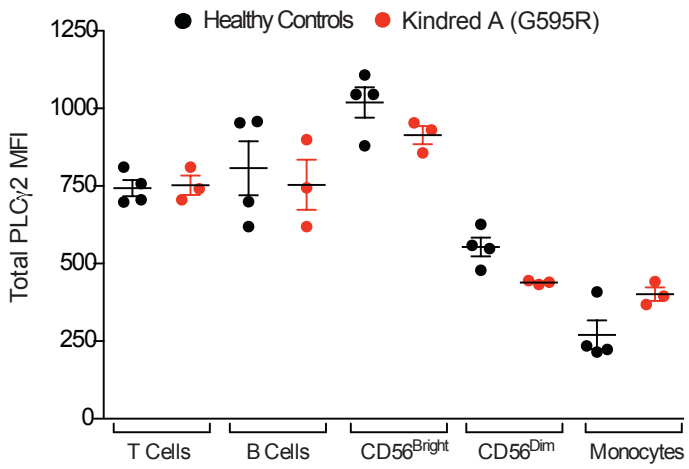

Figure 3.7: Total *PLCG2* Protein Analysis by Cell Type
Total protein levels of *PLCG2* were assessed in healthy controls (black) versus G595R patients (A.I.2, A.II.2 and A.II.3, red) by flow cytometry and intracellular staining. Cells were gated and the mean fluorescent intensity of *PLCG2* was quantified. T cells, $CD3^+$; B cells, $CD3^-$ $CD19^+$; NK T Cells, $CD3^+$ $CD56^+$; $CD56^{Bright}$ NK cells, $CD3^-$ $CD56^{++}$, $CD16^-$; $CD56^{Dim}$ NK Cells, $CD3^-$ $CD56^+$ $CD16^+$; Monocytes, $HLADR^+$ $CD14^+$ $CD16^-$. Error bars represent standard deviation from the mean. Each data point represents a unique individual. Data is representative of two independent experiments.

Section 3.6 *PLCG2* Mutations Occur in Critical Structural Motifs

Bioinformatic and structural analyses of G595 and L183 suggest that these residues are intolerant to mutation. The G595R and L183F mutations occur at highly-conserved sites in the nSH2 domain and N-terminus of *PLCG2,* respectively (Figure 3.8). Only two other individuals in ExAC are reported to have missense variants at G595, while no missense variants in L183 have been reported[205]. Although no structure exists for the PH domain, nSH2 structures from murine *PLCG2*[225] and human *PLCG1*[224] facilitated analysis of the G595R mutation with molecular dynamics (MD), which has been used to understand the structural effects of mutations previously[232,233]. Simulations of wild-type and G595R sequences were analyzed by this approach and revealed conformational disturbances in the nSH2 βD-βE loop, potentially compromising the LAT phosphotyrosine binding site (Figure 3.8B, 3.8C). In support of the βD-βE loop being critical in SH2 function, a structurally-analogous mutation (G60R) in the loop of SHP-2 has been previously reported as pathogenic and this loop serves as a protein-protein interaction site in the nSH2 of *PLCG1*[164,234].

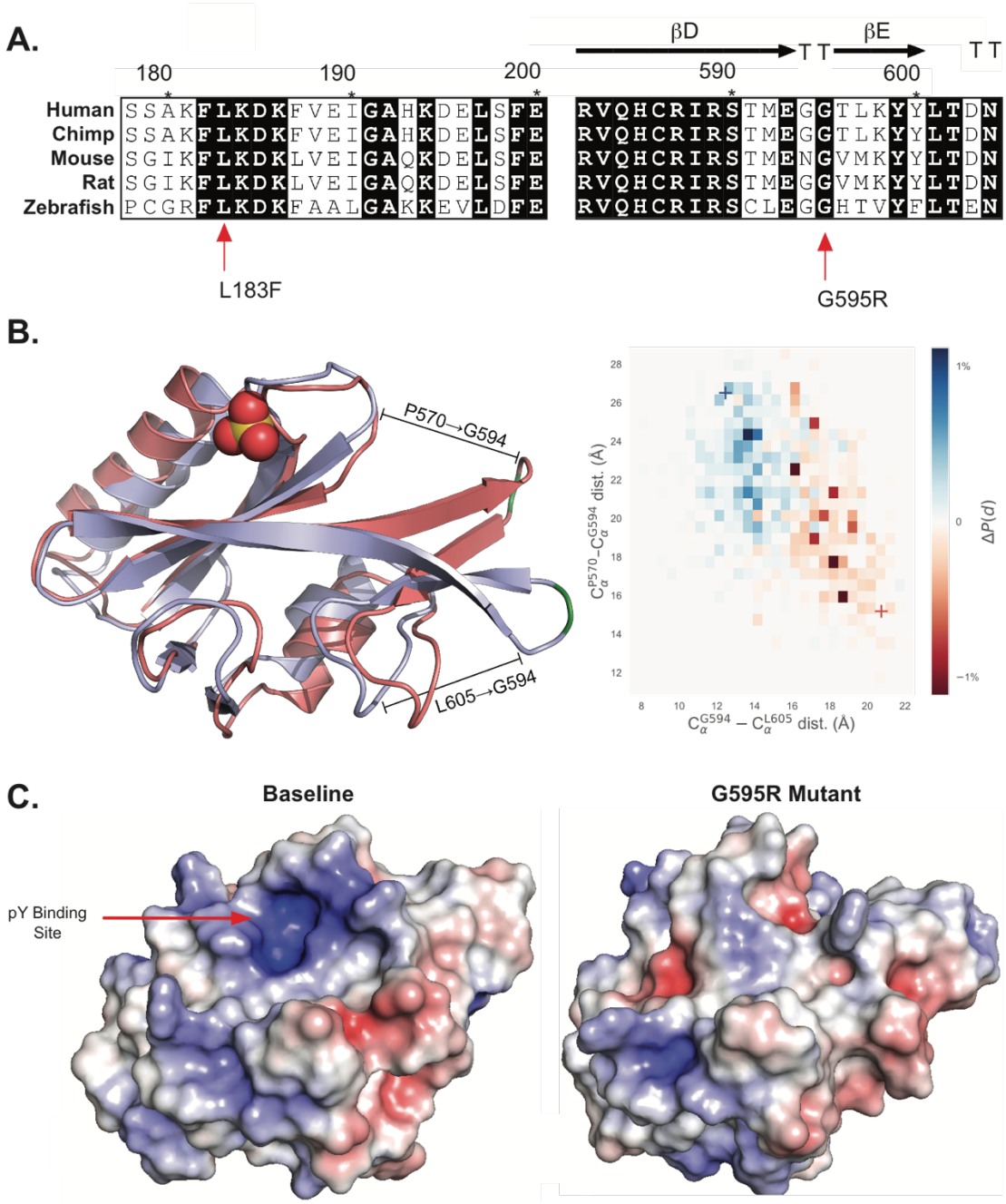

Figure 3.8: Conservation of *PLCG2* and Molecular Dynamics Analysis (Continued Next Page)

Figure 3.8: Conservation of *PLCG2* and Molecular Dynamics Analysis
(A) Conservation analysis of the G595 and L183 residues was generated using M-Coffee with ESPript secondary structure analysis[216-218]. (B) Molecular dynamics analysis was performed to identify principal differences between the wild-type and G595R nSH2 domain of *PLCG2* to understand potential structural effects from the G595R mutation. Molecular dynamics simulations of both sequences were ran and a shared state space Markov state model (MSM) was built for each sequence. One of the outputs of each MSM is the equilibrium probability that each state in the shared state space is occupied by each sequence. This allows direct comparison of each microstate's energetic favorability between sequences. Because there are more than two thousand microstates in this model, differences were systematically identified by computing the all-to-all $C\alpha$–$C\alpha$ distances for each microstate, weighting each state by its population in the wild-type and G595R sequences, and comparing the means of these two distributions. The two distances that the highest positive (i.e. wild-type favored) and negative (mutant-favored) mean differences were chosen and are displayed (left). These two distances were the P570–G594 α-carbon distance and the L605–G594 α-carbon distance. The difference in their joint distributions across all microstates is plotted as a 2-dimensional histogram (right). This analysis shows a clear change in the preference for adopting the P570-near, L605-far conformation in the mutant sequence and P570-far, L605-near conformation in the wild-type sequence. Green indicates site of mutation. Red, mutant preferred state. Blue, wild-type referred state. Bars identify key $C\alpha$–$C\alpha$ distances. (C) APBS[235] generated electrostatics and surface map of baseline versus G595R MD simulated structures. Red arrow depicts phosphotyrosine binding site.

Section 3.7 Reduced NK Cell Calcium Flux

The catalytic activity of *PLCG2* is initiated by phosphorylation, leading to calcium flux and granule movement/polarization. Consistent with *PLCG2* hypophosphorylation, calcium flux in patient A.II.3 was stably reduced in $CD56^{Dim}$ NK cells after NKG2D and 2B4 receptor crosslinking (Figure 3.4D). Notably, $CD56^{Bright}$ NK cells, which express higher levels of *PLCG2* protein (figure 3.7), demonstrated normal calcium flux with NKG2D+2B4 crosslinking (3.9A). Calcium flux in CD16-crosslinked NK cells was also normal, consistent with the ability of CD16 to signal through both *PLCG1* and *PLCG2* (Figure 3.9B)[236]. Limited patient sample required expansion of patient B.II.4 NK cells using K562-mbIL15-41BBL cells and IL-2 before analysis[215]. Patient B.II.4 NK cells also showed partially reduced calcium flux (Figure 3.9C-D), although this expansion process largely restored NK cell cytotoxicity.

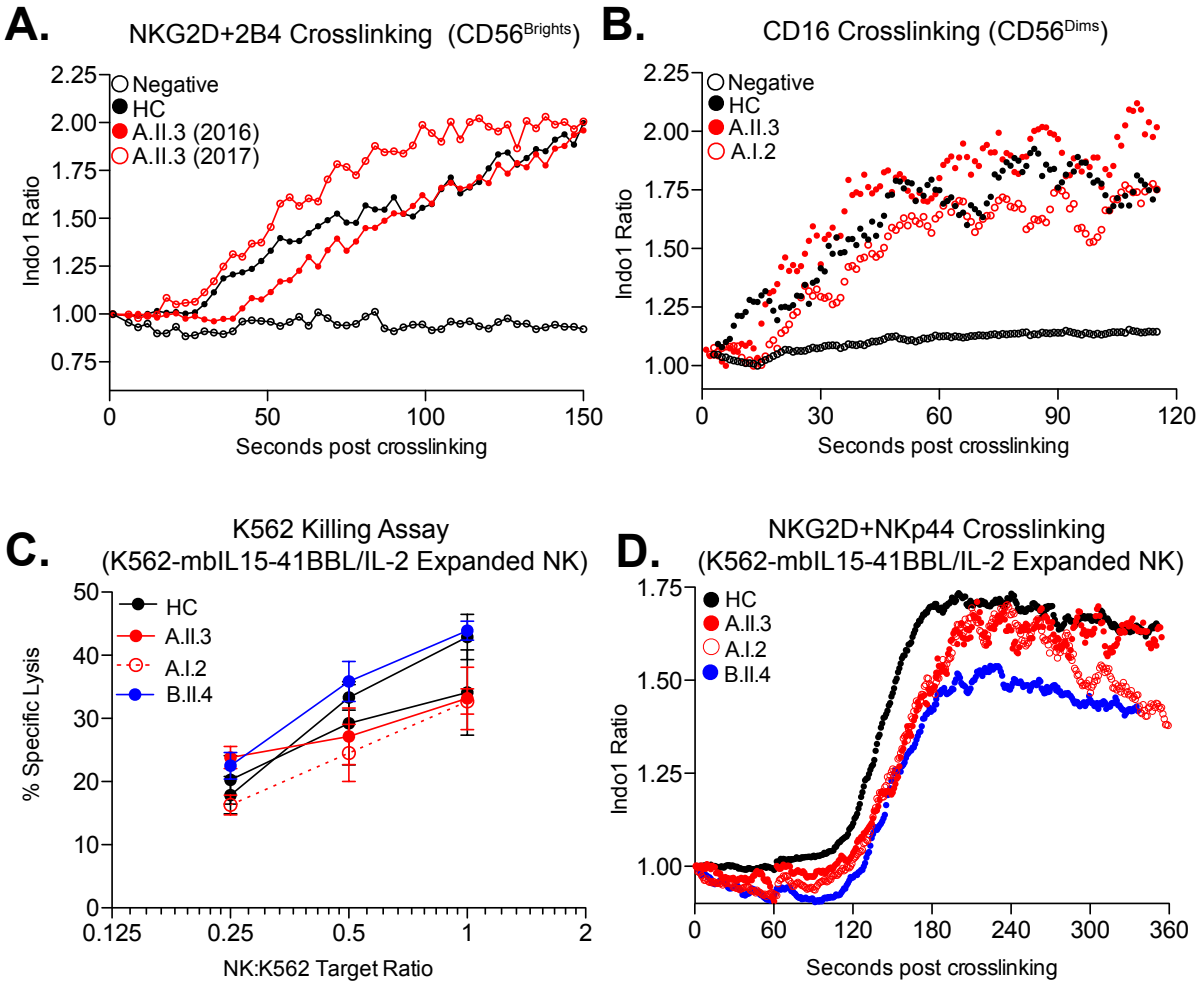

Figure 3.9: Additional Patient Calcium Flux Assays

(A) Indo-1 calcium flux analysis in G595R patient A.II.3 was assessed in $CD56^{Bright}$ NK cells ($CD3^-CD56^{++}CD16^-$) from naïve enriched human NK cells after crosslinking with NKG2D and 2B4. Red circles (filled and empty), patient A.II.3; black filled circles, HC (healthy control); black empty circles, isotype control. (B) Indo-1 calcium flux analysis in G595R patients A.II.3 and A.I.2 was assessed in $CD56^{Dim}$ NK cells ($CD3^-CD56^{++}CD16^-$) after crosslinking with CD16. Red circles (filled), patient A.II.3; red circles (empty), patient A.I.2, black filled circles, HC (healthy control); black empty circles, isotype control. (C) K562 killing assay using co-culture with expanded NK cells at E:T ratios of 1:4, 1:2 and 1:1 for 4 hours before assessment of K562 cytotoxicity. NK cells were expanded as previously described[215]. Briefly, 10^6 PBMCs from patient B.II.4 or healthy control were co-incubated with 10^6 irradiated (100Gy) K562-mbIL15-41bbl (Kind gift from Dario Campana, National University of Singapore) for 7 days. After 7 days, cells were removed and assessed for purity. T cells ($CD3^+$) were present at less than <1%. 100U/mL of recombinant IL-2 was added to the culture and incubated for 7 more days, with partial media exchange every 2 days. After 14 days total, NK cells expanded 10 to 15-fold with >95% purity ($CD56^+CD3^-$) and were then used for cytotoxicity and calcium flux assays. (D) Indo-1 calcium flux analysis in G595R patients A.II.3 and A.I.2 and L183F patient B.II.4 was assessed in expanded NK cells (as in C) after crosslinking with NKG2D and NKp44. Red circles (filled), patient A.II.3; red circles (empty), patient A.I.2, black filled circles, HC (healthy control); blue circles, patient B.II.4

Section 3.8 *PLCG2* Variants are Expressed but Nonfunctional

To establish that G595R and L183F are loss-of-function mutations, wild-type or mutant FLAG-*PLCG2* was expressed in 293T cells (which do not natively express *PLCG2*) and analyzed for protein expression and pervanadate-induced phosphorylation. Although both mutants were expressed normally (Figure 3.4E), FLAG-*PLCG2*^{G595R} and FLAG-*PLCG2*^{L183F} were hypophosphorylated compared to FLAG-*PLCG2*^{Wildtype} (Figure 3.4F). Together, these data demonstrate that the G595R and L183F mutations are loss-of-function mutations and likely contribute to functional *PLCG2* haploinsufficiency.

Section 3.9 Hypomobile Cytotoxic Granule Movement

Cytotoxic granule movement was analyzed by microscopy in NK cells conjugated to K562 target cells (Figure 3.10A). The microtubule organizing center (MTOC) to granule (MGD) and MTOC to synapse (MSD) distances were quantified. Both distances were increased in patient A.II.3, indicating dysregulated cytotoxic granule movement (Figure 3.10B). Synaptic actin accumulation, regulated independently of *PLCG2*, was unchanged (Figure 3.10B). In T cells, calcium flux kinetics and DAG localization influence the path and directionality of granule movement, respectively[70,71]. The observed defect in NK killing despite intact CD107 degranulation (Figure 3.10C) suggests that defects in both of these processes may lead to delayed/adirectional degranulation. Although methods to monitor DAG are limited, the defect in MAPKAPK2 phosphorylation downstream of PKC implies that this branch of *PLCG2* signaling is also dysregulated (Figure 3.6). Additionally, K562 induced NK cell IFN-γ secretion was unchanged in either family A or B (data not shown), suggesting that NK cell cytotoxicity is the primary pathway affected by these mutations.

Section 3.10 Increased NK Cell Maturity and Decreased Adaptive NK Cell Responses

CyTOF was also used to examine NK cell development and receptor expression (panel in Table 3.3). Clustering of NK cells with visual stochastic neighbor embedding (viSNE) enabled visualization of this high-dimensional data, whereby each point represents a cell and groups represent subpopulations which may be identified by marker expression[213]. Activating and inhibitory receptor expression were comparable between patient A.II.3 and control (data not shown); however, patient NK cell density was increased in the viSNE region corresponding to $CD57^+$ maturation stages 3 and 4, indicating increased NK cell maturity (Figure 3.10D). This phenotype was also noted by flow cytometry in patient B.II.4 (data not shown). $CD57^+$ acquisition is typically cytokine-driven and associated with increased cytotoxicity, suggesting either persistently-elevated cytokine levels (perhaps from increased viral burden) or a potential compensatory mechanism to increase NK cell killing[237]. Additionally, a distinct subpopulation of $NKG2C^+$ NK cells was absent in both patient A.II.3 (Figure 3.10E) and patient B.II.4 (data not shown). In most individuals, $NKG2C^+$ NK cells expand during CMV infection and persist thereafter, referred to as the adaptive NK cell response[238-240]. The absence of this population despite CMV seropositivity in both patients suggests this process may be impacted.

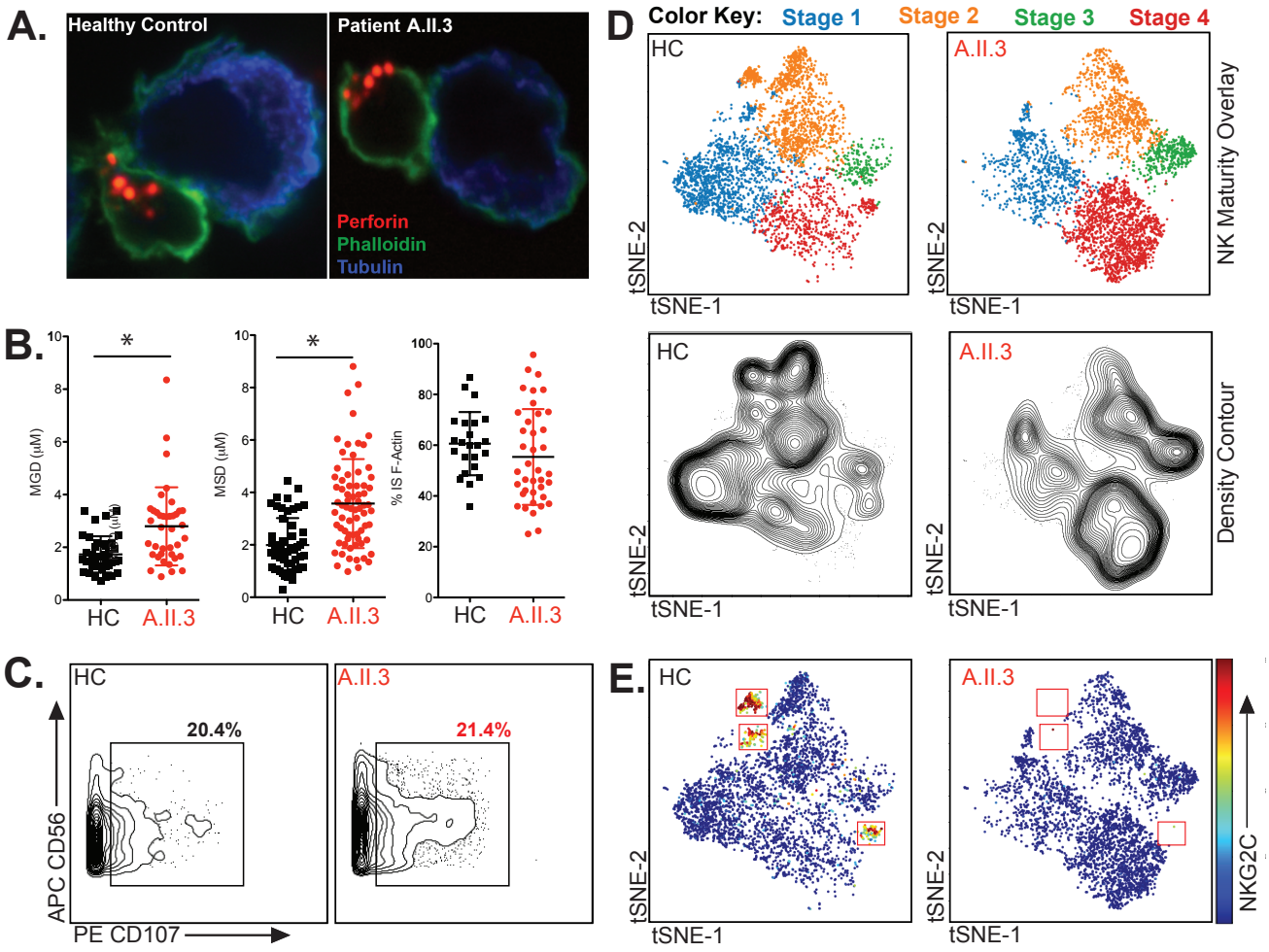

Figure 3.10: *PLCG2* Haploinsufficiency Alters Cytotoxic Granule Mobility, NK Cell Maturation, and the Adaptive NK Cell Response

(A) Representative immunofluorescence of cytotoxic granule microscopy upon K562 target conjugation in healthy versus patient A.II.3 NK cells. (B) Quantification of microtubule organizing center (MTOC) to granule distance (MGD), MTOC to synapse distance (MSD), and synaptic actin accumulation in healthy control (HC) versus patient A.II.3. * $P<0.001$, Mann-Whitney U Test. (C) CD107 Degranulation against K562 target cells is quantified by CyTOF after 1:1 incubation with healthy control or patient A.II.3 PBMCs for 6 hours. (D) viSNE on NK cells ($CD3^{-}$ $CD56^{+}$) overlaid with maturity subpopulations identified by traditional bivariate gating (top) with density visualized by contour (bottom) in both healthy control (HC) and patient A.II.3. Stage 1, $NKG2A^{-}$ $CD57^{-}$; stage 2, $NKG2A^{+}CD57^{-}$; stage 3, $NKG2A^{+}CD57^{+}$; stage 4, $NKG2A^{-}CD57^{+}$. tSNE, *t*-distributed stochastic neighbor embedding. (E) Similar graphical representation as in subfigure D is shown for the adaptive NK cell response marker NKG2C. All data is representative of two or more independent experiments using two patient blood samples drawn more than 1 year apart. All error bars represent standard deviation from the mean.

Table 3.3: CyTOF Panel for NK Cell Development and Function

Antigen	Clone	Tag
CD45	HI30	89 Y
Barcoding	Barcoding	Barcoding
KIR2DL4 (CD158d)	181703	141 PR
CD19	HIB19	142 Nd
KIR3DS1/L1 (CD158e1, e2)	Z27	143 Nd
CD3	UCHT1	144 Nd
KIR2DS4 (CD158i)	FES172	145 Nd
KIR2DL1/DS1 (CD158a,h)	EB6B	146 Nd
NKG2D	1D11	147 Sm
KIR2DL2/2DL3 (CD158b)	CH-L	148 Nd
CD127	A019D5	149 Sm
MIP-1a	93342	150 Nd
CD107a	H4A3	151 Eu
TNF-a	Mab11	152 Sm
CD62L	DREG-56	153 Eu
KIR2DL5 (CD158f)	UP-R1	154 Sm
CD27	L128	155 Gd
KIR3DL1 (CD158e)	DX9	156 Gd
CD137	4B4-1	158 Gd
NKG2C	134591	159 Tb
CD69	FN50	160 Gd
NKp30	P30-15	161 Dy
Ki67	B56	162 Dy
CD94	DX22	163 Er
CD16	3G8	165 Ho
NKG2A	Z199	166 Er
NKp44	P44-8	167 Dy
IFN-g	B27	168 Er
CD25	2A3	169 Tm
NKp80	239127	170 Er
GzmB	GB11	171 Yb
CD57	HCD57	172 Yb
CXCR6	K041E54	173 Yb
NKp46	195314	174 Yb
Perforin	B-D48	175 Lu
CD56	HCD56	176 Yb
CD11b	ICRF44	209 Bi
DNA	Intercalator-IR	191 /193
Cisplatin	NA	194 /195 Pt

Section 3.11 *Plcg2+/-* Mice Phenocopy Human *PLCG2* Haploinsufficiency

To establish that *PLCG2* haploinsufficiency is sufficient to cause NKD, a mouse model of haploinsufficiency was validated by comparing wild-type and *Plcg2*+/- mice. While *Plcg2*-/- mice have been previously described with severe B cell and NK cell defects, defects in *Plcg2*+/- mice have not been previously reported[178,200]. Subpopulation analysis was performed using flow cytometry and viSNE. As expected, major perturbations were seen in *Plcg2*-/- mice, including altered B cell development; however, B cell and NK cell development were intact in *Plcg2*+/- mice (Figure 3.11A-B). Similar to our patients, NK cell maturation was increased in *Plcg2*+/- mice (Figure 3.11C). Calcium flux analysis was performed in both B cells and NK cells. Although IgM-induced calcium flux was normal in *Plcg2*+/- B cells, NK1.1-induced calcium flux was attenuated in *Plcg2*+/- NK cells (Figure 3.11D). Correlating with reduced calcium flux, NK cell killing of YAC-1 and RMA-S target cells was inhibited in *Plcg2*+/- mice (Figure 3.11E). Similar to the clinical findings in our patients, *Plcg2*+/-mice had normal degranulation despite reduced cytotoxicity (data not shown). This combination of enhanced NK cell maturation, decreased NK cell calcium flux, and decreased NK cell killing phenocopies our patients and demonstrates that one-copy loss of *PLCG2* is sufficient to cause functional NKD.

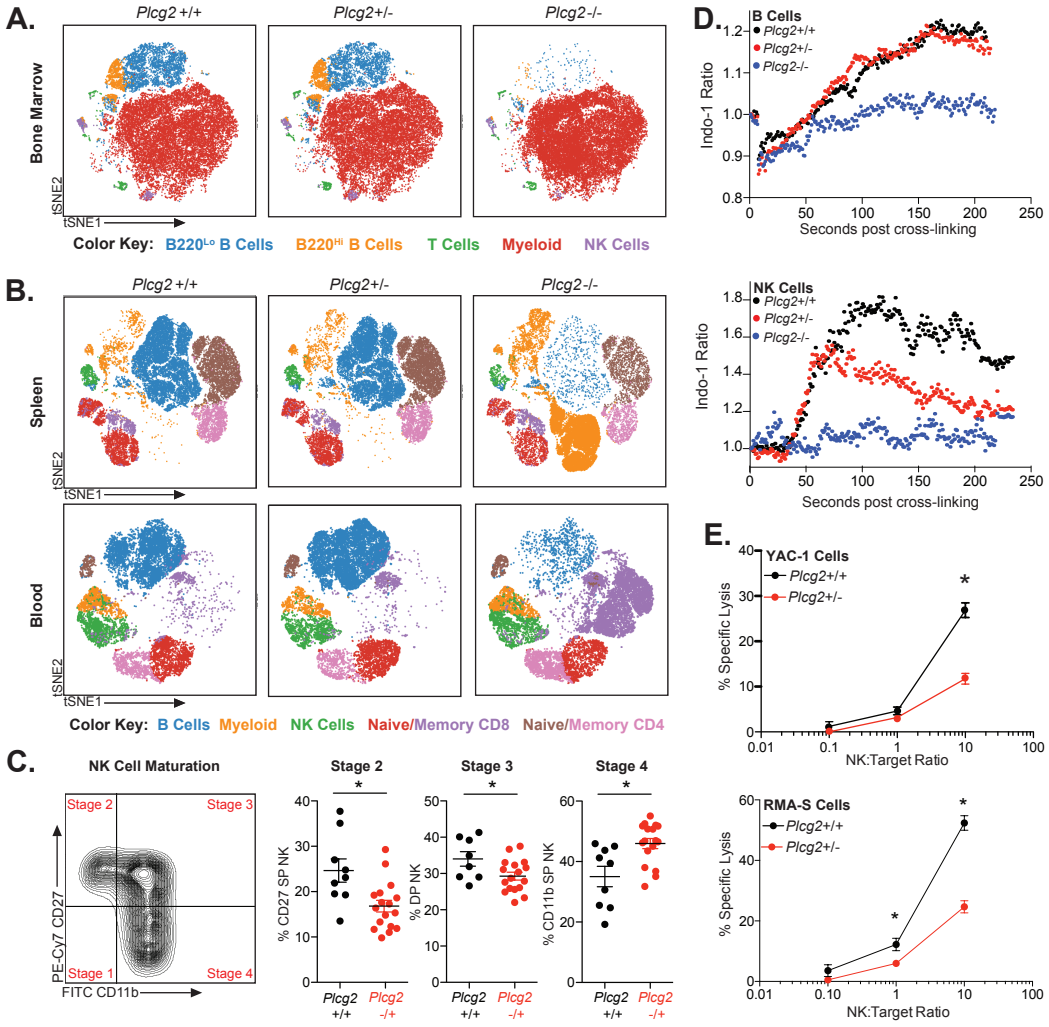

Figure 3.11: Heterozygous *Plcg2* Mice Phenocopy Human *PLCG2* Haploinsufficiency
Analysis of mouse immune cell subpopulations in the bone marrow (A), spleen and peripheral blood (B) of *Plcg2* wild-type (+/+), heterozygous (+/-), and homozygous (-/-) littermates using flow cytometry and displayed using viSNE clustering as in figure 3D. Color key for cell types identified by traditional bivariate is located beneath each subfigure. tSNE, *t*-distributed stochastic neighbor embedding. (C) Analysis of splenic murine NK cell maturity in wild-type littermate control versus heterozygous *Plcg2* mice using CD27 and CD11b expression. DP, double positive. SP, single positive. Example bivariate gating of murine NK cell maturation is shown. Each point represents a unique biologic replicate. * $P<0.05$, Mann Whitney U Test. (D) Indo-1 calcium flux analysis of littermate *Plcg2* +/+, +/- and -/- mice is displayed after crosslinking with anti-IgM antibody (B cells gated from whole splenocytes) or anti-NK.1.1 antibody (NK cells enriched from spleen). (E) NK cell killing against YAC-1 and RMA-S target cells was analyzed in littermate wild-type control versus heterozygous *Plcg2* mice using enriched splenic NK cells at NK to target ratios of 1:10, 1:1 and 10:1. Pairwise comparisons at each time point performed using *t*-test, * $P<0.05$, after test for normality. All data is representative of two or more independent experiments. All error bars represent standard deviation from the mean.

Section 3.12 G595R and L183F CRISPR Mice Recapitulate Human Disease

To conclusively link the heterozygous *PLCG2* mutations to the phenotypes observed in our patients, we generated CRISPR knock-in mice with heterozygous G595R and L183F mutations. These mice were evaluated for immune phenotype and natural killer cell function. Similar to patients in both families, NK cell counts were preserved (Figure 3.12A). Despite normal B cell function, family A presented with low B cell counts which was not recapitulated in the G595R CRISPR mice, indicating this likely represents a kindred effect and is separate from the mechanism of disease in *PLCG2* haploinsufficiency (Figure 3.12A). L183F CRISPR mice also demonstrated normal B cell counts, and both G595R and L183F CRISPR mice had normal memory B formation (Figure 3.12A). NK cell function was tested by examination of NK cell cytotoxicity and calcium flux. Similar to our human patients and haploinsufficient *Plcg2* mice, G595R and L183F CRISPR mice had decreased NK1.1-induced calcium flux (Figure 3.12B) and correspondingly low NK cell cytotoxicity against YAC-1 target cells (Figure 3.12C). Together, these data demonstrate the G595R and L183F mutations are loss-of-function mutations resulting in functional *PLCG2* haploinsufficiency and NK cell functional defects without perturbance of B cell function.

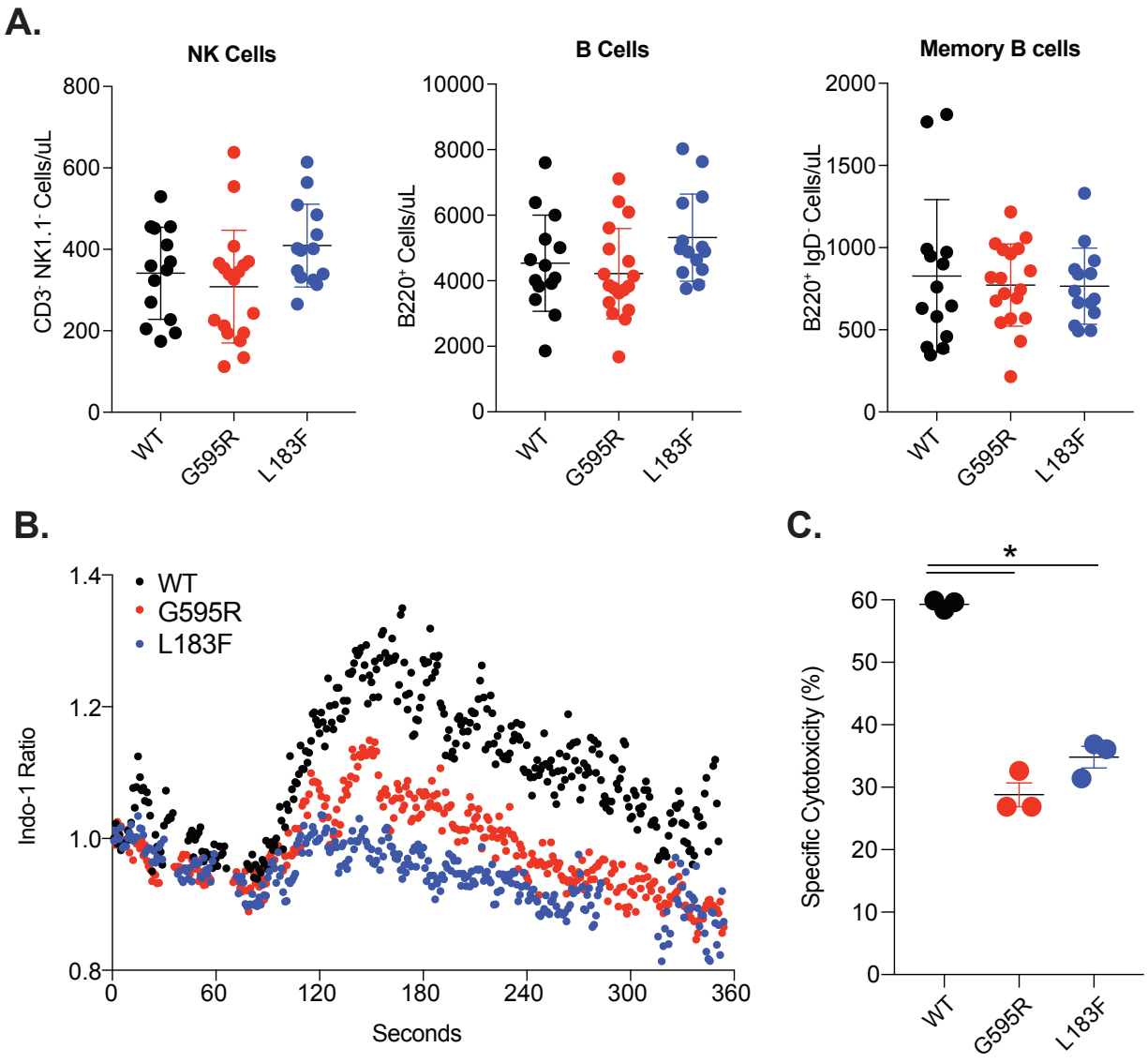

Figure 3.12: *Plcg2* G595R and L183F CRISPR Mice Demonstrate Normal B Cell Development and Perturbed NK Cell Function

(A) Analysis of NK cells, B cells, and memory B cells, in the peripheral blood from heterozygous G595R knock-in, L183F knock- in or wild-type littermate controls using flow cytometry. Data points represent unique biological replicates. (B) Indo-1 calcium flux analysis G595R knock-in, L183F knock- in or wild-type littermate controls is displayed after crosslinking with anti-NK.1.1 antibody (NK cells enriched from spleen). (C) NK cell killing against YAC-1 target cells was analyzed in G595R knock-in, L183F knock- in or wild-type littermate controls at a NK to target ratio of 10:1. Pairwise comparisons were performed using *t*-test, * $P<0.05$, after test for normality. Data points represent technical replicates. All data is representative of two or more independent experiments. All error bars represent standard deviation from the mean.

Section 3.13 Discussion

The heterozygous loss-of-function mutations presented herein result in *PLCG2* haploinsufficiency, NK cell dysfunction, and herpesvirus infections. Despite the role of *PLCG2* in B cells, these cells are functionally intact in *PLCG2* haploinsufficiency. Based on the differential regulation of *PLCG2* expression among lymphocytes, we propose a threshold model wherein cell types with homeostatically low levels of *PLCG2* (i.e. $CD56^{Dim}$ NK cells) are uniquely susceptible to further reductions in *PLCG2* function. As a result, most lymphocytes are likely shielded from haploinsufficiency by virtue of their high *PLCG2* expression or use of alternative pathways (i.e. *PLCG1* in T cells). This model also suggests that *PLCG2* may serve as a rate-limiting checkpoint against erroneous cytotoxicity in NK cells, requiring strong *PLCG2* activation for accurate and directional degranulation. Extrapolating this model further, monocytopenia was also observed in all patients, and monocytes express the lowest levels of *PLCG2* of all cell types examined. While the role of monocytopenia to the observed clinical phenotypes is not clear, this may also contribute to certain features of disease, including herpesvirus and bacterial susceptibility.

Despite a number of similarities (Table S1), family A and B each possess unique features as well. Notably, B cell output was reduced in family A (including A.II.2), but not family B. This is likely a result from other genetic background effects, as B cell development was unaffected in G595R CRISPR knock-in mice. Families A and B also differed in the nature of their phosphorylation defect. Family A had reduced magnitude of *PLCG2* phosphorylation while family B displayed a slower accumulation of phospho-*PLCG2*. An analysis of each domain's function provides insight into this difference. The L183F mutation in family B occurs nears the PH and EF-hand domains, which bind PIP_3 and PIP_2 (respectively) at the immunologic synapse and facilitate localization of

PLCG2 to the membrane[145]. Upon reaching the membrane, the nSH2 (affected by G595R in family A) binds to phosphorylated LAT, enabling assembly of the NK cell signalosome and interaction of *PLCG2* with its kinase (Btk/Itk)[73,241]. Therefore, *PLCG2* with diminished membrane localization would be capable of normal signalosome interaction, but diffusion-limited and kinetically altered. In contrast, *PLCG2* lacking a functional nSH2 domain would be blocked from signalosome interaction and phosphorylation altogether, reducing the magnitude of calcium flux. This hypothesis is consistent with the patterns observed in our patients and suggests that *PLCG2* loss-of-function mutations may have domain-specific phenotypes. Nonetheless, future studies are needed to further delineate the exact mechanisms by which these mutations diminish *PLCG2* function.

Pathogenic variants are commonly modifiable by both genetic and environmental factors. Genetic epistasis likely plays a role in the incomplete penetrance and variable expressivity observed in many autosomal dominant syndromes[228]. Immunologic context, such as the cytokine environment, may also modulate cellular and clinical phenotypes. For example, IL-2 incubation partially reverses NK cell killing defects in *STX11*-deficient patients[242], reminiscent of the restoration of patient NK cell killing after IL-15/IL-2 cytokine exposure herein (Figure 3.9C). The use of collateral immunologic pathways may also alter phenotypes. For example, the versatile use of either *PLCG1* or *PLCG2* by some NK cell receptors (i.e., CD16) may allow compensatory signaling through these pathways. Moreover, the variable nature of the adaptive immune response may compensate for innate defects to different degrees. A combination of these likely contributes to the phenotypic differences and incomplete penetrance seen in *PLCG2* haploinsufficiency. This manipulability may also present an opportunity to therapeutically modify defects, for example with

modulation of IL-15 signaling using ALT-803, an investigational drug previously shown to rectify NK cell cytotoxicity defects in vivo and aid CMV clearance in humans[243].

Whereas PLAID and APLAID represent the autosomal dominant manifestations of dominant-negative and gain-of-function mutations, the present patients illustrate haploinsufficiency and expand the spectrum of *PLCG2*-related disease. A fourth possibility, autosomal recessive loss-of-function, remains either undiscovered or is incompatible with life. While these three syndromes may be mechanistically distinct, there remains unexplained overlap (i.e. autoimmunity) that merits further investigation. Nonetheless, *PLCG2* haploinsufficiency results in clinical phenotypes distinct from PLAID/APLAID and requires a different diagnostic and therapeutic approach.

At present, the lack of a clear etiology complicates the management of many patients with unusually severe and/or recurrent herpesvirus infections. This study highlights a potential role for *PLCG2* mutations in these patients, provides insight into the regulation of human NK cell cytotoxicity, and unifies *PLCG2*-associated disease along a clinical spectrum that now includes PLAID, APLAID, and *PLCG2* haploinsufficiency. Unlike PLAID and APLAID which require deletions or mutations at specific locations, loss-of-function mutations could plausibly occur in many domains beyond the SH2 and PH domains, including the catalytic, SH3 and C2 domains. Of the 60,000 healthy exomes in ExAC, only 402 of 1265 residues in *PLCG2* have been reported with missense variants[205]. This evolutionary pressure against mutations in *PLCG2* implicates a number of residues where variants may disrupt *PLCG2* function. As a result, heterozygous *PLCG2* mutations should be considered in the differential diagnosis of patients with a number of

presentations beyond cold urticaria, antibody deficiency, and autoinflammation, including but not limited to NK cell immunodeficiency and herpesvirus infections.

Chapter 4: The Spectrum of *PLCG2*-related Disease

PLCG2 is closely related to the ubiquitously expressed *PLCG1*; however, while *PLCG1* and *PLCG2* are redundant in many cell types including T cells, *PLCG2* is non-redundant in B cells and NK cells, among others. As such, *Plcg2*-/- mice exhibit abnormal B cell development and function, as well as reduced NK cell cytotoxicity[177-179]. The role of *PLCG2* in other cell types is ever-expanding, with new roles in neutrophils[201], platelets[173], macrophages[170], and osteoclasts[244] being uncovered.

N-ethyl-N-nitrosourea (ENU) mouse models have also been informative about the potential spectrum of disease due to genetic alterations in *Plcg2*. The *Ali5* and *Ali14* mouse, heterozygous for gain-of-function mutations at D993G and Y495C, respectively, develop spontaneous and dominantly inherited autoinflammation resulting in cutaneous and joint inflammation[142,181,245]. Contrastingly, the *Queen* mouse, with a point mutation at I346R in the catalytic domain, exhibits only defects in B cell antibody responses[246].

Three syndromes have been reported due to human mutations in *PLCG2*: PLAID, APLAID, and more recently, *PLCG2* Haploinsufficiency. Each syndrome exhibits unique clinical manifestations that underscore the diverse spectrum of disease phenotypes possible with *PLCG2* mutations. PLAID (PLCγ2-associated antibody deficiency and immune dysregulation) was first reported in patients with familial cold urticaria[188]. Linkage analysis revealed exonic deletions in these patients, either deletions of exon 19 or exons 20-22, deleting portions of the C-terminal SH2 and SH3

domains of *PLCG2*. These patients, without exception, present with cold urticaria, but also present with varying degrees of antibody deficiency due to decreased B cell class switching (75% of patients), antinuclear antibodies (62%), allergic disease (56%), and recurrent sinopulmonary infections (44%). Some patients also develop granulomatous dermatitis, as well as autoimmune disorders including autoimmune thyroiditis and vitiligo[189]. The molecular mechanism underlying PLAID is unique in its temperature-sensitive nature. At physiologic temperatures, deletion of the normally autoinhibitory C-terminal SH2 domain leads to dominant-negative dysfunction in signalosome assembly, resulting in a loss-of-function phenotype in most cell types and thus B cell immunodeficiency[159]. However, at sub-physiologic temperatures, dysfunction of the autoinhibitory domain leads to gain-of-function activity, resulting most noticeably in cold-induced mast cell degranulation and cold urticaria. The treatment of these patients is mostly supportive, including the avoidance of evaporative cooling (i.e. when getting out of the shower or pool) and intravenous immunoglobulin to treat antibody deficiencies as they arise; however, future use of *PLCG2* inhibitors could be therapeutic in these patients[189].

While PLAID represents a complex dominant-negative loss-of-function and temperature-sensitive gain-of-function phenotype, APLAID (autoinflammation and PLCγ2-associated antibody deficiency and immune dysregulation) was discovered in patients with bonafide heterozygous gain-of-function mutations[191,192]. The clinical phenotypes of these patients are extensive, with multiple autoinflammatory features affecting several organ systems. Granulomatous skin lesions, enterocolitis, uveitis, arthralgias, interstitial lung disease, and mild humoral immunodeficiencies may all be present in these patients, reported with gain-of-function mutations at either S707Y in the C-terminal SH2 or L848P in the split PH domain. These mutations, unlike PLAID, do not lead

to cold urticaria or autoantibodies (despite the amount of autoinflammation present). These patients respond to high-dose corticosteroids, but symptoms are largely refractory to nonsteroidal anti-inflammatory drugs, TNF inhibitors, or IL-1 inhibitors.

Most recently, *PLCG2* Haploinsufficiency has been described in patients with heterozygous loss-of-function mutations. Unlike PLAID, these mutations are not dominant-negative or temperature sensitive, affecting a more restricted cellular repertoire that includes NK cells, but not B cells. These patients primarily present with NK cell dysfunction, monocytopenia, and severe or recurrent Herpesvirus infections, including Herpes Simplex Virus 1 (HSV1) and Cytomegalovirus (CMV) infections that require antiviral prophylaxis. The mutations in these patients occur in distinct domains, G595R in the N-terminal SH2 domain, or L183F in the EF hand domain, likely compromising the ability of *PLCG2* to associate with the signalosome or target properly to the membrane. Unlike PLAID or APLAID, the humoral responses in these patients is intact. However, several other features such as bacterial infections, autoantibody formation, and arthralgias are shared with the other syndromes affecting *PLCG2*. The mechanism of this overlap is not clear; however impaired monocyte function and dysfunctional follicular T cell regulation by NK cells may be responsible for certain aspects of all three syndromes.

The differing phenotypes among these three syndromes (summarized in table 4.1) serves as an interesting study in how gene dosage and domain-specific mutations may impact phenotype in a genetic disease. As *PLCG2* is expressed at different levels among hematopoietic cells, the relative susceptibility of a given cell type to either a loss-of-function or gain-of-function mutation is dictated by the physiologic level of *PLCG2* at baseline. In cell types with higher expression of

PLCG2, such as neutrophils and B cells, gain-of-function mutations impact function more so than in cell types with lower physiologic expression of *PLCG2*, such as NK cells. Contrastingly, loss-of-function mutations largely spare cell types with higher baseline *PLCG2* expression as is the case in *PLCG2* haploinsufficiency which appears not to impact higher *PLCG2* expressing cells such as B cells but renders lower *PLCG2* expressing NK cells susceptible to dysfunction. The unique dominant-negative loss-of-function and gain-of-function mechanism of PLAID affects a variety of cell types independent of cellular *PLCG2* expression as the dominant-negative nature of the deletion renders all copies of *PLCG2* inert even in B cells that express high levels of *PLCG2*. Indeed, the phenotypes of each disease can be well predicted based on the expression of *PLCG2* in a given cell type (see figure 4.1).

PLCG2 is a key signaling molecule in a variety of hematopoietic cells and thus, not surprisingly, the dysregulation of this enzyme in human patients leads to a variety of clinical phenotypes. Each syndrome presents with both unique and shared clinical features that may be explained by the role and differential expression level of *PLCG2* in immune cells. As the clinical presentation may range dramatically from cold urticaria to severe autoinflammation to viral immunodeficiency, it is critical for the clinician to recognize mutations in *PLCG2* as potentially pathogenic variants underlying disease in a diverse set of patients.

Table 4.1: Clinical Characteristics of PLAID, APLAID and *PLCG2* Haploinsufficiency

	PLAID[188]	**APLAID[191]**	***PLCG2* Haploinsufficiency**
Mutation	cSH2 Deletions	S707Y	G595R, L183F
Mechanism of Disease	Dominant-negative or Gain-of-function*	Gain-of-function	Loss-of-function (haploinsufficiency)
Cold Urticaria	+	-	-
Inflammatory Skin Lesions and Cutaneous Granulomas	+	+	-
Allergic Disease	+	-	-
Arthralgias	-	+	+
Autoantibodies/Autoimmunity	+	-	+
Bacterial Susceptibility	+	+	+
Herpesvirus Susceptibility	-	-	+
NK Cell Count	Decreased	Normal	Normal
NK Cell Killing	NR	NR	Decreased
NK Cell Degranulation	Decreased	NR	Normal
NK Cell Calcium Influx	Decreased	NR	Decreased
B Cell Count	Decreased	NR	Normal/Decreased
B Cell Class Switching	Decreased	Decreased	Normal
IgG/IgA/IgM levels	Decreased	Normal	Normal
B Cell Calcium Influx	Decreased/Increased†	Increased	Normal
Mast Cell Degranulation	Normal/Increased†	NR	NR

Table 4.1 Legend
NR, not reported. PLAID, *PLCG2*-associated Antibody Deficiency and Immune Dysregulation. APLAID, Autoinflammation & *PLCG2*-associated Antibody Deficiency and Immune Dysregulation. *Temperature dependent mechanism. †At 37°C, B cell calcium is inhibited while mast cell degranulation is unchanged. At sub-physiologic temperatures B cell calcium and mast cell degranulation are increased.

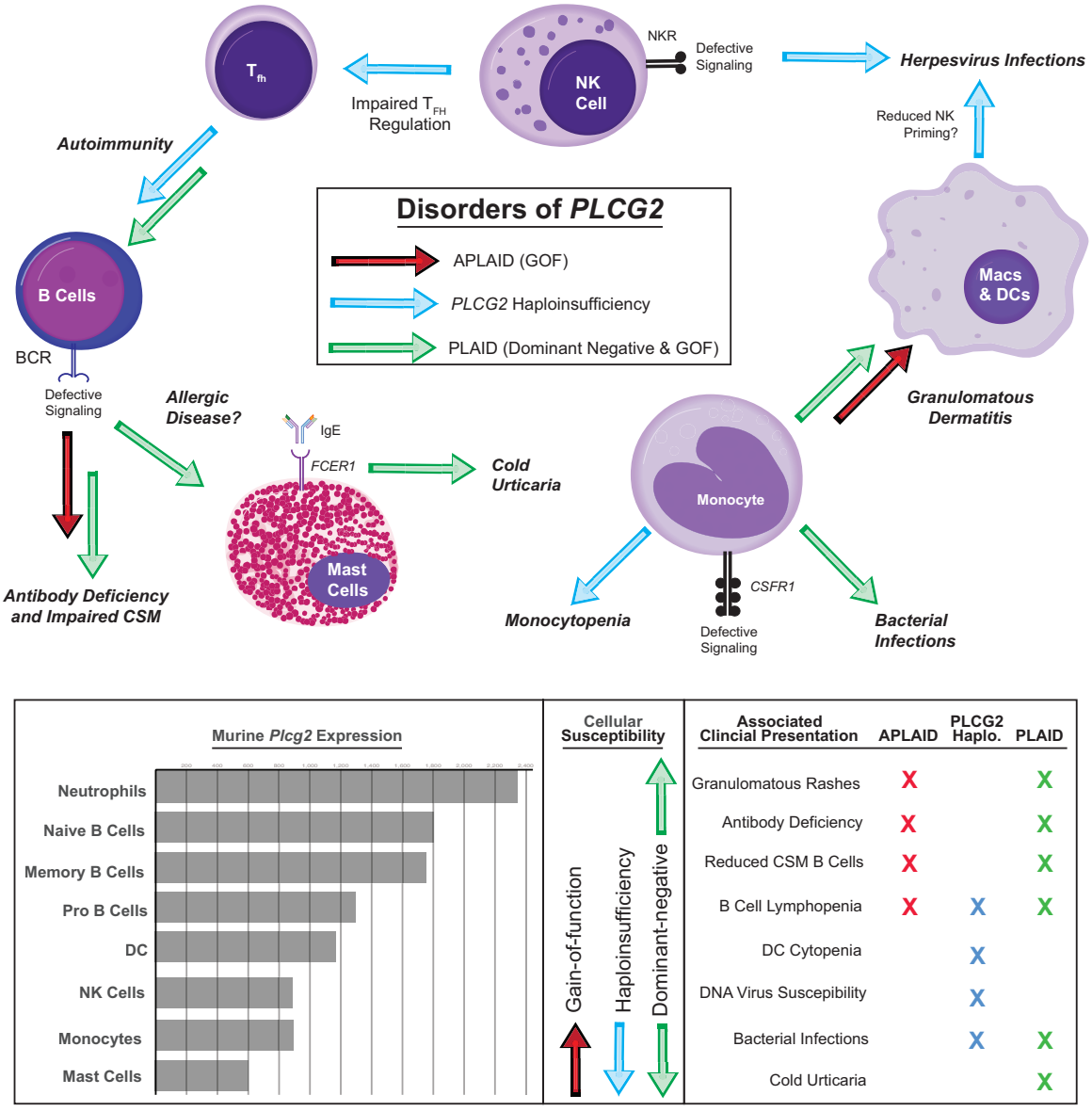

Figure 4.1: Human Disorders of *PLCG2*

The proposed cellular mechanism behind PLAID (PLCγ2-associated antibody deficiency and immune dysregulation), APLAID (autoinflammation and PLCγ2-associated antibody deficiency and immune dysregulation), and *PLCG2* Haploinsufficiency are summarized.

References

1 Griffin, B. D., Verweij, M. C. & Wiertz, E. J. Herpesviruses and immunity: the art of evasion. *Veterinary microbiology* **143**, 89-100, doi:10.1016/j.vetmic.2010.02.017 (2010).

2 Yokoyama, W. M., Kim, S. & French, A. R. The dynamic life of natural killer cells. *Annual review of immunology* **22**, 405-429, doi:10.1146/annurev.immunol.22.012703.104711 (2004).

3 Smith, H. R. *et al.* Recognition of a virus-encoded ligand by a natural killer cell activation receptor. *Proc Natl Acad Sci U S A* **99**, 8826-8831, doi:10.1073/pnas.092258599 (2002).

4 Arase, H., Mocarski, E. S., Campbell, A. E., Hill, A. B. & Lanier, L. L. Direct recognition of cytomegalovirus by activating and inhibitory NK cell receptors. *Science (New York, N.Y.)* **296**, 1323-1326, doi:10.1126/science.1070884 (2002).

5 Alexandre, Y. O., Cocita, C. D., Ghilas, S. & Dalod, M. Deciphering the role of DC subsets in MCMV infection to better understand immune protection against viral infections. *Frontiers in microbiology* **5**, 378, doi:10.3389/fmicb.2014.00378 (2014).

6 Katzenstein, D. A., Yu, G. S. & Jordan, M. C. Lethal infection with murine cytomegalovirus after early viral replication in the spleen. *The Journal of infectious diseases* **148**, 406-411 (1983).

7 Upton, J. W., Kaiser, W. J. & Mocarski, E. S. Cytomegalovirus M45 cell death suppression requires receptor-interacting protein (RIP) homotypic interaction motif (RHIM)-dependent interaction with RIP1. *The Journal of biological chemistry* **283**, 16966-16970, doi:10.1074/jbc.C800051200 (2008).

8 Delale, T. *et al.* MyD88-dependent and -independent murine cytomegalovirus sensing for IFN-alpha release and initiation of immune responses in vivo. *Journal of immunology (Baltimore, Md. : 1950)* **175**, 6723-6732 (2005).

9 Doring, M. *et al.* M27 expressed by cytomegalovirus counteracts effective type I interferon induction of myeloid cells but not of plasmacytoid dendritic cells. *Journal of virology* **88**, 13638-13650, doi:10.1128/jvi.00216-14 (2014).

10 Martinez-Moczygemba, M., Gutch, M. J., French, D. L. & Reich, N. C. Distinct STAT structure promotes interaction of STAT2 with the p48 subunit of the interferon-alpha-stimulated transcription factor ISGF3. *The Journal of biological chemistry* **272**, 20070-20076 (1997).

11 Cocita, C. *et al.* Natural Killer Cell Sensing of Infected Cells Compensates for MyD88 Deficiency but Not IFN-I Activity in Resistance to Mouse Cytomegalovirus. *PLoS pathogens* **11**, e1004897, doi:10.1371/journal.ppat.1004897 (2015).

12 Burkett, P. R. *et al.* Coordinate expression and trans presentation of interleukin (IL)-15Ralpha and IL-15 supports natural killer cell and memory CD8+ T cell homeostasis. *J Exp Med* **200**, 825-834, doi:10.1084/jem.20041389 (2004).

13 Mortier, E., Woo, T., Advincula, R., Gozalo, S. & Ma, A. IL-15Ralpha chaperones IL-15 to stable dendritic cell membrane complexes that activate NK cells via trans presentation. *J Exp Med* **205**, 1213-1225, doi:10.1084/jem.20071913 (2008).

14 Lucas, M., Schachterle, W., Oberle, K., Aichele, P. & Diefenbach, A. Dendritic cells prime natural killer cells by trans-presenting interleukin 15. *Immunity* **26**, 503-517, doi:10.1016/j.immuni.2007.03.006 (2007).

15 Ranson, T. *et al.* IL-15 is an essential mediator of peripheral NK-cell homeostasis. *Blood* **101**, 4887-4893, doi:10.1182/blood-2002-11-3392 (2003).

16 Carson, W. E. *et al.* Interleukin (IL) 15 is a novel cytokine that activates human natural killer cells via components of the IL-2 receptor. *J Exp Med* **180**, 1395-1403 (1994).

17 Carson, W. E. *et al.* A potential role for interleukin-15 in the regulation of human natural killer cell survival. *The Journal of clinical investigation* **99**, 937-943, doi:10.1172/jci119258 (1997).

18 French, A. R., Holroyd, E. B., Yang, L., Kim, S. & Yokoyama, W. M. IL-18 acts synergistically with IL-15 in stimulating natural killer cell proliferation. *Cytokine* **35**, 229-234, doi:10.1016/j.cyto.2006.08.006 (2006).

19 Kuwajima, S. *et al.* Interleukin 15-dependent crosstalk between conventional and plasmacytoid dendritic cells is essential for CpG-induced immune activation. *Nat Immunol* **7**, 740-746, doi:10.1038/ni1348 (2006).

20 Orange, J. S. & Biron, C. A. An absolute and restricted requirement for IL-12 in natural killer cell IFN-gamma production and antiviral defense. Studies of natural killer and T cell responses in contrasting viral infections. *Journal of immunology (Baltimore, Md. : 1950)* **156**, 1138-1142 (1996).

21 Madera, S. *et al.* Type I IFN promotes NK cell expansion during viral infection by protecting NK cells against fratricide. *J Exp Med* **213**, 225-233, doi:10.1084/jem.20150712 (2016).

22 Mack, E. A., Kallal, L. E., Demers, D. A. & Biron, C. A. Type 1 interferon induction of natural killer cell gamma interferon production for defense during lymphocytic choriomeningitis virus infection. *mBio* **2**, doi:10.1128/mBio.00169-11 (2011).

23 McRae, B. L., Semnani, R. T., Hayes, M. P. & van Seventer, G. A. Type I IFNs inhibit human dendritic cell IL-12 production and Th1 cell development. *Journal of immunology (Baltimore, Md. : 1950)* **160**, 4298-4304 (1998).

24 Chaix, J. *et al.* Cutting edge: Priming of NK cells by IL-18. *Journal of immunology (Baltimore, Md. : 1950)* **181**, 1627-1631 (2008).

25 Scalzo, A. A. & Yokoyama, W. M. Cmv1 and natural killer cell responses to murine cytomegalovirus infection. *Current topics in microbiology and immunology* **321**, 101-122 (2008).

26 Dokun, A. O. *et al.* Specific and nonspecific NK cell activation during virus infection. *Nat Immunol* **2**, 951-956, doi:10.1038/ni714 (2001).

27 Mitrovic, M. *et al.* The NK cell response to mouse cytomegalovirus infection affects the level and kinetics of the early CD8(+) T-cell response. *Journal of virology* **86**, 2165-2175, doi:10.1128/jvi.06042-11 (2012).

28 Cheng, T. P. *et al.* Ly49h is necessary for genetic resistance to murine cytomegalovirus. *Immunogenetics* **60**, 565-573, doi:10.1007/s00251-008-0313-3 (2008).

29 Keppel, M. P., Saucier, N., Mah, A. Y., Vogel, T. P. & Cooper, M. A. Activation-specific metabolic requirements for NK Cell IFN-gamma production. *Journal of immunology (Baltimore, Md. : 1950)* **194**, 1954-1962, doi:10.4049/jimmunol.1402099 (2015).

30 Tripathy, S. K., Smith, H. R., Holroyd, E. A., Pingel, J. T. & Yokoyama, W. M. Expression of m157, a murine cytomegalovirus-encoded putative major histocompatibility class I (MHC-I)-like protein, is independent of viral regulation of host MHC-I. *Journal of virology* **80**, 545-550, doi:10.1128/jvi.80.1.545-550.2006 (2006).

31 Parikh, B. A. *et al.* Dual Requirement of Cytokine and Activation Receptor Triggering for Cytotoxic Control of Murine Cytomegalovirus by NK Cells. *PLoS pathogens* **11**, e1005323, doi:10.1371/journal.ppat.1005323 (2015).

32 Loh, J., Chu, D. T., O'Guin, A. K., Yokoyama, W. M. & Virgin, H. W. t. Natural killer cells utilize both perforin and gamma interferon to regulate murine cytomegalovirus infection in the spleen and liver. *Journal of virology* **79**, 661-667, doi:10.1128/jvi.79.1.661-667.2005 (2005).

33 Orange, J. S. Natural killer cell deficiency. *J Allergy Clin Immunol* **132**, 515-525; quiz 526, doi:10.1016/j.jaci.2013.07.020 (2013).

34 Biron, C. A., Byron, K. S. & Sullivan, J. L. Severe herpesvirus infections in an adolescent without natural killer cells. *N Engl J Med* **320**, 1731-1735, doi:10.1056/NEJM198906293202605 (1989).

35 Mace, E. M. *et al.* Mutations in GATA2 cause human NK cell deficiency with specific loss of the CD56(bright) subset. *Blood* **121**, 2669-2677, doi:10.1182/blood-2012-09-453969 (2013).

36 Mace, E. M. *et al.* Biallelic mutations in IRF8 impair human NK cell maturation and function. *The Journal of clinical investigation* **127**, 306-320, doi:10.1172/jci86276 (2017).

37 Gineau, L. *et al.* Partial MCM4 deficiency in patients with growth retardation, adrenal insufficiency, and natural killer cell deficiency. *The Journal of clinical investigation* **122**, 821-832, doi:10.1172/JCI61014 (2012).

38 Rubin, T. S. *et al.* Perforin and CD107a testing is superior to NK cell function testing for screening patients for genetic HLH. *Blood* **129**, 2993-2999, doi:10.1182/blood-2016-12-753830 (2017).

39 Jawahar, S. *et al.* Natural Killer (NK) cell deficiency associated with an epitope-deficient Fc receptor type IIIA (CD16-II). *Clin Exp Immunol* **103**, 408-413, doi:10.1111/j.1365-2249.1996.tb08295.x (1996).

40 de Vries, E. *et al.* Identification of an unusual Fc gamma receptor IIIa (CD16) on natural killer cells in a patient with recurrent infections. *Blood* **88**, 3022-3027 (1996).

41 Akdis, M., Palomares, O., van de Veen, W., van Splunter, M. & Akdis, C. A. TH17 and TH22 cells: a confusion of antimicrobial response with tissue inflammation versus protection. *J Allergy Clin Immunol* **129**, 1438-1449; quiz1450-1431, doi:10.1016/j.jaci.2012.05.003 (2012).

42 Fogel, L. A., Yokoyama, W. M. & French, A. R. Natural killer cells in human autoimmune disorders. *Arthritis research & therapy* **15**, 216, doi:10.1186/ar4232 (2013).

43 Baxter, A. G. & Smyth, M. J. The role of NK cells in autoimmune disease. *Autoimmunity* **35**, 1-14 (2002).

44 Flodstrom, M., Shi, F. D., Sarvetnick, N. & Ljunggren, H. G. The natural killer cell -- friend or foe in autoimmune disease? *Scand J Immunol* **55**, 432-441 (2002).

45 French, A. R. & Yokoyama, W. M. Natural killer cells and autoimmunity. *Arthritis research & therapy* **6**, 8-14, doi:10.1186/ar1034 (2004).

46 Flodstrom-Tullberg, M., Bryceson, Y. T., Shi, F. D., Hoglund, P. & Ljunggren, H. G. Natural killer cells in human autoimmunity. *Curr Opin Immunol* **21**, 634-640, doi:10.1016/j.coi.2009.09.012 (2009).

47 Park, Y. W. *et al.* Impaired differentiation and cytotoxicity of natural killer cells in systemic lupus erythematosus. *Arthritis and rheumatism* **60**, 1753-1763, doi:10.1002/art.24556 (2009).

48 Bossowski, A., Urban, M. & Stasiak-Barmuta, A. Analysis of circulating T gamma/delta lymphocytes and CD16/56 cell populations in children and adolescents with Graves' disease. *Pediatr Res* **54**, 425-429, doi:10.1203/01.Pdr.0000076663.94850.44 (2003).

49 Ciampolillo, A. *et al.* Modifications of the immune responsiveness in patients with autoimmune thyroiditis: evidence for a systemic immune alteration. *Curr Pharm Des* **9**, 1946-1950 (2003).

50 Cameron, A. L., Kirby, B. & Griffiths, C. E. Circulating natural killer cells in psoriasis. *Br J Dermatol* **149**, 160-164, doi:10.1046/j.1365-2133.2003.05319.x (2003).

51 Wouters, C. H., Ceuppens, J. L. & Stevens, E. A. Different circulating lymphocyte profiles in patients with different subtypes of juvenile idiopathic arthritis. *Clinical and experimental rheumatology* **20**, 239-248 (2002).

52 Throm, A. A. *et al.* Dysregulated NK cell PLCgamma2 signaling and activity in juvenile dermatomyositis. *JCI Insight* **3**, doi:10.1172/jci.insight.123236 (2018).

53 Mehrotra, P. T. *et al.* Production of IL-10 by human natural killer cells stimulated with IL-2 and/or IL-12. *Journal of immunology (Baltimore, Md. : 1950)* **160**, 2637-2644 (1998).

54 Deniz, G. *et al.* Regulatory NK cells suppress antigen-specific T cell responses. *Journal of immunology (Baltimore, Md. : 1950)* **180**, 850-857, doi:10.4049/jimmunol.180.2.850 (2008).

55 Pallmer, K. & Oxenius, A. Recognition and Regulation of T Cells by NK Cells. *Frontiers in immunology* **7**, 251, doi:10.3389/fimmu.2016.00251 (2016).

56 Cook, K. D., Kline, H. C. & Whitmire, J. K. NK cells inhibit humoral immunity by reducing the abundance of CD4+ T follicular helper cells during a chronic virus infection. *Journal of leukocyte biology* **98**, 153-162, doi:10.1189/jlb.4HI1214-594R (2015).

57 Gensous, N. *et al.* T Follicular Helper Cells in Autoimmune Disorders. *Frontiers in immunology* **9**, 1637, doi:10.3389/fimmu.2018.01637 (2018).

58 Nagler, A., Lanier, L. L., Cwirla, S. & Phillips, J. H. Comparative studies of human FcRIII-positive and negative natural killer cells. *Journal of immunology (Baltimore, Md. : 1950)* **143**, 3183-3191 (1989).

59 Cooper, M. A., Fehniger, T. A. & Caligiuri, M. A. The biology of human natural killer-cell subsets. *Trends Immunol* **22**, 633-640 (2001).

60 Caligiuri, M. A. Human natural killer cells. *Blood* **112**, 461-469, doi:10.1182/blood-2007-09-077438 (2008).

61 Wagner, J. A. *et al.* CD56bright NK cells exhibit potent antitumor responses following IL-15 priming. *The Journal of clinical investigation* **127**, 4042-4058, doi:10.1172/JCI90387 (2017).

62 Biassoni, R. *et al.* Human natural killer cell receptors and co-receptors. *Immunological reviews* **181**, 203-214 (2001).

63 Vivier, E., Nunes, J. A. & Vely, F. Natural killer cell signaling pathways. *Science (New York, N.Y.)* **306**, 1517-1519, doi:10.1126/science.1103478 (2004).

64 Diefenbach, A. *et al.* Selective associations with signaling proteins determine stimulatory versus costimulatory activity of NKG2D. *Nat Immunol* **3**, 1142-1149, doi:10.1038/ni858 (2002).

65 Wu, J., Cherwinski, H., Spies, T., Phillips, J. H. & Lanier, L. L. DAP10 and DAP12 form distinct, but functionally cooperative, receptor complexes in natural killer cells. *J Exp Med* **192**, 1059-1068, doi:10.1084/jem.192.7.1059 (2000).

66 Jevremovic, D. *et al.* Cutting edge: a role for the adaptor protein LAT in human NK cell-mediated cytotoxicity. *Journal of immunology (Baltimore, Md. : 1950)* **162**, 2453-2456 (1999).

67 Cella, M. *et al.* Differential requirements for Vav proteins in DAP10- and ITAM-mediated NK cell cytotoxicity. *J Exp Med* **200**, 817-823, doi:10.1084/jem.20031847 (2004).

68 Cruz-Orcutt, N., Vacaflores, A., Connolly, S. F., Bunnell, S. C. & Houtman, J. C. Activated PLC-gamma1 is catalytically induced at LAT but activated PLC-gamma1 is localized at both LAT- and TCR-containing complexes. *Cell Signal* **26**, 797-805, doi:10.1016/j.cellsig.2013.12.022 (2014).

69 Zhang, W., Sloan-Lancaster, J., Kitchen, J., Trible, R. P. & Samelson, L. E. LAT: the ZAP-70 tyrosine kinase substrate that links T cell receptor to cellular activation. *Cell* **92**, 83-92, doi:10.1016/s0092-8674(00)80901-0 (1998).

70 Quann, E. J., Merino, E., Furuta, T. & Huse, M. Localized diacylglycerol drives the polarization of the microtubule-organizing center in T cells. *Nat Immunol* **10**, 627-635, doi:10.1038/ni.1734 (2009).

71 Beal, A. M. *et al.* Kinetics of early T cell receptor signaling regulate the pathway of lytic granule delivery to the secretory domain. *Immunity* **31**, 632-642, doi:10.1016/j.immuni.2009.09.004 (2009).

72 Mace, E. M. *et al.* Cell biological steps and checkpoints in accessing NK cell cytotoxicity. *Immunol Cell Biol* **92**, 245-255, doi:10.1038/icb.2013.96 (2014).

73 Matalon, O. *et al.* Dephosphorylation of the adaptor LAT and phospholipase C-gamma by SHP-1 inhibits natural killer cell cytotoxicity. *Sci Signal* **9**, ra54, doi:10.1126/scisignal.aad6182 (2016).

74 Zompi, S. *et al.* NKG2D triggers cytotoxicity in mouse NK cells lacking DAP12 or Syk family kinases. *Nat Immunol* **4**, 565-572, doi:10.1038/ni930 (2003).

75 Kim, H. S., Das, A., Gross, C. C., Bryceson, Y. T. & Long, E. O. Synergistic signals for natural cytotoxicity are required to overcome inhibition by c-Cbl ubiquitin ligase. *Immunity* **32**, 175-186, doi:10.1016/j.immuni.2010.02.004 (2010).

76 Bryceson, Y. T., March, M. E., Ljunggren, H. G. & Long, E. O. Synergy among receptors on resting NK cells for the activation of natural cytotoxicity and cytokine secretion. *Blood* **107**, 159-166, doi:10.1182/blood-2005-04-1351 (2006).

77 Guerra, N. *et al.* NKG2D-deficient mice are defective in tumor surveillance in models of spontaneous malignancy. *Immunity* **28**, 571-580, doi:10.1016/j.immuni.2008.02.016 (2008).

78 Vitale, M. *et al.* Identification of NKp80, a novel triggering molecule expressed by human NK cells. *European journal of immunology* **31**, 233-242, doi:10.1002/1521-4141(200101)31:1<233::AID-IMMU233>3.0.CO;2-4 (2001).

79 Welte, S., Kuttruff, S., Waldhauer, I. & Steinle, A. Mutual activation of natural killer cells and monocytes mediated by NKp80-AICL interaction. *Nat Immunol* **7**, 1334-1342, doi:10.1038/ni1402 (2006).

80 Ruckrich, T. & Steinle, A. Attenuated natural killer (NK) cell activation through C-type lectin-like receptor NKp80 is due to an anomalous hemi-immunoreceptor tyrosine-based activation motif (HemITAM) with impaired Syk kinase recruitment capacity. *The Journal of biological chemistry* **288**, 17725-17733, doi:10.1074/jbc.M113.453548 (2013).

81 Shibuya, A. *et al.* DNAM-1, a novel adhesion molecule involved in the cytolytic function of T lymphocytes. *Immunity* **4**, 573-581 (1996).

82 Bottino, C. *et al.* Identification of PVR (CD155) and Nectin-2 (CD112) as cell surface ligands for the human DNAM-1 (CD226) activating molecule. *J Exp Med* **198**, 557-567, doi:10.1084/jem.20030788 (2003).

83 Zhang, Z. *et al.* DNAM-1 controls NK cell activation via an ITT-like motif. *J Exp Med* **212**, 2165-2182, doi:10.1084/jem.20150792 (2015).

84 Sivori, S. *et al.* 2B4 functions as a co-receptor in human NK cell activation. *European journal of immunology* **30**, 787-793, doi:10.1002/1521-4141(200003)30:3<787::AID-IMMU787>3.0.CO;2-I (2000).

85 Brown, M. H. *et al.* 2B4, the natural killer and T cell immunoglobulin superfamily surface protein, is a ligand for CD48. *J Exp Med* **188**, 2083-2090, doi:10.1084/jem.188.11.2083 (1998).

86 Latchman, Y., McKay, P. F. & Reiser, H. Identification of the 2B4 molecule as a counter-receptor for CD48. *Journal of immunology (Baltimore, Md. : 1950)* **161**, 5809-5812 (1998).

87 Duev-Cohen, A. *et al.* The human 2B4 and NTB-A receptors bind the influenza viral hemagglutinin and co-stimulate NK cell cytotoxicity. *Oncotarget* **7**, 13093-13105, doi:10.18632/oncotarget.7597 (2016).

88 Tangye, S. G., Cherwinski, H., Lanier, L. L. & Phillips, J. H. 2B4-mediated activation of human natural killer cells. *Molecular immunology* **37**, 493-501 (2000).

89 Tangye, S. G. *et al.* Cutting edge: human 2B4, an activating NK cell receptor, recruits the protein tyrosine phosphatase SHP-2 and the adaptor signaling protein SAP. *Journal of immunology (Baltimore, Md. : 1950)* **162**, 6981-6985 (1999).

90 McNerney, M. E., Lee, K. M. & Kumar, V. 2B4 (CD244) is a non-MHC binding receptor with multiple functions on natural killer cells and CD8+ T cells. *Molecular immunology* **42**, 489-494, doi:10.1016/j.molimm.2004.07.032 (2005).

91 Bottino, C. *et al.* NTB-A [correction of GNTB-A], a novel SH2D1A-associated surface molecule contributing to the inability of natural killer cells to kill Epstein-Barr virus-infected B cells in X-linked lymphoproliferative disease. *J Exp Med* **194**, 235-246, doi:10.1084/jem.194.3.235 (2001).

92 Flaig, R. M., Stark, S. & Watzl, C. Cutting edge: NTB-A activates NK cells via homophilic interaction. *Journal of immunology (Baltimore, Md. : 1950)* **172**, 6524-6527, doi:10.4049/jimmunol.172.11.6524 (2004).

93 Katz, G., Krummey, S. M., Larsen, S. E., Stinson, J. R. & Snow, A. L. SAP facilitates recruitment and activation of LCK at NTB-A receptors during restimulation-induced cell death. *Journal of immunology (Baltimore, Md. : 1950)* **192**, 4202-4209, doi:10.4049/jimmunol.1303070 (2014).

94 Eissmann, P. & Watzl, C. Molecular analysis of NTB-A signaling: a role for EAT-2 in NTB-A-mediated activation of human NK cells. *Journal of immunology (Baltimore, Md. : 1950)* **177**, 3170-3177, doi:10.4049/jimmunol.177.5.3170 (2006).

95 Moretta, A. *et al.* Activating receptors and coreceptors involved in human natural killer cell-mediated cytolysis. *Annual review of immunology* **19**, 197-223, doi:10.1146/annurev.immunol.19.1.197 (2001).

96 Pende, D. *et al.* Identification and molecular characterization of NKp30, a novel triggering receptor involved in natural cytotoxicity mediated by human natural killer cells. *J Exp Med* **190**, 1505-1516, doi:10.1084/jem.190.10.1505 (1999).

97 Brandt, C. S. *et al.* The B7 family member B7-H6 is a tumor cell ligand for the activating natural killer cell receptor NKp30 in humans. *J Exp Med* **206**, 1495-1503, doi:10.1084/jem.20090681 (2009).

98 Pogge von Strandmann, E. *et al.* Human leukocyte antigen-B-associated transcript 3 is released from tumor cells and engages the NKp30 receptor on natural killer cells. *Immunity* **27**, 965-974, doi:10.1016/j.immuni.2007.10.010 (2007).

99 Mavoungou, E., Held, J., Mewono, L. & Kremsner, P. G. A Duffy binding-like domain is involved in the NKp30-mediated recognition of Plasmodium falciparum-parasitized erythrocytes by natural killer cells. *The Journal of infectious diseases* **195**, 1521-1531, doi:10.1086/515579 (2007).

100 Cantoni, C. *et al.* NKp44, a triggering receptor involved in tumor cell lysis by activated human natural killer cells, is a novel member of the immunoglobulin superfamily. *J Exp Med* **189**, 787-796, doi:10.1084/jem.189.5.787 (1999).

101 Shemesh, A. *et al.* NKp44-Derived Peptide Binds Proliferating Cell Nuclear Antigen and Mediates Tumor Cell Death. *Frontiers in immunology* **9**, 1114, doi:10.3389/fimmu.2018.01114 (2018).

102 Parodi, M. *et al.* NKp44-NKp44 Ligand Interactions in the Regulation of Natural Killer Cells and Other Innate Lymphoid Cells in Humans. *Frontiers in immunology* **10**, 719, doi:10.3389/fimmu.2019.00719 (2019).

103 Campbell, K. S., Yusa, S., Kikuchi-Maki, A. & Catina, T. L. NKp44 triggers NK cell activation through DAP12 association that is not influenced by a putative cytoplasmic inhibitory sequence. *Journal of immunology (Baltimore, Md. : 1950)* **172**, 899-906, doi:10.4049/jimmunol.172.2.899 (2004).

104 Vitale, M. *et al.* NKp44, a novel triggering surface molecule specifically expressed by activated natural killer cells, is involved in non-major histocompatibility complex-restricted tumor cell lysis. *J Exp Med* **187**, 2065-2072, doi:10.1084/jem.187.12.2065 (1998).

105 Pessino, A. *et al.* Molecular cloning of NKp46: a novel member of the immunoglobulin superfamily involved in triggering of natural cytotoxicity. *J Exp Med* **188**, 953-960, doi:10.1084/jem.188.5.953 (1998).

106 Sivori, S. *et al.* p46, a novel natural killer cell-specific surface molecule that mediates cell activation. *J Exp Med* **186**, 1129-1136, doi:10.1084/jem.186.7.1129 (1997).

107 Narni-Mancinelli, E. *et al.* Complement factor P is a ligand for the natural killer cell-activating receptor NKp46. *Sci Immunol* **2**, doi:10.1126/sciimmunol.aam9628 (2017).

108 Mandelboim, O. *et al.* Recognition of haemagglutinins on virus-infected cells by NKp46 activates lysis by human NK cells. *Nature* **409**, 1055-1060, doi:10.1038/35059110 (2001).

109 Bauer, S. *et al.* Activation of NK cells and T cells by NKG2D, a receptor for stress-inducible MICA. *Science (New York, N.Y.)* **285**, 727-729 (1999).

110 Holmes, M. A., Li, P., Petersdorf, E. W. & Strong, R. K. Structural studies of allelic diversity of the MHC class I homolog MIC-B, a stress-inducible ligand for the activating immunoreceptor NKG2D. *Journal of immunology (Baltimore, Md. : 1950)* **169**, 1395-1400, doi:10.4049/jimmunol.169.3.1395 (2002).

111 Cosman, D. *et al.* ULBPs, novel MHC class I-related molecules, bind to CMV glycoprotein UL16 and stimulate NK cytotoxicity through the NKG2D receptor. *Immunity* **14**, 123-133 (2001).

112 Wu, J. *et al.* An activating immunoreceptor complex formed by NKG2D and DAP10. *Science (New York, N.Y.)* **285**, 730-732, doi:10.1126/science.285.5428.730 (1999).

113 Braud, V. M. *et al.* HLA-E binds to natural killer cell receptors CD94/NKG2A, B and C. *Nature* **391**, 795-799, doi:10.1038/35869 (1998).

114 Kaiser, B. K., Pizarro, J. C., Kerns, J. & Strong, R. K. Structural basis for NKG2A/CD94 recognition of HLA-E. *Proc Natl Acad Sci U S A* **105**, 6696-6701, doi:10.1073/pnas.0802736105 (2008).

115 Lanier, L. L., Corliss, B., Wu, J. & Phillips, J. H. Association of DAP12 with activating CD94/NKG2C NK cell receptors. *Immunity* **8**, 693-701 (1998).

116 Lopez-Verges, S. *et al.* Expansion of a unique CD57(+)NKG2Chi natural killer cell subset during acute human cytomegalovirus infection. *Proc Natl Acad Sci U S A* **108**, 14725-14732, doi:10.1073/pnas.1110900108 (2011).

117 Vivier, E. *et al.* Tyrosine phosphorylation of the Fc gamma RIII(CD16): zeta complex in human natural killer cells. Induction by antibody-dependent cytotoxicity but not by natural killing. *Journal of immunology (Baltimore, Md. : 1950)* **146**, 206-210 (1991).

118 Simmons, D. & Seed, B. The Fc gamma receptor of natural killer cells is a phospholipid-linked membrane protein. *Nature* **333**, 568-570, doi:10.1038/333568a0 (1988).

119 Ravetch, J. V. & Perussia, B. Alternative membrane forms of Fc gamma RIII(CD16) on human natural killer cells and neutrophils. Cell type-specific expression of two genes that differ in single nucleotide substitutions. *J Exp Med* **170**, 481-497, doi:10.1084/jem.170.2.481 (1989).

120 Lanier, L. L., Yu, G. & Phillips, J. H. Co-association of CD3 zeta with a receptor (CD16) for IgG Fc on human natural killer cells. *Nature* **342**, 803-805, doi:10.1038/342803a0 (1989).

121 Cognet, C. *et al.* Expression of the HLA-C2-specific activating killer-cell Ig-like receptor KIR2DS1 on NK and T cells. *Clin Immunol* **135**, 26-32, doi:10.1016/j.clim.2009.12.009 (2010).

122 Katz, G., Markel, G., Mizrahi, S., Arnon, T. I. & Mandelboim, O. Recognition of HLA-Cw4 but not HLA-Cw6 by the NK cell receptor killer cell Ig-like receptor two-domain short tail number 4. *Journal of immunology (Baltimore, Md. : 1950)* **166**, 7260-7267, doi:10.4049/jimmunol.166.12.7260 (2001).

123 Graef, T. *et al.* KIR2DS4 is a product of gene conversion with KIR3DL2 that introduced specificity for HLA-A*11 while diminishing avidity for HLA-C. *J Exp Med* **206**, 2557-2572, doi:10.1084/jem.20091010 (2009).

124 Sim, M. J. W. *et al.* Human NK cell receptor KIR2DS4 detects a conserved bacterial epitope presented by HLA-C. *Proc Natl Acad Sci U S A* **116**, 12964-12973, doi:10.1073/pnas.1903781116 (2019).

125 Kiani, Z., Bruneau, J., Geraghty, D. E. & Bernard, N. F. HLA-F on autologous HIV infected cells activates primary NK cells expressing the activating killer immunoglobulin-like receptor KIR3DS1. *Journal of virology*, doi:10.1128/JVI.00933-19 (2019).

126 Carr, W. H. *et al.* Cutting Edge: KIR3DS1, a gene implicated in resistance to progression to AIDS, encodes a DAP12-associated receptor expressed on NK cells that triggers NK cell activation. *Journal of immunology (Baltimore, Md. : 1950)* **178**, 647-651, doi:10.4049/jimmunol.178.2.647 (2007).

127 Raulet, D. H., Vance, R. E. & McMahon, C. W. Regulation of the natural killer cell receptor repertoire. *Annual review of immunology* **19**, 291-330, doi:10.1146/annurev.immunol.19.1.291 (2001).

128 Lopez-Botet, M. *et al.* Paired inhibitory and triggering NK cell receptors for HLA class I molecules. *Hum Immunol* **61**, 7-17 (2000).

129 Miah, S. M., Hughes, T. L. & Campbell, K. S. KIR2DL4 differentially signals downstream functions in human NK cells through distinct structural modules. *Journal of immunology (Baltimore, Md. : 1950)* **180**, 2922-2932, doi:10.4049/jimmunol.180.5.2922 (2008).

130 Gresset, A., Sondek, J. & Harden, T. K. The phospholipase C isozymes and their regulation. *Subcell Biochem* **58**, 61-94, doi:10.1007/978-94-007-3012-0_3 (2012).

131 Hofmann, S. L. & Majerus, P. W. Identification and properties of two distinct phosphatidylinositol-specific phospholipase C enzymes from sheep seminal vesicular glands. *The Journal of biological chemistry* **257**, 6461-6469 (1982).

132 Ryu, S. H., Cho, K. S., Lee, K. Y., Suh, P. G. & Rhee, S. G. Two forms of phosphatidylinositol-specific phospholipase C from bovine brain. *Biochem Biophys Res Commun* **141**, 137-144, doi:10.1016/s0006-291x(86)80345-x (1986).

133 Ryu, S. H., Cho, K. S., Lee, K. Y., Suh, P. G. & Rhee, S. G. Purification and characterization of two immunologically distinct phosphoinositide-specific phospholipases C from bovine brain. *The Journal of biological chemistry* **262**, 12511-12518 (1987).

134 Ryu, S. H., Suh, P. G., Cho, K. S., Lee, K. Y. & Rhee, S. G. Bovine brain cytosol contains three immunologically distinct forms of inositolphospholipid-specific phospholipase C. *Proc Natl Acad Sci U S A* **84**, 6649-6653, doi:10.1073/pnas.84.19.6649 (1987).

135 Takenawa, T. & Nagai, Y. Purification of phosphatidylinositol-specific phospholipase C from rat liver. *The Journal of biological chemistry* **256**, 6769-6775 (1981).

136 Meisenhelder, J., Suh, P. G., Rhee, S. G. & Hunter, T. Phospholipase C-gamma is a substrate for the PDGF and EGF receptor protein-tyrosine kinases in vivo and in vitro. *Cell* **57**, 1109-1122, doi:10.1016/0092-8674(89)90048-2 (1989).

137 Wahl, M. I. *et al.* Platelet-derived growth factor induces rapid and sustained tyrosine phosphorylation of phospholipase C-gamma in quiescent BALB/c 3T3 cells. *Molecular and cellular biology* **9**, 2934-2943, doi:10.1128/mcb.9.7.2934 (1989).

138 Morris, A. J., Waldo, G. L., Downes, C. P. & Harden, T. K. A receptor and G-protein-regulated polyphosphoinositide-specific phospholipase C from turkey erythrocytes. II. P2Y-purinergic receptor and G-protein-mediated regulation of the purified enzyme reconstituted with turkey erythrocyte ghosts. *The Journal of biological chemistry* **265**, 13508-13514 (1990).

139 Suh, P. G., Ryu, S. H., Moon, K. H., Suh, H. W. & Rhee, S. G. Cloning and sequence of multiple forms of phospholipase C. *Cell* **54**, 161-169, doi:10.1016/0092-8674(88)90548-x (1988).

140 Nishizuka, Y. Intracellular signaling by hydrolysis of phospholipids and activation of protein kinase C. *Science (New York, N.Y.)* **258**, 607-614, doi:10.1126/science.1411571 (1992).

141 Feske, S. *et al.* A mutation in Orai1 causes immune deficiency by abrogating CRAC channel function. *Nature* **441**, 179-185, doi:10.1038/nature04702 (2006).

142 Everett, K. L. *et al.* Characterization of phospholipase C gamma enzymes with gain-of-function mutations. *The Journal of biological chemistry* **284**, 23083-23093, doi:10.1074/jbc.M109.019265 (2009).

143 Rebecchi, M. J. & Scarlata, S. Pleckstrin homology domains: a common fold with diverse functions. *Annu Rev Biophys Biomol Struct* **27**, 503-528, doi:10.1146/annurev.biophys.27.1.503 (1998).

144 Essen, L. O., Perisic, O., Cheung, R., Katan, M. & Williams, R. L. Crystal structure of a mammalian phosphoinositide-specific phospholipase C delta. *Nature* **380**, 595-602, doi:10.1038/380595a0 (1996).

145 Falasca, M. *et al.* Activation of phospholipase C gamma by PI 3-kinase-induced PH domain-mediated membrane targeting. *EMBO J* **17**, 414-422, doi:10.1093/emboj/17.2.414 (1998).

146 Singh, S. M. & Murray, D. Molecular modeling of the membrane targeting of phospholipase C pleckstrin homology domains. *Protein Sci* **12**, 1934-1953, doi:10.1110/ps.0358803 (2003).

147 Illenberger, D., Walliser, C., Nurnberg, B., Diaz Lorente, M. & Gierschik, P. Specificity and structural requirements of phospholipase C-beta stimulation by Rho GTPases versus G protein beta gamma dimers. *The Journal of biological chemistry* **278**, 3006-3014, doi:10.1074/jbc.M208282200 (2003).

148 Kouchi, Z. *et al.* The role of EF-hand domains and C2 domain in regulation of enzymatic activity of phospholipase Czeta. *The Journal of biological chemistry* **280**, 21015-21021, doi:10.1074/jbc.M412123200 (2005).

149 Nomikos, M. *et al.* Essential Role of the EF-hand Domain in Targeting Sperm Phospholipase Czeta to Membrane Phosphatidylinositol 4,5-Bisphosphate (PIP2). *The Journal of biological chemistry* **290**, 29519-29530, doi:10.1074/jbc.M115.658443 (2015).

150 Waldo, G. L. *et al.* Kinetic scaffolding mediated by a phospholipase C-beta and Gq signaling complex. *Science (New York, N.Y.)* **330**, 974-980, doi:10.1126/science.1193438 (2010).

151 Katan, M. & Williams, R. L. Phosphoinositide-specific phospholipase C: structural basis for catalysis and regulatory interactions. *Semin Cell Dev Biol* **8**, 287-296, doi:10.1006/scdb.1997.0150 (1997).

152 Jezyk, M. R. *et al.* Crystal structure of Rac1 bound to its effector phospholipase C-beta2. *Nat Struct Mol Biol* **13**, 1135-1140, doi:10.1038/nsmb1175 (2006).

153 Everett, K. L. *et al.* Membrane environment exerts an important influence on rac-mediated activation of phospholipase Cgamma2. *Molecular and cellular biology* **31**, 1240-1251, doi:10.1128/MCB.01408-10 (2011).

154 Piechulek, T. *et al.* Isozyme-specific stimulation of phospholipase C-gamma2 by Rac GTPases. *The Journal of biological chemistry* **280**, 38923-38931, doi:10.1074/jbc.M509396200 (2005).

155 Walliser, C. *et al.* rac regulates its effector phospholipase Cgamma2 through interaction with a split pleckstrin homology domain. *The Journal of biological chemistry* **283**, 30351-30362, doi:10.1074/jbc.M803316200 (2008).

156 Bubeck Wardenburg, J. *et al.* Phosphorylation of SLP-76 by the ZAP-70 protein-tyrosine kinase is required for T-cell receptor function. *The Journal of biological chemistry* **271**, 19641-19644, doi:10.1074/jbc.271.33.19641 (1996).

157 Braiman, A., Barda-Saad, M., Sommers, C. L. & Samelson, L. E. Recruitment and activation of PLCgamma1 in T cells: a new insight into old domains. *EMBO J* **25**, 774-784, doi:10.1038/sj.emboj.7600978 (2006).

158 Poulin, B., Sekiya, F. & Rhee, S. G. Intramolecular interaction between phosphorylated tyrosine-783 and the C-terminal Src homology 2 domain activates phospholipase C-gamma1. *Proc Natl Acad Sci U S A* **102**, 4276-4281, doi:10.1073/pnas.0409590102 (2005).

159 Wang, J., Sohn, H., Sun, G., Milner, J. D. & Pierce, S. K. The autoinhibitory C-terminal SH2 domain of phospholipase C-gamma2 stabilizes B cell receptor signalosome assembly. *Sci Signal* **7**, ra89, doi:10.1126/scisignal.2005392 (2014).

160 Mitchell, A. L. *et al.* InterPro in 2019: improving coverage, classification and access to protein sequence annotations. *Nucleic Acids Res* **47**, D351-D360, doi:10.1093/nar/gky1100 (2019).

161 Gresset, A., Hicks, S. N., Harden, T. K. & Sondek, J. Mechanism of phosphorylation-induced activation of phospholipase C-gamma isozymes. *The Journal of biological chemistry* **285**, 35836-35847, doi:10.1074/jbc.M110.166512 (2010).

162 Devkota, S., Joseph, R. E., Min, L., Bruce Fulton, D. & Andreotti, A. H. Scaffold Protein SLP-76 Primes PLCgamma1 for Activation by ITK-Mediated Phosphorylation. *Journal of molecular biology* **427**, 2734-2747, doi:10.1016/j.jmb.2015.04.012 (2015).

163 Todderud, G., Wahl, M. I., Rhee, S. G. & Carpenter, G. Stimulation of phospholipase C-gamma 1 membrane association by epidermal growth factor. *Science (New York, N.Y.)* **249**, 296-298, doi:10.1126/science.2374928 (1990).

164 Bae, J. H. *et al.* The selectivity of receptor tyrosine kinase signaling is controlled by a secondary SH2 domain binding site. *Cell* **138**, 514-524, doi:10.1016/j.cell.2009.05.028 (2009).

165 Coggeshall, K. M., McHugh, J. C. & Altman, A. Predominant expression and activation-induced tyrosine phosphorylation of phospholipase C-gamma 2 in B lymphocytes. *Proc Natl Acad Sci U S A* **89**, 5660-5664, doi:10.1073/pnas.89.12.5660 (1992).

166 Nakamura, Y. & Fukami, K. Regulation and physiological functions of mammalian phospholipase C. *J Biochem* **161**, 315-321, doi:10.1093/jb/mvw094 (2017).

167 Nishida, M. *et al.* Amplification of receptor signalling by Ca2+ entry-mediated translocation and activation of PLCgamma2 in B lymphocytes. *EMBO J* **22**, 4677-4688, doi:10.1093/emboj/cdg457 (2003).

168 Engelke, M. *et al.* Cutting edge: feed-forward activation of phospholipase Cgamma2 via C2 domain-mediated binding to SLP65. *Journal of immunology (Baltimore, Md. : 1950)* **191**, 5354-5358, doi:10.4049/jimmunol.1301326 (2013).

169 Bunney, T. D. *et al.* Structural insights into formation of an active signaling complex between Rac and phospholipase C gamma 2. *Molecular cell* **34**, 223-233, doi:10.1016/j.molcel.2009.02.023 (2009).

170 Chiang, C. Y., Veckman, V., Limmer, K. & David, M. Phospholipase Cgamma-2 and intracellular calcium are required for lipopolysaccharide-induced Toll-like receptor 4 (TLR4) endocytosis and interferon regulatory factor 3 (IRF3) activation. *The Journal of biological chemistry* **287**, 3704-3709, doi:10.1074/jbc.C111.328559 (2012).

171 Obba, S. *et al.* The PRKAA1/AMPKalpha1 pathway triggers autophagy during CSF1-induced human monocyte differentiation and is a potential target in CMML. *Autophagy* **11**, 1114-1129, doi:10.1080/15548627.2015.1034406 (2015).

172 Leon, C. M. *et al.* Requirement for PLCgamma2 in IL-3 and GM-CSF-stimulated MEK/ERK phosphorylation in murine and human hematopoietic stem/progenitor cells. *J Cell Physiol* **226**, 1780-1792, doi:10.1002/jcp.22507 (2011).

173 Mangin, P. *et al.* Signaling role for phospholipase C gamma 2 in platelet glycoprotein Ib alpha calcium flux and cytoskeletal reorganization. Involvement of a pathway distinct from FcR gamma chain and Fc gamma RIIA. *The Journal of biological chemistry* **278**, 32880-32891, doi:10.1074/jbc.M302333200 (2003).

174 Ichise, H., Ichise, T., Ohtani, O. & Yoshida, N. Phospholipase Cgamma2 is necessary for separation of blood and lymphatic vasculature in mice. *Development* **136**, 191-195, doi:10.1242/dev.025353 (2009).

175 Yablonski, D., Kadlecek, T. & Weiss, A. Identification of a phospholipase C-gamma1 (PLC-gamma1) SH3 domain-binding site in SLP-76 required for T-cell receptor-

mediated activation of PLC-gamma1 and NFAT. *Molecular and cellular biology* **21**, 4208-4218, doi:10.1128/mcb.21.13.4208-4218.2001 (2001).

176 Ji, Q. S. *et al.* Essential role of the tyrosine kinase substrate phospholipase C-gamma1 in mammalian growth and development. *Proc Natl Acad Sci U S A* **94**, 2999-3003, doi:10.1073/pnas.94.7.2999 (1997).

177 Hashimoto, A. *et al.* Cutting edge: essential role of phospholipase C-gamma 2 in B cell development and function. *Journal of immunology (Baltimore, Md. : 1950)* **165**, 1738-1742 (2000).

178 Tassi, I. *et al.* Phospholipase C-gamma 2 is a critical signaling mediator for murine NK cell activating receptors. *Journal of immunology (Baltimore, Md. : 1950)* **175**, 749-754 (2005).

179 Caraux, A. *et al.* Phospholipase C-gamma2 is essential for NK cell cytotoxicity and innate immunity to malignant and virally infected cells. *Blood* **107**, 994-1002, doi:10.1182/blood-2005-06-2428 (2006).

180 Ichise, H., Ichise, T. & Yoshida, N. Phospholipase Cgamma2 Is Required for Luminal Expansion of the Epididymal Duct during Postnatal Development in Mice. *PLoS One* **11**, e0150521, doi:10.1371/journal.pone.0150521 (2016).

181 Yu, P. *et al.* Autoimmunity and inflammation due to a gain-of-function mutation in phospholipase C gamma 2 that specifically increases external Ca2+ entry. *Immunity* **22**, 451-465, doi:10.1016/j.immuni.2005.01.018 (2005).

182 Gossmann, J. *et al.* A Gain-Of-Function Mutation in the Plcg2 Gene Protects Mice from Helicobacter felis-Induced Gastric MALT Lymphoma. *PLoS One* **11**, e0150411, doi:10.1371/journal.pone.0150411 (2016).

183 Arnold, C. N. *et al.* A forward genetic screen reveals roles for Nfkbid, Zeb1, and Ruvbl2 in humoral immunity. *Proc Natl Acad Sci U S A* **109**, 12286-12293, doi:10.1073/pnas.1209134109 (2012).

184 Liu, T. M. *et al.* Hypermorphic mutation of phospholipase C, gamma2 acquired in ibrutinib-resistant CLL confers BTK independency upon B-cell receptor activation. *Blood* **126**, 61-68, doi:10.1182/blood-2015-02-626846 (2015).

185 Woyach, J. A. *et al.* BTK(C481S)-Mediated Resistance to Ibrutinib in Chronic Lymphocytic Leukemia. *J Clin Oncol* **35**, 1437-1443, doi:10.1200/JCO.2016.70.2282 (2017).

186 Woyach, J. A. *et al.* Resistance mechanisms for the Bruton's tyrosine kinase inhibitor ibrutinib. *N Engl J Med* **370**, 2286-2294, doi:10.1056/NEJMoa1400029 (2014).

187 Ahn, I. E. *et al.* Clonal evolution leading to ibrutinib resistance in chronic lymphocytic leukemia. *Blood* **129**, 1469-1479, doi:10.1182/blood-2016-06-719294 (2017).

188 Ombrello, M. J. *et al.* Cold urticaria, immunodeficiency, and autoimmunity related to PLCG2 deletions. *N Engl J Med* **366**, 330-338, doi:10.1056/NEJMoa1102140 (2012).

189 Milner, J. D. PLAID: a Syndrome of Complex Patterns of Disease and Unique Phenotypes. *J Clin Immunol* **35**, 527-530, doi:10.1007/s10875-015-0177-x (2015).

190 Aderibigbe, O. M. *et al.* Distinct Cutaneous Manifestations and Cold-Induced Leukocyte Activation Associated With PLCG2 Mutations. *JAMA Dermatol* **151**, 627-634, doi:10.1001/jamadermatol.2014.5641 (2015).

191 Zhou, Q. *et al.* A hypermorphic missense mutation in PLCG2, encoding phospholipase Cgamma2, causes a dominantly inherited autoinflammatory disease with immunodeficiency. *Am J Hum Genet* **91**, 713-720, doi:10.1016/j.ajhg.2012.08.006 (2012).

192 Neves, J. F. *et al.* Novel PLCG2 Mutation in a Patient With APLAID and Cutis Laxa. *Frontiers in immunology* **9**, 2863, doi:10.3389/fimmu.2018.02863 (2018).

193 Sims, R. *et al.* Rare coding variants in PLCG2, ABI3, and TREM2 implicate microglial-mediated innate immunity in Alzheimer's disease. *Nature genetics* **49**, 1373-1384, doi:10.1038/ng.3916 (2017).

194 Magno, L. *et al.* Alzheimer's disease phospholipase C-gamma-2 (PLCG2) protective variant is a functional hypermorph. *Alzheimers Res Ther* **11**, 16, doi:10.1186/s13195-019-0469-0 (2019).

195 Beutler, B. *Phenotypic Mutation 'queen'* <https://mutagenetix.utsouthwestern.edu/phenotypic/phenotypic_rec.cfm?pk=480> (2010).

196 Rosenthal, S. L. *et al.* Seroprevalence of herpes simplex virus types 1 and 2 and cytomegalovirus in adolescents. *Clinical infectious diseases : an official publication of the Infectious Diseases Society of America* **24**, 135-139 (1997).

197 Ornstein, B. W., Hill, E. B., Geurs, T. L. & French, A. R. Natural killer cell functional defects in pediatric patients with severe and recurrent herpesvirus infections. *The Journal of infectious diseases* **207**, 458-468, doi:10.1093/infdis/jis701 (2013).

198 Mace, E. M. & Orange, J. S. Genetic Causes of Human NK Cell Deficiency and Their Effect on NK Cell Subsets. *Frontiers in immunology* **7**, 545, doi:10.3389/fimmu.2016.00545 (2016).

199 Lanier, L. L. Up on the tightrope: natural killer cell activation and inhibition. *Nat Immunol* **9**, 495-502, doi:10.1038/ni1581 (2008).

200 Wang, D. *et al.* Phospholipase Cgamma2 is essential in the functions of B cell and several Fc receptors. *Immunity* **13**, 25-35 (2000).

201 Volmering, S., Block, H., Boras, M., Lowell, C. A. & Zarbock, A. The Neutrophil Btk Signalosome Regulates Integrin Activation during Sterile Inflammation. *Immunity* **44**, 73-87, doi:10.1016/j.immuni.2015.11.011 (2016).

202 Milner, J. D. *et al.* Early-onset lymphoproliferation and autoimmunity caused by germline STAT3 gain-of-function mutations. *Blood* **125**, 591-599, doi:10.1182/blood-2014-09-602763 (2015).

203 Yang, Y. *et al.* Molecular findings among patients referred for clinical whole-exome sequencing. *JAMA* **312**, 1870-1879, doi:10.1001/jama.2014.14601 (2014).

204 Yang, Y. *et al.* Clinical whole-exome sequencing for the diagnosis of mendelian disorders. *N Engl J Med* **369**, 1502-1511, doi:10.1056/NEJMoa1306555 (2013).

205 Lek, M. *et al.* Analysis of protein-coding genetic variation in 60,706 humans. *Nature* **536**, 285-291, doi:10.1038/nature19057 (2016).

206 Picard, C. *et al.* International Union of Immunological Societies: 2017 Primary Immunodeficiency Diseases Committee Report on Inborn Errors of Immunity. *J Clin Immunol* **38**, 96-128, doi:10.1007/s10875-017-0464-9 (2018).

207 George, M. R. Hemophagocytic lymphohistiocytosis: review of etiologies and management. *J Blood Med* **5**, 69-86, doi:10.2147/JBM.S46255 (2014).

208 Hughes, C. R. *et al.* MCM4 mutation causes adrenal failure, short stature, and natural killer cell deficiency in humans. *The Journal of clinical investigation* **122**, 814-820, doi:10.1172/jci60224 (2012).

209 Banerjee, P. P. & Orange, J. S. Quantitative measurement of F-actin accumulation at the NK cell immunological synapse. *J Immunol Methods* **355**, 1-13, doi:10.1016/j.jim.2010.02.003 (2010).

210 Mentlik, A. N., Sanborn, K. B., Holzbaur, E. L. & Orange, J. S. Rapid lytic granule convergence to the MTOC in natural killer cells is dependent on dynein but not cytolytic commitment. *Mol Biol Cell* **21**, 2241-2256, doi:10.1091/mbc.E09-11-0930 (2010).

211 Newell, E. W., Sigal, N., Bendall, S. C., Nolan, G. P. & Davis, M. M. Cytometry by time-of-flight shows combinatorial cytokine expression and virus-specific cell niches within a continuum of CD8+ T cell phenotypes. *Immunity* **36**, 142-152, doi:10.1016/j.immuni.2012.01.002 (2012).

212 Bendall, S. C. *et al.* Single-cell mass cytometry of differential immune and drug responses across a human hematopoietic continuum. *Science (New York, N.Y.)* **332**, 687-696, doi:10.1126/science.1198704 (2011).

213 Amir el, A. D. *et al.* viSNE enables visualization of high dimensional single-cell data and reveals phenotypic heterogeneity of leukemia. *Nat Biotechnol* **31**, 545-552, doi:10.1038/nbt.2594 (2013).

214 Kotecha, N., Krutzik, P. O. & Irish, J. M. Web-based analysis and publication of flow cytometry experiments. *Curr Protoc Cytom* **Chapter 10**, Unit10 17, doi:10.1002/0471142956.cy1017s53 (2010).

215 Fujisaki, H. *et al.* Expansion of highly cytotoxic human natural killer cells for cancer cell therapy. *Cancer Res* **69**, 4010-4017, doi:10.1158/0008-5472.CAN-08-3712 (2009).

216 Robert, X. & Gouet, P. Deciphering key features in protein structures with the new ENDscript server. *Nucleic Acids Res* **42**, W320-324, doi:10.1093/nar/gku316 (2014).

217 Notredame, C., Higgins, D. G. & Heringa, J. T-Coffee: A novel method for fast and accurate multiple sequence alignment. *Journal of molecular biology* **302**, 205-217, doi:10.1006/jmbi.2000.4042 (2000).

218 Moretti, S. *et al.* The M-Coffee web server: a meta-method for computing multiple sequence alignments by combining alternative alignment methods. *Nucleic Acids Res* **35**, W645-648, doi:10.1093/nar/gkm333 (2007).

219 Abraham, M. J. *et al.* GROMACS: High performance molecular simulations through multi-level parallelism from laptops to supercomputers. *SoftwareX* **1**, 19-25 (2015).

220 Duan, Y. *et al.* A point-charge force field for molecular mechanics simulations of proteins based on condensed-phase quantum mechanical calculations. *J Comput Chem* **24**, 1999-2012, doi:10.1002/jcc.10349 (2003).

221 Jorgensen, W. L., Chandrasekhar, J., Madura, J. D., Impey, R. W. & Klein, M. L. Comparison of simple potential functions for simulating liquid water. *Journal of Chemical Physics* **79**, 926-935 (1983).

222 Hess, B., Bekker, H., Berendsen, H. & Fraaojie, J. LINCS: A Linear Constraint Solver for Molecular Simulations. *Journal of Computational Chemistry* **18**, 1463-1472 (1997).

223 Bussi, G., Donadio, D. & Parrinello, M. Canonical sampling through velocity rescaling. *J Chem Phys* **126**, 014101, doi:10.1063/1.2408420 (2007).

224 Bunney, T. D. *et al.* Structural and functional integration of the PLCgamma interaction domains critical for regulatory mechanisms and signaling deregulation. *Structure* **20**, 2062-2075, doi:10.1016/j.str.2012.09.005 (2012).

225 Handa, N. *et al.* (ed Structural Genomics/Proteomics Initiative (RSGI)) (RCSB PDB, 2006).

226 Beauchamp, K. A. *et al.* MSMBuilder2: Modeling Conformational Dynamics at the Picosecond to Millisecond Scale. *J Chem Theory Comput* **7**, 3412-3419, doi:10.1021/ct200463m (2011).

227 Bowman, G. R., Pande, V. S. & Noe, F. *An Introduction to Markov State Models and Their Application to Long Timescale Molecular Simulation*. (Springer Science & Business Media, 2013).

228 Rieux-Laucat, F. & Casanova, J. L. Immunology. Autoimmunity by haploinsufficiency. *Science (New York, N.Y.)* **345**, 1560-1561, doi:10.1126/science.1260791 (2014).

229 Garcia, P. *et al.* The pleckstrin homology domain of phospholipase C-delta 1 binds with high affinity to phosphatidylinositol 4,5-bisphosphate in bilayer membranes. *Biochemistry* **34**, 16228-16234, doi:10.1021/bi00049a039 (1995).

230 Ueno, H. T follicular helper cells in human autoimmunity. *Curr Opin Immunol* **43**, 24-31, doi:10.1016/j.coi.2016.08.003 (2016).

231 Ueda, Y. *et al.* Protein kinase C activates the MEK-ERK pathway in a manner independent of Ras and dependent on Raf. *The Journal of biological chemistry* **271**, 23512-23519 (1996).

232 Zimmerman, M. I. *et al.* Prediction of New Stabilizing Mutations Based on Mechanistic Insights from Markov State Models. *ACS Cent Sci* **3**, 1311-1321, doi:10.1021/acscentsci.7b00465 (2017).

233 Hart, K. M., Ho, C. M., Dutta, S., Gross, M. L. & Bowman, G. R. Modelling proteins' hidden conformations to predict antibiotic resistance. *Nat Commun* **7**, 12965, doi:10.1038/ncomms12965 (2016).

234 Lappalainen, I., Thusberg, J., Shen, B. & Vihinen, M. Genome wide analysis of pathogenic SH2 domain mutations. *Proteins* **72**, 779-792, doi:10.1002/prot.21970 (2008).

235 Baker, N. A., Sept, D., Joseph, S., Holst, M. J. & McCammon, J. A. Electrostatics of nanosystems: application to microtubules and the ribosome. *Proc Natl Acad Sci U S A* **98**, 10037-10041, doi:10.1073/pnas.181342398 (2001).

236 Upshaw, J. L., Schoon, R. A., Dick, C. J., Billadeau, D. D. & Leibson, P. J. The isoforms of phospholipase C-gamma are differentially used by distinct human NK activating receptors. *Journal of immunology (Baltimore, Md. : 1950)* **175**, 213-218 (2005).

237 Lopez-Verges, S. *et al.* CD57 defines a functionally distinct population of mature NK cells in the human CD56dimCD16+ NK-cell subset. *Blood* **116**, 3865-3874, doi:10.1182/blood-2010-04-282301 (2010).

238 Guma, M. *et al.* Imprint of human cytomegalovirus infection on the NK cell receptor repertoire. *Blood* **104**, 3664-3671, doi:10.1182/blood-2004-05-2058 (2004).

239 Cerwenka, A. & Lanier, L. L. Natural killer cell memory in infection, inflammation and cancer. *Nature reviews. Immunology* **16**, 112-123, doi:10.1038/nri.2015.9 (2016).

240 Muntasell, A., Vilches, C., Angulo, A. & Lopez-Botet, M. Adaptive reconfiguration of the human NK-cell compartment in response to cytomegalovirus: a different perspective of the host-pathogen interaction. *European journal of immunology* **43**, 1133-1141, doi:10.1002/eji.201243117 (2013).

241 Paz, P. E. *et al.* Mapping the Zap-70 phosphorylation sites on LAT (linker for activation of T cells) required for recruitment and activation of signalling proteins in T cells. *The Biochemical journal* **356**, 461-471 (2001).

242 Bryceson, Y. T. *et al.* Defective cytotoxic lymphocyte degranulation in syntaxin-11 deficient familial hemophagocytic lymphohistiocytosis 4 (FHL4) patients. *Blood* **110**, 1906-1915, doi:10.1182/blood-2007-02-074468 (2007).

243 Mah, A. Y. *et al.* Glycolytic requirement for NK cell cytotoxicity and cytomegalovirus control. *JCI Insight* **2**, doi:10.1172/jci.insight.95128 (2017).

244 Mao, D., Epple, H., Uthgenannt, B., Novack, D. V. & Faccio, R. PLCgamma2 regulates osteoclastogenesis via its interaction with ITAM proteins and GAB2. *The Journal of clinical investigation* **116**, 2869-2879, doi:10.1172/JCI28775 (2006).

245 Abe, K. *et al.* A novel N-ethyl-N-nitrosourea-induced mutation in phospholipase Cgamma2 causes inflammatory arthritis, metabolic defects, and male infertility in vitro in a murine model. *Arthritis and rheumatism* **63**, 1301-1311, doi:10.1002/art.30280 (2011).

246 Arnold, C. N. & Beutler, B. Queen is an allele of Plcg2 and causes a deficiency in T-independent antibody responses. *MGI Direct Data Submission* (2010).